

Report

Fowler, David; Cape, Neil; Smith, Ron; Nemitz, Eiko; Sutton, Mark; Dore, Tony; Coyle, Mhairi; Crossley, Alan; Storeton-West, Robert; Muller, Jennifer; Phillips, Gavin; Thomas, Rick; Vieno, Massimo; Yang, Sim; Famulari, Daniela; Twigg, Marsailidh; Bealey, Bill; Benham, David; Hayman, Garry; Lawrence, Helen; Vincent, Keith; Fagerli, Hilde; Simpson, David. 2007 *Acid Deposition Processes. Final report to Defra*. NERC/Centre for Ecology & Hydrology, 110pp. (CEH Project Number: C02379, RMP 2258)

Copyright © 2007, NERC/Centre for Ecology & Hydrology

This version available at <http://nora.nerc.ac.uk/4558/>

NERC has developed NORA to enable users to access research outputs wholly or partially funded by NERC. Copyright and other rights for material on this site are retained by the authors and/or other rights owners. Users should read the terms and conditions of use of this material at <http://nora.nerc.ac.uk/policies.html#access>

This report is an official document prepared under contract between the customer and the Natural Environment Research Council. It should not be quoted without the permission of both the Centre for Ecology and Hydrology and the customer.

Contact CEH NORA team at
nora@ceh.ac.uk

Acid Deposition Processes

RMP 2258

Final Report to Defra

David Fowler, Neil Cape, Ron Smith, Eiko Nemitz, Mark Sutton, Tony Dore, Mhairi Coyle
Alan Crossley, Robert Storeton-West, Jennifer Muller, Gavin Phillips, Rick Thomas,
Massimo Vieno, Sim Yang, Daniela Famulari, Marsailidh Twigg and Bill Bealey ^a

David Benham ^b

Garry Hayman, Helen Lawrence, Keith Vincent ^c

Hilde Fagerli, David Simpson ^d

*a, Centre for Ecology and Hydrology (Edinburgh Research Station)
Bush Estate, Penicuik, Midlothian, EH26 0QB, UK.*

*b Centre for Ecology and Hydrology (Lancaster Environment Centre)
Library Avenue, Bailrigg, Lancaster, LA1 4AP, UK*

*c, AEA Energy & Environment
The Gemini Building, Fermi Avenue, Harwell International Business Centre, Didcot OX11 0QR*

*d. NILU Norwegian Institute for Air Research
P.O.Box 100, 2027 Kjeller, Norway*

February 2007

Client: Department for Environment Food and Rural Affairs	
Client Project number: RMP2258	CEH Project number: C02379NEW
Project Title: Acid Deposition Processes	
Start date: 1. November 2003	Completion date: 31 December 2006
Client Project Officer: Samantha Baker	
CEH Project Officer: David Fowler/Mark Sutton	
Main authors: David Fowler, Neil Cape, Ron Smith, Eiko Nemitz, Mark Sutton, Tony Dore, Mhairi Coyle Alan Crossley, Robert Storeton-West, Jennifer Muller, Gavin Phillips, Rick Thomas, Massimo Vieno, Sim Yang, Daniela Famulari, Marsailidh Twigg, Bill Bealey, David Benham, Garry Hayman, Helen Lawrence, Keith Vincent	
Report approved for release by: M. Sutton or D. Fowler as appropriate	
Reporting period: Final Report (1 November 2003 – 31 December 2006)	
Report date: January 2007	
Report Number: AS 07/01	
Report Status: Final	

This report is a confidential document prepared under contract between Defra and the Natural Environment Research Council (NERC). It should not be distributed or quoted without the permission of both the Centre for Ecology and Hydrology (CEH) and Defra

EXECUTIVE SUMMARY

- 1. Measurement of SO₂ dry deposition fluxes and model development:** deposition of SO₂ to Auchencorth Moss has remained constant over the past 10 years, despite a fall in average SO₂ concentration from 0.5 to 0.3 µg m⁻³. This is because the canopy resistance has decreased systematically over that period. A similar pattern has been seen for arable crops at Sutton Bonington, Nottingham. The likely cause is an increase in NH₃:SO₂ ratio, and has implications for dry deposition rates across the whole of the UK. An improved parameterisation for modelling deposition has been developed, and applied to the EMEP model; application at sites in the Netherlands and France has greatly improved the comparison between model results and measured concentrations.
- 2. Rural SO₂ monitoring network:** the rural network was stopped in 2005 and has been replaced by measurements from the Nitric Acid network. A full report on the reasons for the change, and a comparison of methods, has been provided by AEA Technology. There was a significant decline in rural SO₂ concentrations, from an average of 1.1 to 0.5 µg m⁻³ between 2001 and 2005.
- 3. Measurement of NH₃ dry deposition rates and model development:** an eddy covariance flux measurement system using a tunable diode laser absorption spectrometer (TDL-AS) has been used for the first time to measure fluxes from a recently fertilised field. Results agreed very well with an independent quantum cascade laser (University of Manchester) and a gradient system based on annular denuders (AMANDA). Although time response is much superior to the gradient system, only large fluxes are currently measurable by eddy covariance.
- 4. Measurement of aerosol dry deposition rates:** an aerosol mass spectrometer (AMS) and a gradient analyser with steam jet aerosol collector (GRAEGOR) have been used to measure particle fluxes over grassland and forest. Deposition velocities to grassland were 1-2 mm s⁻¹, and 2-6 mm s⁻¹ to a pine plantation. Deposition velocities to an oak woodland were small (< 2 mm s⁻¹) but only low wind speed conditions were present during the field measurements. However, the deposition rates to forest are generally about 3 times smaller than currently used values in modelling, which were derived from a mature forest stand in the Netherlands. Details of the processes, especially for nitrate particles, are not well understood, with apparent emission from oak forests.
- 5. UK 5km dry deposition maps:** UK deposition maps for sulphur dioxide, ammonia, nitrogen dioxide, nitric acid gases, and sulphate, nitrate, ammonium, and non-sea calcium particles are presented for 2002, 2003 and 2004. Dry deposition of nitric acid and nitrate particles in 2003 was approximately 50% greater than in the other years because of the long dry summer, which promoted nitric acid formation.
- 6. Monitoring and modelling of cloud water deposition:** the new site in southern Scotland (Bowbeat) showed enhanced capture of cloud water compared with the former site at Dunslair, which had been compromised by growth of nearby trees. Concentration enhancements in cloud compared to rain were less at Bowbeat than at Dunslair, but more similar to early data from Dunslair, before the trees caused interference with cloud water sampling. At Holme Moss (Pennines) a synthesis of data from 1994 to 2006 showed an increasing trend in rain and cloud water volumes, a small downward trend in nitrate and ammonium concentrations and a larger downward trend in non-sea sulphate concentrations. The opposing trends led to little change in cloud deposition over the period. Cloud deposition maps for the whole UK at 5km grid scale are presented for 2002, 2003 and 2004.

7. **Bi-directional exchange in UK dispersion modelling of reduced nitrogen:** a new parameterisation of NH_3 exchange, which permits emission as well as deposition, has been applied in the FRAME model of ammonia emission and transport across the UK. Incorporation of a ‘canopy compensation point’ has improved model results for ammonia concentrations in remote areas, and has demonstrated the need for seasonally-varying emission data for ammonia in source areas.
8. **Integrated deposition monitoring:** the time-averaged gradient technique has been improved by extension to sampling at 5 heights up to 9 m. Although good flux data were obtained for gases (including ammonia, nitric and hydrochloric acids), the much smaller vertical gradients for ammonium particles at Auchencorth Moss (in clean air) could not be resolved. However, use of 5 sampling heights allows better analysis of the measurement uncertainties.
9. **Investigation of primary nitric acid emissions from agricultural activities:** early indications of nitric acid release from manure could not be confirmed. Improved instrumentation (TDL-AS) and a new photoacoustic gas analyzer for NH_3 showed good agreement in the field, next to a chicken farm. A laboratory experiment with slurry showed that ammonia, trimethylamine and organic acids are released initially, followed by secondary emission of other oxygenated volatile organic compounds and nitrous acid. Earlier data apparently showing nitric acid emissions may have been caused by oxidation of nitrous acid on the sampling filters. Emission and deposition fluxes of nitrate and sulphate particles following slurry spreading were also observed, implying rapid formation of ammonium nitrate particles.
10. **Bias from dry deposition on bulk rain collectors:** operation of novel ‘flushing’ rain gauges in triplicate suggested that 15-40% of ammonium, nitrate and sulphate collected by bulk gauges could have come from dry deposition to the exposed funnel surface. There are still some uncertainties about the interpretation of the data and work will continue to identify the reasons for discrepancies.
11. **Mapping wet deposition across the UK:** annual maps of seeder-feeder enhanced wet deposition of non-sea sulphate, non-sea calcium, ammonium and nitrate are presented for 2002, 2003 and 2004. Wet deposition was generally lower in 2003 than in the other years because of lower rainfall.
12. **Total deposition and UK budgets:** maps are presented for the UK for 2002, 2003 and 2004, and budget trends from 1995 to 2004. Wet and dry deposition of non-sea sulphate has decreased from 310 to 167 gG y^{-1} ; oxidised nitrogen (excluding nitric acid) has decreased slightly, from 130 to 116 gG y^{-1} ; reduced nitrogen has stayed almost constant at around 170 gG y^{-1} . Dry deposition of nitric acid (measured from 2000 onwards) shows large year-to-year variability, but is 2-3 times greater, at 60-90 gG y^{-1} , than dry deposition of nitrogen dioxide (NO_2).
13. **Critical load exceedance maps:** these show no significant change in 2002-2004 from the previous period 1999-2001.
14. **Mapping annual AOT40 for ozone:** the 5-year mean AOT40 map for the UK at 1 km resolution is presented for the period 1999-2003.
15. **Communication:** a new internet site <http://www.uk-pollutantdeposition.ceh.ac.uk> has been set up as a framework for integrating all Defra-funded data and mapping by CEH.

CONTENTS

1. INTRODUCTION & HISTORICAL PERSPECTIVE.....	7
2. DRY DEPOSITION AND CLOUD DEPOSITION.....	19
2.1. MEASUREMENT OF SO ₂ DRY DEPOSITION FLUXES AND MODEL DEVELOPMENT.....	19
<i>Auchencorth Moss</i>	19
<i>Development of improved parameterisations of NH₃ and SO₂ exchange</i>	21
2.2. RURAL SULPHUR DIOXIDE MONITORING NETWORK.....	24
<i>Introduction</i>	24
<i>Executive Summary</i>	24
2.3. MEASUREMENT OF NH ₃ DRY DEPOSITION RATES AND MODEL DEVELOPMENT.....	26
<i>Continued development of eddy covariance system for the measurements of surface / atmosphere exchange fluxes of atmospheric ammonia</i>	26
<i>Quantification of NH₃ exchange</i>	28
2.4. MEASUREMENT OF AEROSOL DRY DEPOSITION RATES.....	31
<i>Background</i>	31
<i>Measurements over grassland</i>	31
<i>Measurements over coniferous forest</i>	32
<i>Measurements of aerosol deposition rates to deciduous oak forest</i>	32
2.5 UK 5KM DRY DEPOSITION MAPS.....	37
<i>Modelling dry deposition of gases and aerosols</i>	37
2.6. MONITORING AND MODELLING OF CLOUD WATER DEPOSITION.....	44
<i>Comparison of Bowbeat and Dunslair</i>	44
<i>Cloud versus Rain composition</i>	45
<i>Long-term monitoring of ion concentrations in cloud and rainwater at Holme Moss from 1994 to 2006</i>	47
<i>Maps of cloud droplet deposition</i>	67
2.7. BI-DIRECTIONAL EXCHANGE IN UK DISPERSION MODELLING OF REDUCED NITROGEN...	71
<i>Introduction</i>	71
<i>New parameterisation of Bi-directional exchange of ammonia</i>	71
<i>Results of modelling bi-directional exchange of ammonia with FRAME</i>	72
2.8 INTEGRATED DEPOSITION MONITORING.....	76
2.9 INVESTIGATION OF PRIMARY NITRIC ACID EMISSIONS FROM AGRICULTURAL ACTIVITIES.	80
<i>Measurements of NH₃ and HNO₃ at farmyard locations</i>	80
<i>Laboratory based cuvette measurements of HNO₃ emission from slurry</i>	81
<i>Field experiment of slurry application</i>	86
<i>Scaling-up of the effects of agricultural HNO₃ emissions on UK budgets</i>	90
<i>Summary of the current understanding of HNO₃ emission from livestock wastes</i>	90
2.10. BIAS FROM DRY DEPOSITION – DRY DEPOSITION ON BULK RAIN COLLECTORS.....	92
<i>Use of ‘flushing’ rain gauges to estimate the contribution of dry deposition to bulk rain collectors</i>	92
3. MAPPING DEPOSITION.....	97
3.1 MAPPING WET DEPOSITION ACROSS THE UK.....	97
3.2 MAPS OF TOTAL DEPOSITION AND BUDGETS FOR UK.....	101
<i>UK budgets</i>	101
<i>Deposition for critical load exceedances</i>	106

4. AOT 40	109
4.1. MAPPING ANNUAL AOT40	109
5. SYNTHESIS	110
5.1. SYNTHESIS OF UK TRENDS TO SUPPORT POLICY NEGOTIATIONS	110
5.2 COMMUNICATION, REPORTING AND DEVELOPMENT OF INTERNET SITE.....	110

INTRODUCTION & HISTORICAL PERSPECTIVE

This report brings together a range of largely independent work packages, all of which are necessary for the development of our understanding of acid deposition in the UK. The work packages contribute to total deposition maps and budgets for the country, through direct monitoring of gases, precipitation chemistry, improving models of the underlying processes and compiling the total inputs for the country as maps and annual budgets. There is a wider perspective for this work to show how the chemical climate of the UK has changed in response to the very substantial changes in emissions of acid deposition precursor gases and the extent to which the changes observed are understood. This introduction therefore provides a narrative which extends beyond the work packages which follow, both in mechanistic studies and in time, but is necessary to provide the overall context for the work.

There have been dramatic changes in the composition of the air over the UK during the period of high quality measurements (since 1986). Most of the changes are in the expected direction, reductions in concentrations and deposition, following reductions in emission. The surprises are in the magnitudes of the responses, some reductions in deposition greatly exceed those expected from the changes in emission, while other reductions in concentration and deposition are much smaller than those expected from the changes in emissions. This introduction provides some mechanistic explanations of the observed changes.

The subject of acid deposition has a long history, from R.A.Smith's description of rainfall composition in the UK in the late 19th century (1872), which identified links between emissions of pollutants from coal combustion and the chemical composition of precipitation. However, the environmental significance of deposited acidity was not appreciated politically until the 1970's following the discovery of large areas of acidified freshwaters in Southern Scandinavia and associated declines in fish populations. The scientific evidence was presented at the UN conference on the Human Environment at Stockholm in 1971 (Sweden 1971). The case made by Sweden was that the long range transport of sulphur from the main industrial countries of Europe was primarily responsible for the observed trends in freshwater acidification and that therefore the action necessary to reduce these effects required controls of emissions of sulphur in all countries contributing to the problem. In the UK the existing policy was primarily concerned with national issues and the problems of SO₂ and smoke in urban areas, with the focus of effects on human health. Thus this international dimension was very new and a new policy development began following the UN conference in Sweden. The

1970s provided syntheses of existing data, process studies and modelling to assess the fate of UK emissions of sulphur and the magnitude of the UK contribution to Scandinavian acid deposition. The monitoring data within the UK for air quality and the composition of precipitation had been established to address issues of urban air quality, and on smoke and SO₂ thus the data coverage in rural areas was poor. The assessments of the early 1980s concluded that wet and dry not monitored adequately to quantify the spatial and temporal trends in acid deposition throughout the UK, (RGAR 1983). However, for Scotland and Northern England a limited area network of rainfall chemistry samplers demonstrated that precipitation was as acidic in parts of the UK as in Southern Sweden, that sulphur was the main contributor to the acidity, and that long range transport of air pollutants was responsible for the episodic deposition of particularly acidic precipitation (Fowler et al 1981). It was not long before ecological effects of deposited acidity similar to those observed in Scandinavia were reported in the UK (Battarbee et al 1990). Furthermore, methods developed by Battarbee and colleagues provided the time course of acidification of acidification of UK lochs and lakes in acid sensitive catchments since the industrial revolution. This was the period in which electricity production was being actively moved out of the urban centres to large coal fired generating stations, mainly in Nottinghamshire and Yorkshire. This policy was developed in part to remove sulphur emissions from the urban areas, but there were concerns at the time that the tall stacks (typically 200m) were contributing to the long range transport of sulphur.

Following the recommendations of the early RGAR reports a new network of precipitation chemistry monitoring was established and by 1986 this provided the data necessary to quantify the spatial patterns of acid deposition throughout the UK. The report presented here is based on the data from this network, and while substantial changes in the number of sites in the network and some methodological changes have been made, the data have proved adequate to define the spatial patterns in deposition of the major ions in precipitation and trends with time. The networks also provided a concentration field for SO₂, to allow dry deposition to be quantified. In the early period of the network, the majority of the sulphur deposited in the UK was by dry deposition. Thus, in addition to the background monitoring of precipitation and SO₂ concentration, process studies of dry deposition were made to underpin the modelling of dry deposition throughout the UK. It was recognised that at that time a network to monitor dry deposition directly was not practical, or affordable.

At the time the networks were established (1986) UK emissions of sulphur were almost 2 MT (as S), deposition within the UK amounted to about 0.7 MT-S of which 60% was dry

deposited. Export of sulphur from the UK, mainly as $(\text{NH}_4)_2\text{SO}_4$ and H_2SO_4 , therefore amounted to 1.3 MT-S. Thus the two thirds of UK emissions were exported and the majority of the sulphur deposited in the UK was dry deposited, with the Midlands as the area of largest deposition, where annual total S deposition was of the order of 50 kg S ha^{-1} , crops, throughout the UK received a substantial fraction of their sulphur from the atmosphere, large areas of the UK were devoid of most lichen species, limestone buildings were seriously corroded by the deposited acidity and effects on freshwater ecology were widespread in the poorly buffered catchments of upland UK. By contrast, the current (2005) emissions are 400kT-S, a reduction to 20% of the 1986 emissions and to 12% of peak emissions, in 1970. Total deposition within the UK in 2005 is 300kt, so instead of exporting the majority of emissions, two thirds of UK sulphur emissions are now deposited within the UK. Furthermore, the deposition total is dominated by wet deposition, so that the areas of maximum deposition are now the uplands of Northern and Western Britain, where peak deposition is currently about 10 kg-S ha^{-1} . The areas of the English Midlands, which received 50 kg-S ha^{-1} in the early 1980s, now receive less than 10 kg-S ha^{-1} , crops are sulphur deficient, unless supplied with their sulphur needs through fertilizers, lichens are migrating back into the areas in which they were absent, rainwater acidity has declined dramatically throughout the UK and the freshwaters are recovering, some very slowly as the base cations, necessary to restore alkalinity to the water are released very slowly from the parent geology.

The policy objective of reducing UK sulphur emissions, deposition and their effects on the environment has been a considerable success. Emissions of sulphur in the UK at ~400 kT-S, represent only 12% of the peak emissions in 1970. As detailed elsewhere in the report, acidity in precipitation has declined everywhere in the country, with the largest decline, both in absolute and relative terms in the Midlands of England, the areas of largest sulphur emissions, both historically and currently. However, while the reduced deposition is entirely expected, there are many features of the changes in the 'deposition climatology' of the UK which were not expected and which require an explanation, how otherwise can we be confident in the results of further control strategies?

Non-linearities in the relationship between emission and deposition of sulphur in the UK

The emissions and deposition of sulphur in the UK throughout the monitoring period (1986-2005) may be compared graphically as in figure 1. If the fraction of emissions deposited in the UK remains constant with time, then a simple linear relationship between emissions and deposition would be expected. Substantial non-linearities are evident as reported by Fowler et al 2005, 2006, 2007. During the early years, with emissions in the range 1600kT-S to 2000 kT-S deposition declined very quickly following the reductions in emissions, with reductions in deposition amounting to about half of the reduction in emissions. These very large reductions in SO₂ concentrations followed the sharp decline in low level sources, especially domestic coal combustion and low level emissions from industrial coal combustion. This was the period 1986 to 1990. By contrast the period 1990 to 2000, during which emissions declined from 1600 kT-S to 800 kT-S resulted in a slower decline in deposition of only 100 kT-S, the reduction in deposition representing only between 10% and 20% of the decline in emissions. This was the period during which the reduction in coal combustion was mainly by the replacement of coal by gas fired power stations and by flue gas desulphurization at two major power stations.

More recently, the rate of the decline in deposition with emission reduction has again increased, reflecting the more rapid conversion of SO₂ to SO₄, through both gas phase and heterogeneous processes and through the continued increase in dry deposition. This explanation, is not the whole picture as emissions of sulphur elsewhere in Europe and from shipping find their way to the UK, and changes in the contribution to the sulphur budget over the UK from these two sources have not remained constant through the monitoring period. However, in both cases, the data available to quantify their contribution to the observed changes is very limited and would require further analysis. A modelling study to reconstruct the changes in the deposition climate of the UK would be helpful as a part of this analysis, in collaboration with EMEP. However, the emissions in continental Europe contribute only a small fraction of the deposition on the UK and trends in emissions over continental Europe for the same period are of a similar order to those in the UK. It is reasonable to conclude that processes regulating the relationship between emission and deposition of sulphur have changed substantially during the period.

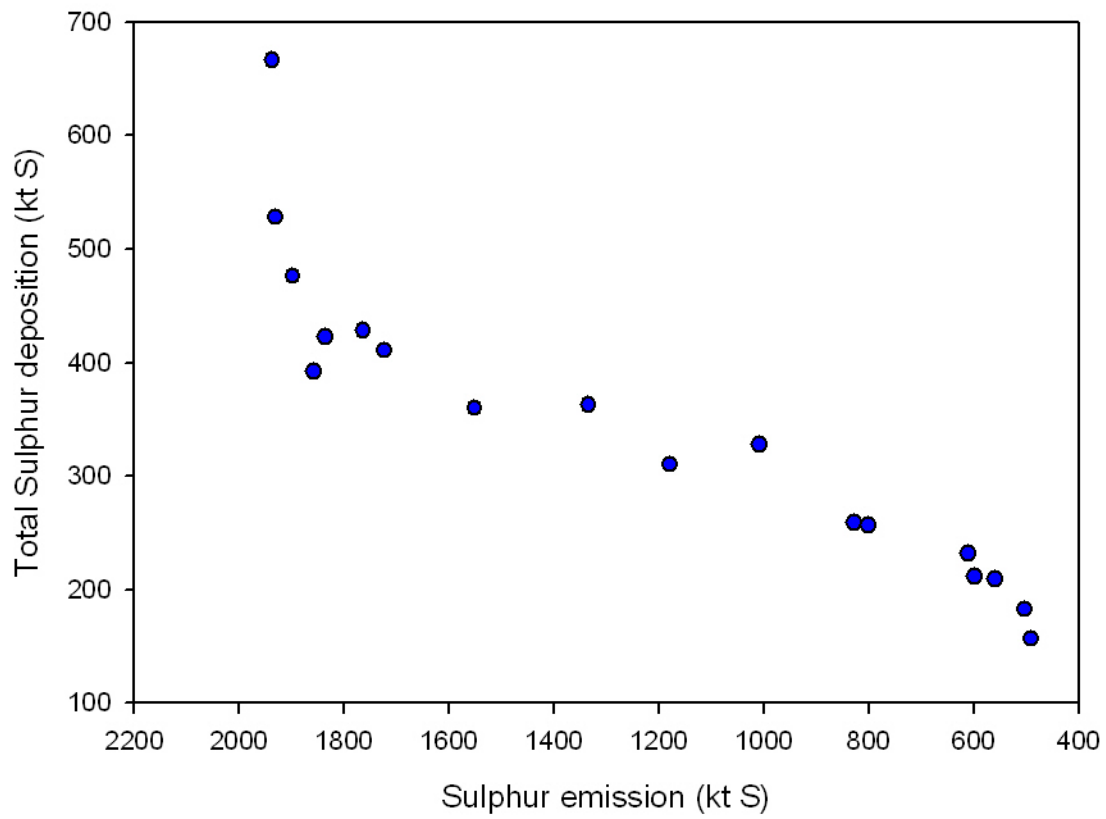


Figure 1. A comparison of UK emissions sulphur and of the total (wet plus dry) deposition of non-sea salt sulphur UK throughout the period 1986 to 2005.

Comparing the atmospheric chemistry and deposition of Sulphur in the UK in the mid 1980s with 2005

In the mid 1980s and throughout the 1960s and 1970s, concentrations of SO₂ were substantial throughout the Midlands of England, central Scotland and close to all major conurbations. In these areas dry deposition dominated the deposition total, but rates of deposition, expressed as a deposition velocity (V_g) averaged between 4 and 8 mm s⁻¹, the dry deposition process was controlled by surface chemistry, and particularly the pH of the surface film of water on vegetation (Flechard et al 1994); the acidic surface film effectively limited the rate of SO₂ deposition. The large concentrations of sulphur in the boundary layer, acidified the cloudwater and also limited the oxidation pathway for the SO₂ in the atmosphere. The presence of atmospheric NH₃ was important in regulating both the dry deposition rate and As SO₂ emissions and concentrations declined the processes of removal by dry deposition and oxidation in the atmosphere increased, accelerating the decline in SO₂ concentration. The ratio of NH₃ to SO₂ has increased, allowing the deposition rate at the surface to increase with time. Thus deposition velocity has increased with time over large areas of the UK as the SO₂ concentrations have declined. The long term measurements of deposition velocity at Auchencorth Moss and Sutton Bonnington reported later in this report and by Fowler et al (2001) provide the direct evidence of this progressive change in deposition velocity. The feedback between the increasing rates of dry deposition further reducing surface SO₂ concentration is an important part of the change in the processing of SO₂ with time. It is notable that in the Trent valley of Nottinghamshire, annual mean concentrations of SO₂ were typically 15 ppb in the 1960s and early 1970s, whereas typical values in recent years are 0.5 to 1.0 ppb.

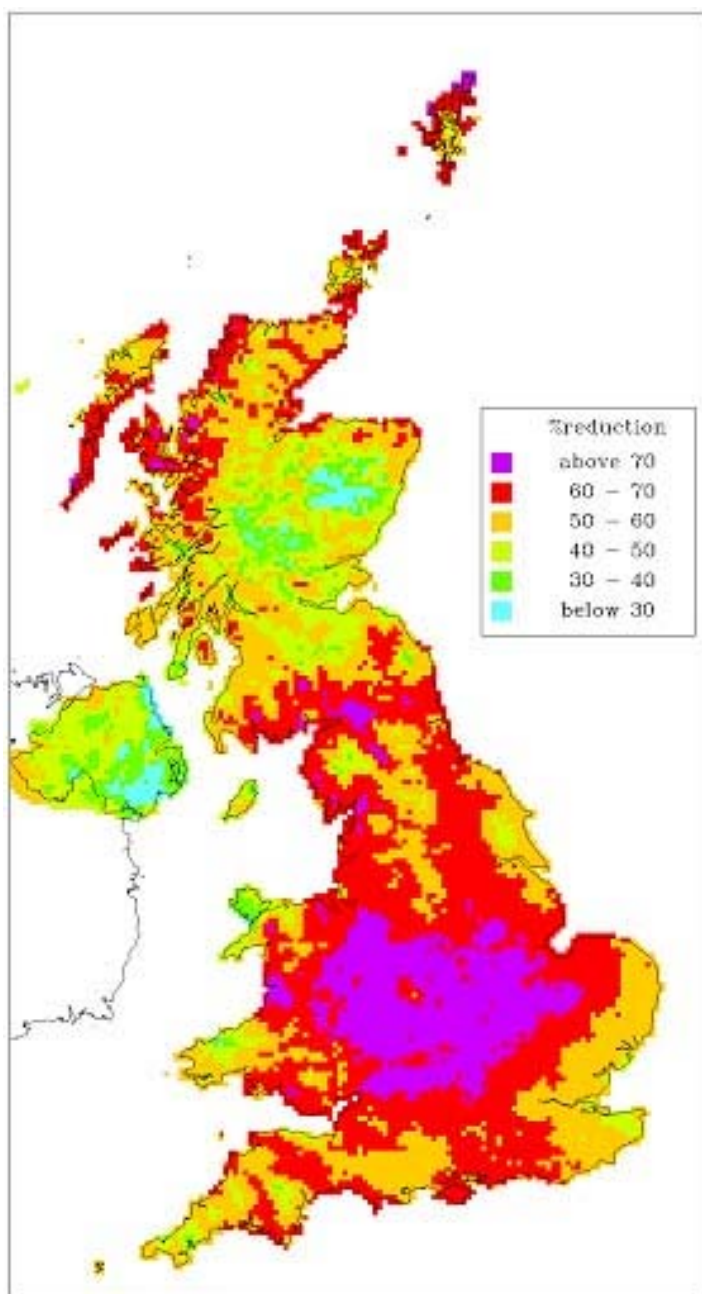


Figure 2 The reduction in total sulphur deposition throughout the UK between 1986 and 2005, expressed as a percentage of values for 1986.

The effect of reductions in SO₂ concentration and dry deposition in the source areas is illustrated in Figure 2, which shows the percentage reduction in total deposition of sulphur since 19986 mapped across the UK. The Midlands of England, where dry deposition dominated the sulphur deposition shows reductions in excess of 70%, whereas the uplands of the West and North, show much smaller reductions in deposition, of the order 30% to 40%. These spatial changes are also reflected in the change from a dry deposition to a wet deposition dominated national deposition budget, shown plotted against time since 1986 in Figure 3.

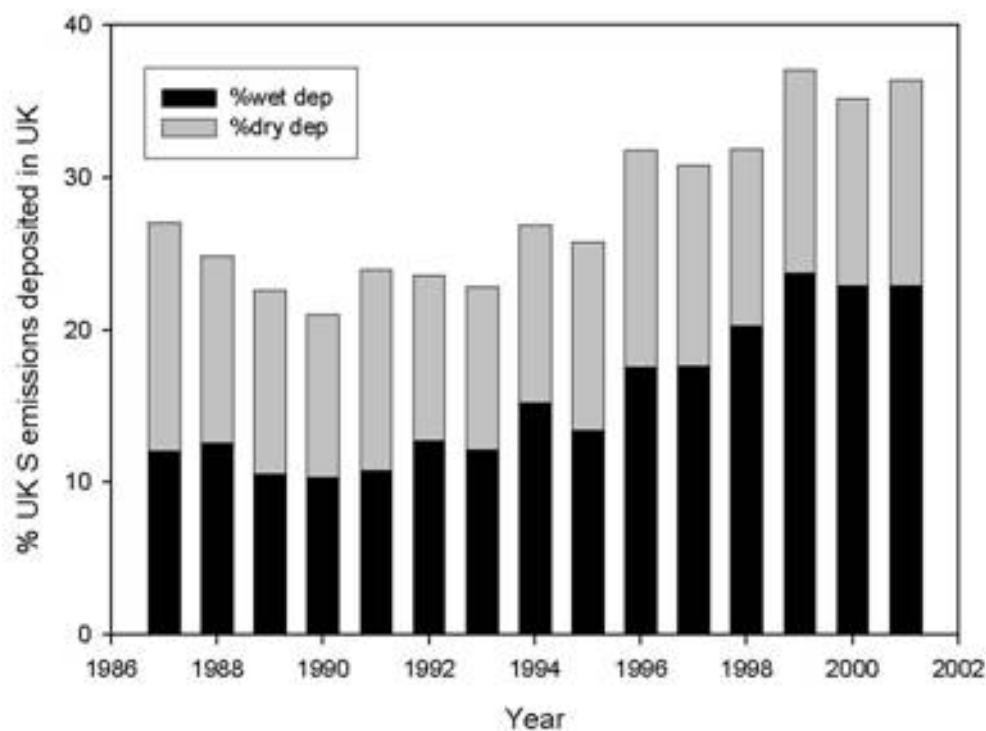


Figure 3 Total, wet and dry deposition of sulphur in the UK expressed as a percentage of emissions plotted annually between 1986 and 2002.

The consequence of these observations is that the greatest benefits of the control strategy adopted have been the areas of the country in which dry deposition was the main source of sulphur, ie the Midlands and the urban areas. The areas benefiting least are the uplands and the wet deposition dominated areas of the country. The uplands are primarily the areas of greatest ecological effects, especially on freshwater biota. The overall acid deposition in the uplands has declined substantially, but less than the reduction in emissions, as illustrated in Fig 2 as the emission reduction in the UK over this period has been about 80%.

Changes in the oxidized nitrogen budget over the UK since 1986

The other main feature of the response to changing emissions since 1986 is the change in oxidized nitrogen deposition. The emissions of NO_x in the UK have declined by approximately 45% since 1986, as shown in Figure 4a.

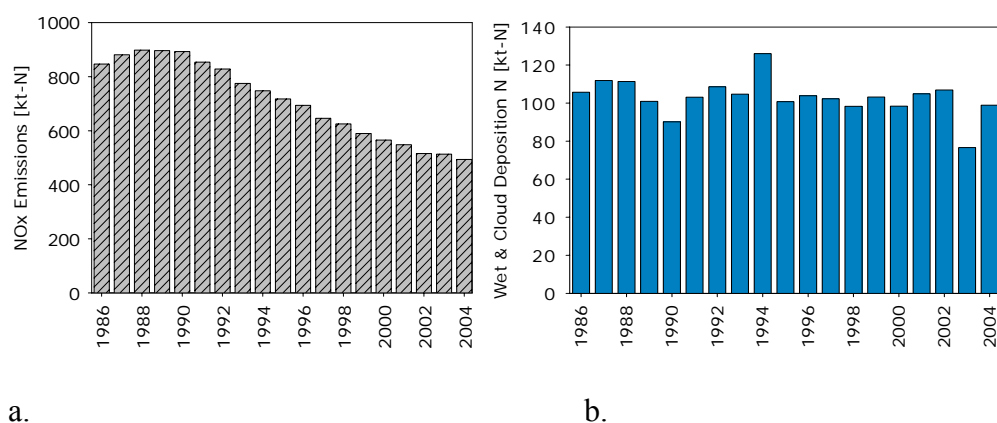


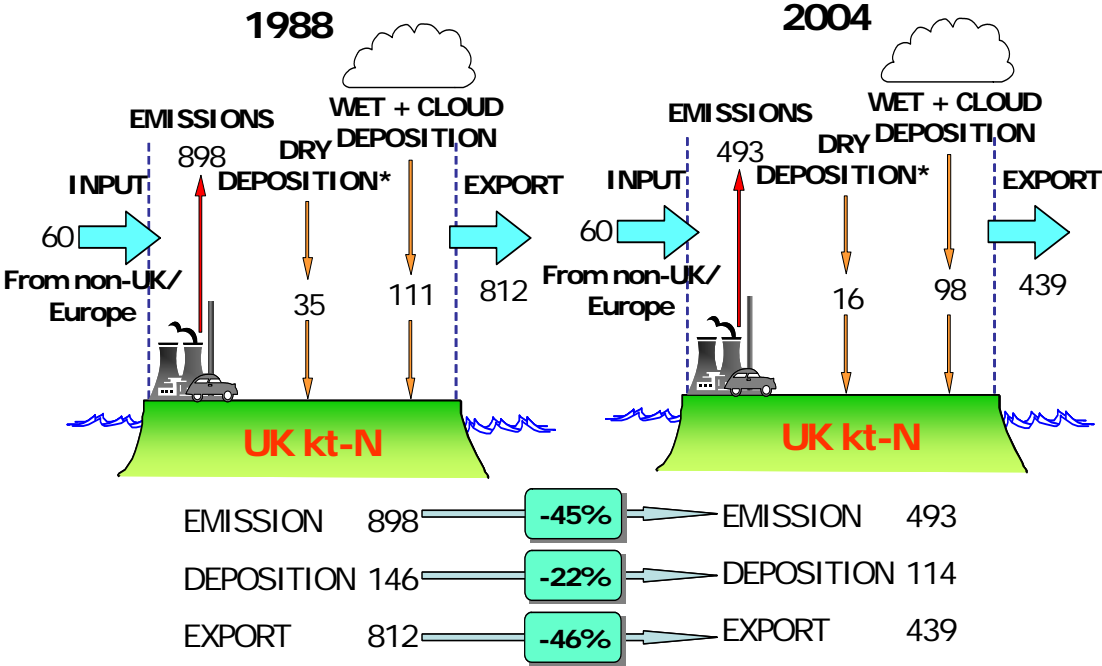
Figure 4 Emissions (a) and wet deposition (b) of oxidized Nitrogen in the UK between 1986 and 2004

Wet deposition, including cloud droplet deposition on the hills, has changed very little over the period of measurements, the notably smaller wet deposition year of 2003 was due to the unusually dry year.

Dry deposition of NO₂ has declined in line with emissions (Fig 5), but the deposition rate of NO₂ is small and overall dry deposition represents only 3 % of the emitted oxidized nitrogen. The other components of the oxidized nitrogen budget are nitric acid and aerosol nitrate, the former being dry deposited rapidly and the latter dry deposited slowly. The relatively recent implementation of a UK network of nitric acid samplers means that we do not have estimates of the nitric acid concentrations for the period 1986 to 2000. However, the lack of a trend in wet deposition and recent data from the NERC Polluted Troposphere programme imply more rapid atmospheric processing of NO_x to NO₃. Thus as for sulphur, substantial non-linearities are apparent. The NERC measurements from a series of circumnavigation of the UK experiments to deduce the net boundary layer budget of a range of pollutants, including

oxidized nitrogen, suggests that oxidized nitrogen in large plumes from urban areas is oxidized more rapidly than NO_x from large combustion plant, most probably because nocturnal processing of the oxidized nitrogen in urban areas is now much faster, as there is now a substantial ozone concentration present in urban air, whereas in the 1980s, urban ozone concentrations were titrated to very small concentrations by the local emissions of nitric oxide.

The consequence of these changes in the oxidized nitrogen budget is that the large reduction in emissions, has caused a much larger reduction in net export of NO_x from the UK than in the oxidized nitrogen deposition, as illustrated schematically in Figure 5. Deposition in the UK has declined, but by



*NO_x only

Figure 5. Illustrating the annual oxidized nitrogen budget of the atmosphere over the UK, contrasting the budgets for 1988 and 2004.

half the extent of the reduction in emissions, as a consequence of the gradual increase in the oxidation of NO_x to NO₃, and the overall shortening of the residence time for NO_x in the boundary layer over the UK. The consequence in environmental effects is that those effects driven by the total input of nitrogen to ecosystems, will have changed little in response to the large changes in emissions.

The other main contributor to emissions and deposition of reactive nitrogen are the reduced Nitrogen components (NH₃ and NH₄). These nitrogen components dominate the nitrogen deposition budget, as shown elsewhere in the report and as emissions and deposition of reduced nitrogen have changed little over the period 1996 to 2005, the ecological effects driven by this deposited nitrogen remain largely unchanged. The monitoring data for UK flora reveal clear links between declines in species diversity throughout the UK and the deposition of nitrogen from the atmosphere. Substantial reductions in both oxidized and reduced nitrogen would be necessary to reduce the current impacts of deposited nitrogen.

REFERENCES

- Smith, R.A. 1872. Air and Rain: The Beginnings of a Chemical Climatology. Longmans-Green, London. 600. pp.290-291
- Royal Ministry of Agriculture 1972: Sweden's case study for the United Nations conference on the human environment. (Air Pollution across national boundaries. The impact on the environment of sulfur in air and precipitation)
- Fowler, D., Cape, J.N., Leith, I.D., Paterson, I.S., Kinnaird, J.W. & Nicholson, I.A. 1982. Rainfall acidity in northern Britain. *Nature*, Lond. **297**, 383-386.
- Barrett C F, Atkins D H F, Cape J N, Fowler D, Irwin J G, Kallend A S, Marint A, Pitman J I, Scriven R A, Tuck A F 1983. Acid Deposition in the United Kingdom. pp50-51
- Battarbee, R.W., Flower, R.J., Stevenson, A.C., Jones, V.J., Harriman, R. & Appleby, P.G. 1988. Diatom and chemical evidence for reversibility of acidification in Scottish lochs. *Nature* 332, 530-2
- Sutton M.A., Tang Y.S. and Fowler D. 1998. Monitoring of atmospheric ammonia: first results. *ECN Newsletter*, **10**, 2-3.
- Fowler, D., Sutton, M.A., Flechard, C., Cape, J.N., Storeton-West, R., Coyle, M. & Smith, R.I. 2001. The control of SO₂ dry deposition on to natural surfaces and its effects on regional deposition. *Water Air Soil Pollution: Focus*, **1**, 39-48.
- Fowler, D., Muller, J., Smith, R.I. and Cape, J.N. 2005. Nonlinearities in source receptor relationships for sulfur and nitrogen compounds. *Ambio*, **34**, 41-46.

- Fowler, D., Muller, J., Smith, R.I., Cape, J.N., Erisman, J.W. 2005. Nonlinearities in source receptor relationships for sulphur and nitrogen compounds. *Ambio*, 34, 41-46.
- Fowler, D., Smith, R.I., Muller, J.B.A., Hayman, G., Vincent, K.J. 2005. Changes in the atmospheric deposition of acidifying compounds in the UK between 1986 and 2001. *Environmental Pollution*, 137, 15-25.
- Fowler, D., Smith, R.I., Muller, J., Cape, J.N., Sutton, M.A., Erisman, J.W., Fagerli, H. Long term trends in sulphur and nitrogen deposition in Europe and the cause of non-linearities. (Presented at Acid Rain Conference 2005 in Prague) *Water, Air, Soil Pollution Focus* (online first doi:10.1007/s11267-006-9102-x)
- Fowler, D., Smith, R., Muller, J., Cape, J.N., Sutton, M., Erisman, J.W., Fagerli, H. 2007. Long Term Trends in Sulphur and Nitrogen Deposition in Europe and the Cause of Non-Linearities. *Water Air Soil Pollut: Focus* (2007) 7:41-47

2. DRY DEPOSITION AND CLOUD DEPOSITION

2.1. Measurement of SO₂ dry deposition fluxes and model development

David Fowler, Mhairi Coyle, Robert Storeton-West, Jennifer Muller

AUCHENCORTH MOSS

Dry deposition measurements have continued to bring surprises, the ambient concentrations have declined from about 0.5ug m⁻³ in 1995 to current values close to 0.3ug m⁻³ and yet the deposition velocity continues to increase due to continued reduction in the canopy resistance (R_c). Over the monitoring period the canopy resistance has almost halved and is now about 70sm⁻¹. The consequence of the steady decline in the canopy resistance along with a decline in ambient concentration is that the flux remains nearly constant at about 2.9 ng m⁻²s⁻¹ (Table 1.1).

The measurements of the atmospheric terms (R_a and R_b) show that the trend is not caused by changes in turbulence, and thus the interpretation of cause in changes in the surface processing of the deposited SO₂ is secure.

The dry deposition measurements have proved very valuable in explaining the consistently larger decline in ambient SO₂ concentration than in emissions. In the absence of these flux measurements it would be a matter of speculation as to the underlying cause of the faster decline in ambient concentration than emission. Even with these measurements there remains the possibility that SO₂ oxidation rates have increased due to the growing oxidizing capacity of the atmosphere and have contributed to the relative changes in emission and deposition (non-linearity.)

It will be necessary in the further analysis and interpretation of the UK pollution climate data to carefully examine the relative importance of the different contributors to the observed trends in concentration and deposition and quantify the relative importance of changes in dry deposition and oxidation rates in the current trends. However, the observation of changes in deposition velocity from this work is now widely known and is being used by EMEP to explain growing discrepancies in the model-measurement comparisons over Europe. The work has also led to modifications of the EMEP code to simulate the temporal trends.

Table1.1 Annual statistics (median) of the dry deposition of SO₂ at Auchencorth Moss

	1995	1996	1997	1998	1999	2000	2001	2002	2003	2004	2005	2006
SO₂(1m) ug.m⁻³	0.55	0.73	0.52	0.35	0.45	0.39	0.38	0.36	0.53	0.34	0.66	0.42
Flux SO₂ ng m⁻² s⁻¹	-2.71	-3.27	-3.36	-2.72	-2.63	-2.95	-2.81	-3.17	-3.74	-1.85	-5.98	-2.65
v_d(1m) mm s⁻¹	4.92	4.51	6.42	7.69	5.80	7.55	7.48	8.83	7.10	5.42	9.00	6.37
R_a(1m) s m⁻¹	34.8	34.3	34.2	30.7	30.3	26.1	30.1	28.9	30.1	27.5	31.5	24.1
R_bSO₂ s m⁻¹	18.4	18.8	18.7	16.8	15.9	17.8	18.0	16.7	17.9	18.5	22.1	21.3
R_cSO₂ s m⁻¹	150.0	168.5	102.9	82.6	126.2	88.6	85.6	67.7	93.0	138.3	57.5	111.5

Auchencorth Moss

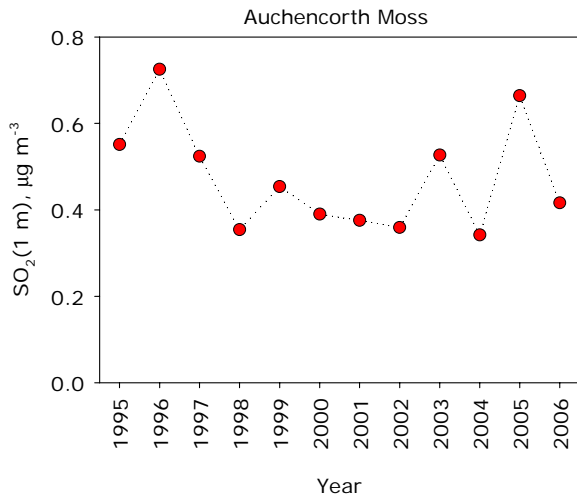


Figure 1.1. Concentrations of SO₂ at a height of 1 m above moorland in southern Scotland (Auchencorth Moss) 1995-2006

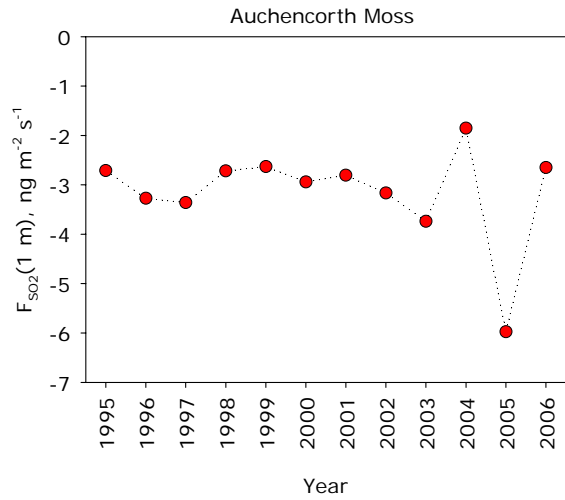


Figure 1.2. Dry deposition fluxes of SO₂ over moorland in southern Scotland (Auchencorth Moss) 1995-2006

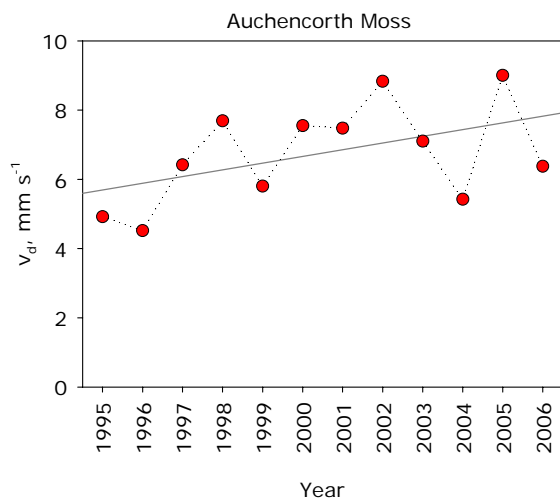


Figure 1.3. Dry deposition velocity of SO₂ over moorland in southern Scotland (Auchencorth Moss) 1995-2006

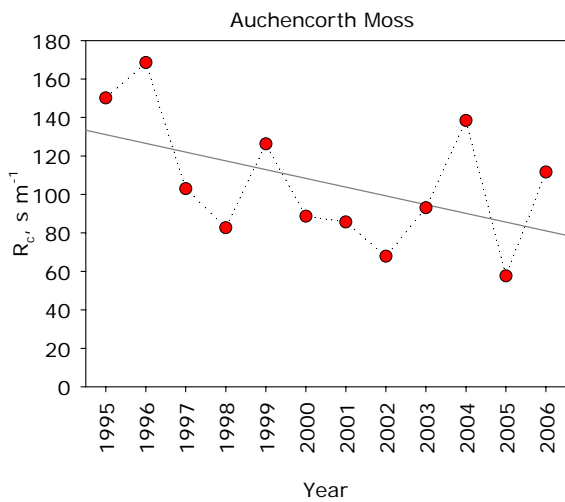


Figure 1.4. Canopy resistance to dry deposition of SO₂ over moorland in southern Scotland (Auchencorth Moss) 1995-2006

Sutton Bonnington

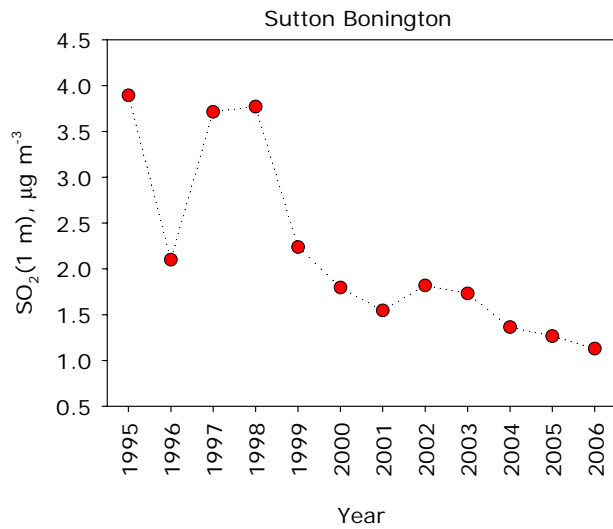


Figure 1.5. Concentrations of SO₂ at a height of 1m above arable cropland at Sutton Bonnington 1994-2006

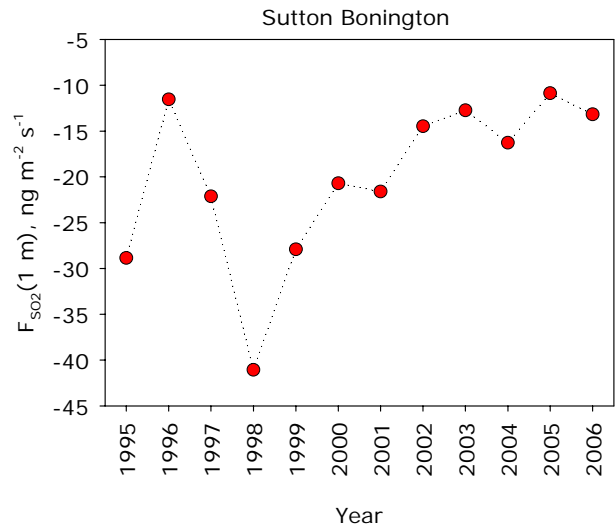


Figure 1.6. Dry deposition fluxes of SO₂ over arable land in the English Midlands (Sutton Bonnington) 1994 to 2006

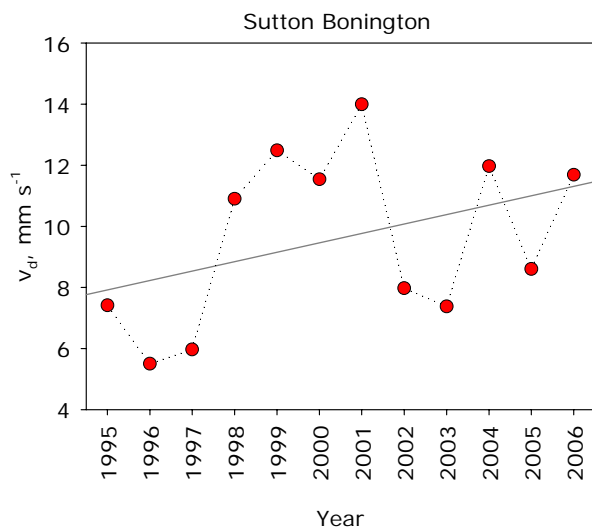


Figure 1.7. Dry deposition velocity of SO₂ over arable land in the English Midlands (Sutton Bonnington) 1994 to 2006

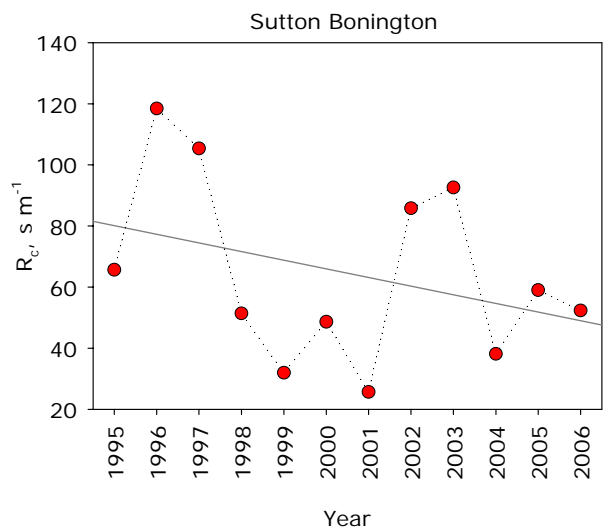


Figure 1.8. Canopy resistance to dry deposition of SO₂ over arable land in the English Midlands (Sutton Bonnington) 1994 to 2006

Eiko Nemitz, Rognvald Smith, Mark Sutton, Hilde Fagerli (EMEP/MSC-W), David Simpson (EMEP/MSC-W) and David Fowler

Current chemical transport models (CTMs) such as the EMEP model tended to reproduce SO₂ concentrations for 1990 well. However, following the reduction on SO₂ emissions since, the models now tend to overestimate SO₂ concentrations. Possible reasons include an overestimation of current emissions and a change in the SO₂ chemistry (e.g. through changes in the OH concentration). An alternative explanation, initially proposed by Fowler *et al.* (2005), suggests that the deposition rate of SO₂ has increased as the SO₂/NH₃ ratio has declined, resulting in an increase in the neutralisation potential for the deposited SO₂. For this reason, existing simultaneous measurements of SO₂ and NH₃ exchange were analysed further to derive parameterisations of stomatal compensation points and cuticular resistances, two important, but poorly understood, parameters controlling the net flux of NH₃ with ecosystems. For example, in collaboration with EMEP/MSC-W measurements of a measurement network operated under the EU LIFE project at three sites across Europe were used to investigate the effect of co-deposition on canopy resistances of NH₃ and SO₂. Figure 1.9a examines the effect of the concentration ratio SO₂/NH₃ of the previous hour on the canopy resistance (in this case of SO₂). The non-stomatal canopy resistance for SO₂ ($R_{ns}(\text{SO}_2)$) increases if the canopy was subjected to high concentrations of SO₂, compared with the concentration of NH₃. It should be noted that this graph combines data from two completely different semi-natural ecosystems: Auchencorth Moss, a moorland 20 km south of Edinburgh, and Speulder Bos a Dutch forest. While concentrations of both gases are larger in the Netherlands, the SO₂/NH₃ ratio is higher. The dependence of R_c on this ratio appears to be continuous across both ecosystems, within the measurement uncertainties.

This analysis will continue and lead to improved parameterisations of co-deposition for inclusion in the EMEP model of MSC-W. This response to SO₂/NH₃ was combined with the response of R_{ns} to relative humidity (fRH) to derive a combined parameterisation:

$$R_{ns}(\text{SO}_2) = 11.84 \text{ s m}^{-1} \times \exp\left(1.1 \times \frac{\text{SO}_2}{\text{NH}_3}\right) fRH^{-1.67} \quad (1)$$

which is shown in Fig. 1.9b, compared with measurements, separated into low and high RH conditions.

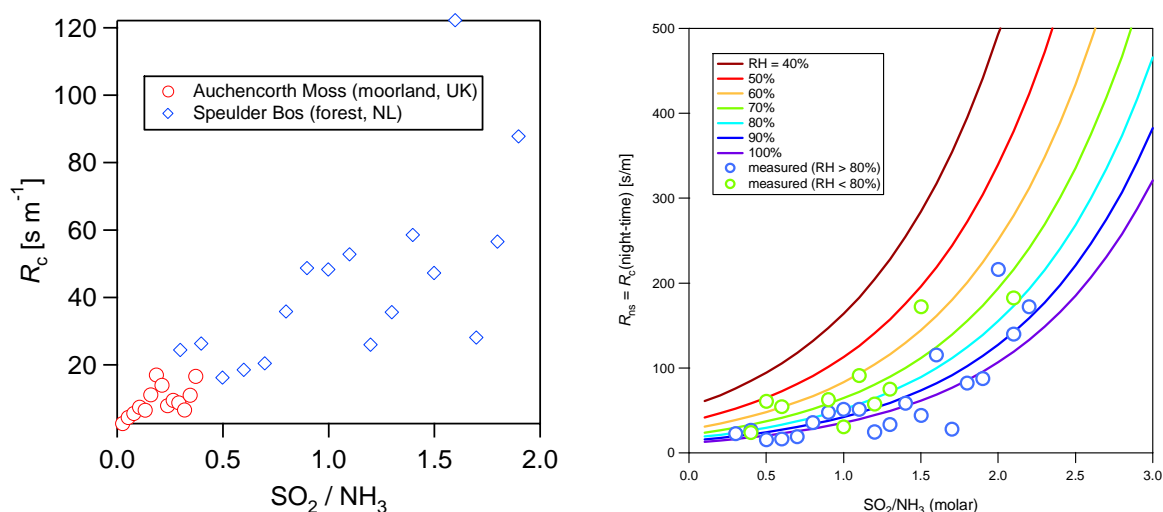


Figure 1.9. Dependence of the SO₂ canopy resistance on the ratio of the SO₂ and NH₃ air concentration of the previous 24 hours, combining data from two different field sites: (a) measurements and (b) parameterisation.

This parameterisation was provided to EMEP/MSC-W and incorporated into the EMEP Eulerian CTM. Figure 1.10 compares the time series of modelled and measured concentrations at four example EMEP stations across Europe, comparing observations (obs) with model results using the old (SO_2/NH_3 independent) and the new (SO_2/NH_3 dependent) description of the non-stomatal resistance, together with the annual average deposition velocity at the site.

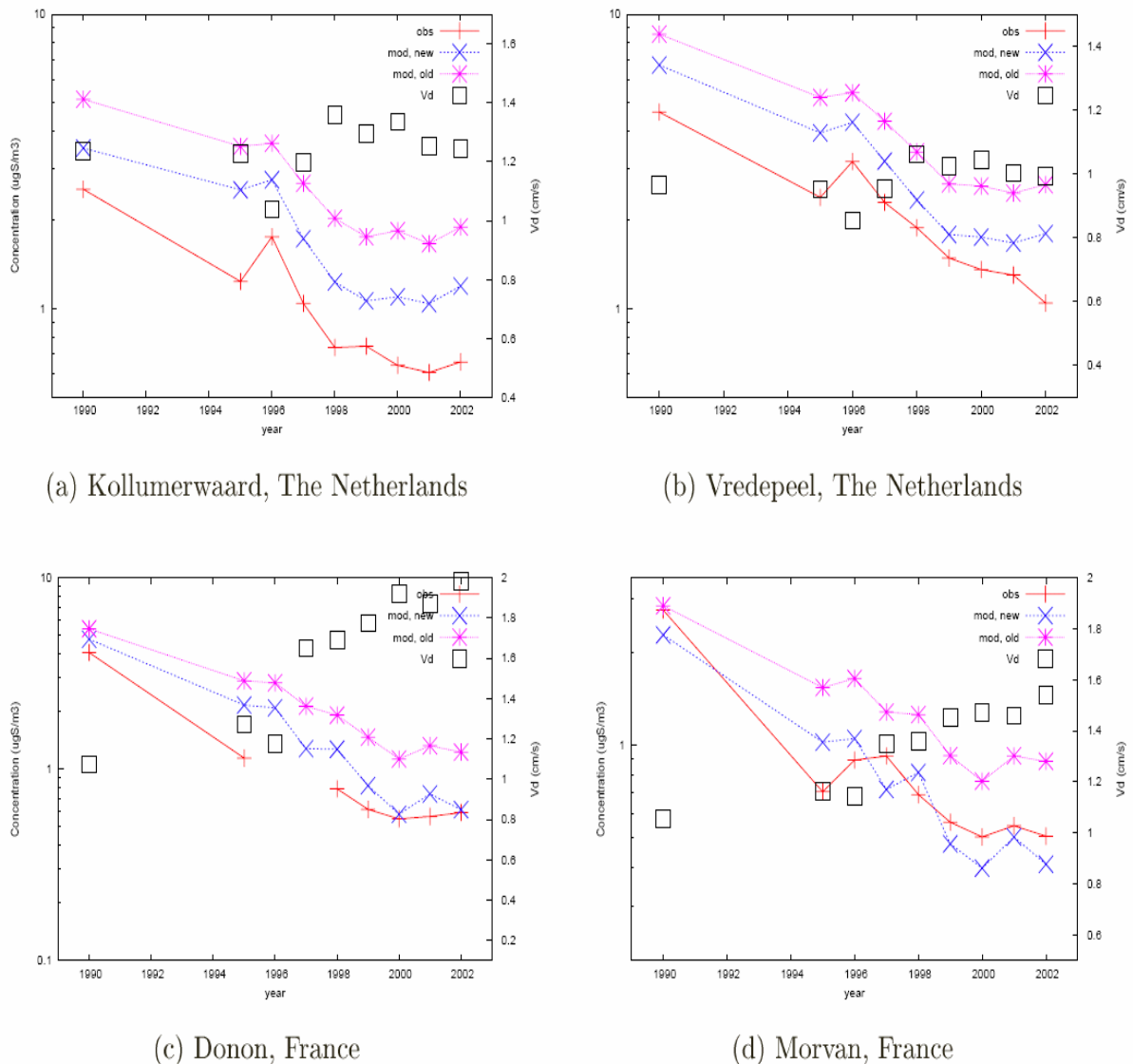


Figure 1.10. Results of the EMEP model, showing the effect of the new model parameterisation on the comparison between observed and modelled SO_2 concentrations at four measurement sites.

An attempt was also made to detect an effect of SO_2/NH_3 on $R_{\text{ns}}(\text{NH}_3)$ in the measurement data, but no clear relationship could be derived. This is possibly due to ammonia's higher solubility in water compared with SO_2 , which would lead to a stronger response to RH than to SO_2/NH_3 .

2.2. Rural Sulphur Dioxide Monitoring Network

Garry Hayman, Helen Lawrence, Keith Vincent (AEA Technology plc)

INTRODUCTION

Following the termination of the Rural Sulphur Dioxide Network in 2005, the following full report on the period 2001-2005 was produced:

Rural Sulphur Dioxide Monitoring in the UK: Data Summary 2001-2005

Report to Natural Environment Research Council - Centre for Ecology and Hydrology (Edinburgh) (Final Customer: Department for Environment, Food and Rural Affairs and the Devolved Administrations) ED48204 AEAT/ENV/R/2292 Issue 1. Date December 2006

This report is available from the UK Air Quality Archive web site as the pdf:

http://www.airquality.co.uk/archive/reports/cat04/0701151519_2001_2005_so2datareport_iss ue1.pdf

and the executive summary from the report is reproduced below.

EXECUTIVE SUMMARY

Sulphur deposition is known to have acidifying effects on freshwater, soils and vegetation. For these effects to be assessed the total sulphur deposition must be estimated from both its wet and dry deposition pathways. The Department for Environment, Food and Rural Affairs (Defra) has placed a contract with the Centre for Ecology and Hydrology at Edinburgh (CEH) on *Acid Deposition Processes in the UK* (EPG 1/3/166 and RMP 2125) to quantify *inter alia* the wet and dry deposition budgets of sulphur for the United Kingdom.

As part of this contract, AEA Technology manages and operates the UK Rural Sulphur Dioxide Monitoring Network. This network provides monthly- and annual averaged concentrations of sulphur dioxide (SO₂), which are subsequently used to produce concentration maps for the UK. The dry sulphur deposition across the UK is then derived by CEH by combining the sulphur dioxide concentration field with estimated deposition velocities.

The SO₂ concentrations measured at some of the sites in the UK Acid Deposition Monitoring and the UK Rural Sulphur Dioxide Monitoring networks during the late 1990's, especially the daily sites in remote areas, were at or below the Limit of Detection (LOD) of the bubbler method. This would make it more difficult to determine reliable trends and could compromise the application of the monitoring data, for example, in identifying the cause of the non-linear response of ambient concentrations to change in emissions at such sites. A method intercomparison exercise was undertaken in collaboration with CEH at the Auchincorth Moss site near Edinburgh between September 1998 and May 1999 to evaluate potential replacement methods which will provide a lower Limit of Detection while retaining data integrity and consistency. On the basis of this exercise, the choice of methods to replace the bubbler method was limited to the denuder or the filter-pack methods on the grounds of cost, improved sensitivity, method robustness, ease of operation and the quality of the measurements. The filter-pack method was preferred for practical reasons and the new samplers were introduced into the monitoring network between April and November 2001.

The Rural Sulphur Dioxide Monitoring programme was terminated at the end of 2005. The monitoring programme has been replaced by the SO₂ measurements made in the expanded denuder network operated by CEH as part of Defra's Acid Deposition Monitoring programme.

This report provides a complete dataset of the SO₂ measurements for all sites in the UK Acid Deposition and Rural Sulphur Dioxide Monitoring Networks for the years 2001 to 2005.

During the period covered by this report and as indicated above, the SO₂ sampler was changed from a H₂O₂ bubbler making daily/weekly measurements to a filter-pack sampler, making fortnightly measurements initially and four-weekly measurements from 2004. The introduction of the new sampler and the need to ensure coverage of the high emission area in Yorkshire led to some site changes.

The report also includes a comparison of the measurements made by the new filter-pack sampler with the previous H₂O₂ bubbler method. A comparison was also made with the measurements made in the Nitric Acid Denuder Network operated by CEH. This comparison allowed the following statements to be made:

- The three samplers generally showed the same qualitative behaviour with time
- The filter-pack and denuder measurements were in good agreement although the denuder measurements were slightly larger.
- Both the filter-pack and denuder measurements are lower than those of the bubbler. This is especially noticeable during the period from Spring 2002 when there was a significant discrepancy between the filter-pack and bubbler measurement.

To identify the cause of the lower filter-pack measurements, about 200 aerosol filters were retained and analysed between 2002 and 2005 from a number of the filter-pack monitoring sites. These measurements were then used to derive monthly sulphate and combined with the monthly sulphur dioxide concentrations to give total sulphur concentrations for comparison with the measurements made by the denuders and with the daily sulphate measurements. The results provided no clear evidence that the low sulphur dioxide measurements on the filter-pack sampler were a result of absorption by or loss onto the untreated filter used to remove particulate sulphate.

In terms of UK concentrations, there has been a significant decline in sulphur dioxide concentrations during this period, with the network mean concentration falling by a factor of 2 from 1.06 to 0.5 µg SO₂ as S m⁻³ between 2001 and 2005. This fall has continued the long-term decline in sulphur dioxide concentrations.

Maps of the annual and monthly mean sulphur dioxide (SO₂) concentration fields have been derived for the UK. The spatial distribution of SO₂ is similar to that observed in previous years with the highest concentrations in the Yorkshire/Nottinghamshire and Thames estuary areas. The recent measurements show that SO₂ concentrations have continued to decline in rural areas, a trend which has been observed since the establishment of the network in the early 1990s. The trend for sites closest to emission sources is consistent with the reduction in UK SO₂ emissions calculated over this period.

The measurement data have already been provided to CEH for interpretation and further analysis as part of its programme of work and to the Pollution Climate Mapping team at AEA Environment & Energy.

2.3. Measurement of NH₃ dry deposition rates and model development

Eiko Nemitz, Marsailidh Twigg, Daniela Famulari, Mark Sutton

CONTINUED DEVELOPMENT OF EDDY COVARIANCE SYSTEM FOR THE MEASUREMENTS OF SURFACE / ATMOSPHERE EXCHANGE FLUXES OF ATMOSPHERIC AMMONIA

The standard technique for the measurement of surface / atmosphere exchange fluxes of NH₃ is the gradient technique, in which fluxes are derived indirectly from measurements of the vertical concentration gradient at several heights above vegetation, using slow response chemical sensors, together with information on atmospheric turbulence. Fast response sensors, suitable for application to superior eddy-covariance flux measurements, which derive the flux more directly as the co-variance of the concentration with the vertical wind component, are still in their infancy. We have here used a dual tunable diode laser absorption spectrometer (TDL-AS; Aerodyne Research Inc.) to develop and test one of the first eddy-covariance flux systems for NH₃ (Famulari *et al.*, 2004). The instrument was characterised in the laboratory (Twigg, 2006). This work focussed on the characterisation of the TDL-AS system for ammonia and its response time with different inlet configurations and materials (e.g. Fig. 1.11).

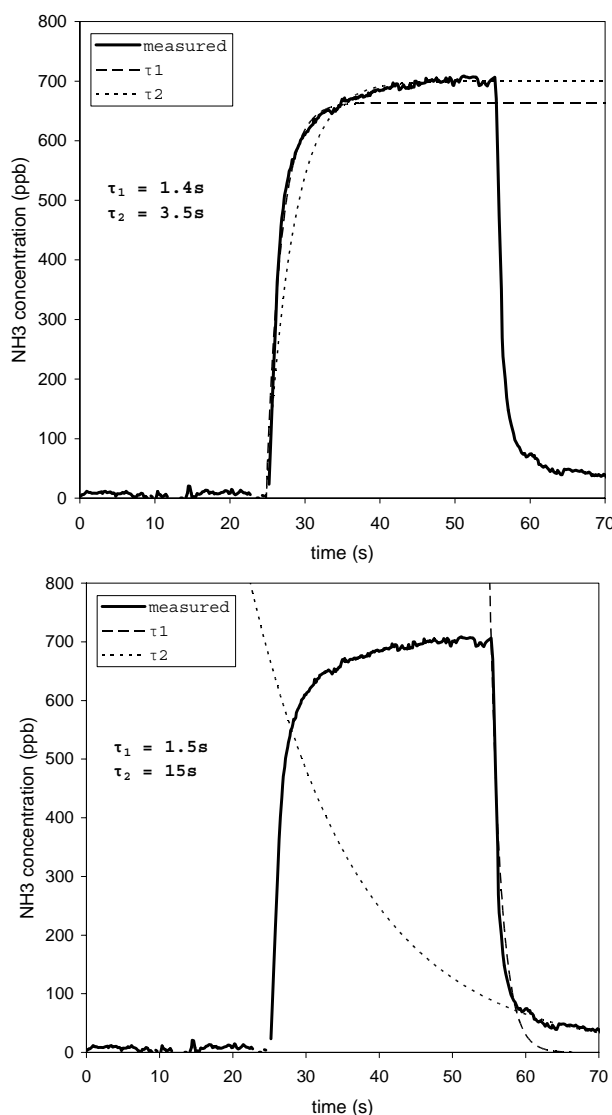


Figure 1.11. Response time measurements of TDL-AS system for changes from (a) low to high and (b) high to low concentration.

The instrument was then used in two intercomparison exercises at the Easter Bush agricultural grassland site near CEH Edinburgh, during periods of large fluxes following slurry applications which were arranged with the farm manager of this Edinburgh University farm for this purpose. During these measurements the TDL-AS was compared with a second eddy covariance system (quantum cascade laser absorption spectrometer or QCL-AS) operated by Manchester University and a more traditional AMANDA gradient system. Figures 1.12 & 1.13 show the comparison of the concentrations and fluxes measured with the two optical spectrometer systems (Whitehead *et al.*, 2007). The comparison is extremely encouraging, but the measurements were made after fertilisation when concentrations and fluxes were large. It is estimated that the TDL-AS eddy-covariance system is now able to resolve fluxes of $100 \text{ ng m}^{-2} \text{ s}^{-1}$, which is still much larger than that of the AMANDA gradient system ($5 \text{ ng m}^{-2} \text{ s}^{-1}$).

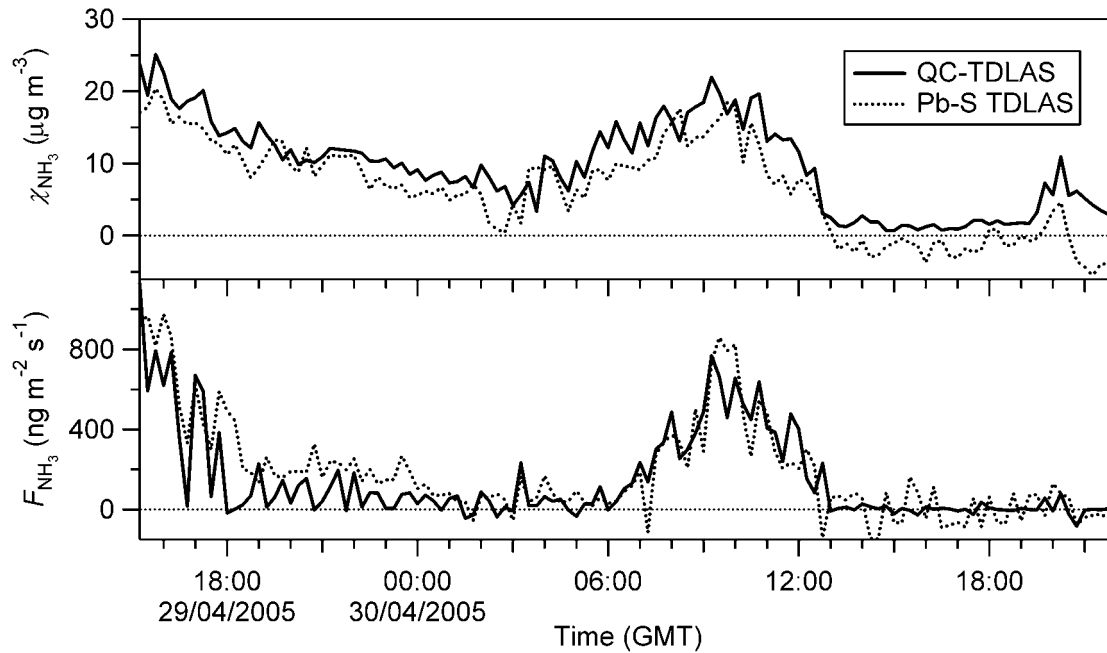


Figure 1.12. Time-series of NH_3 concentration and flux after slurry application during the second Easter Bush experiment, comparing the QCL laser system (QC-TDLAS) and the lead-salt (Pb-S) TDL.

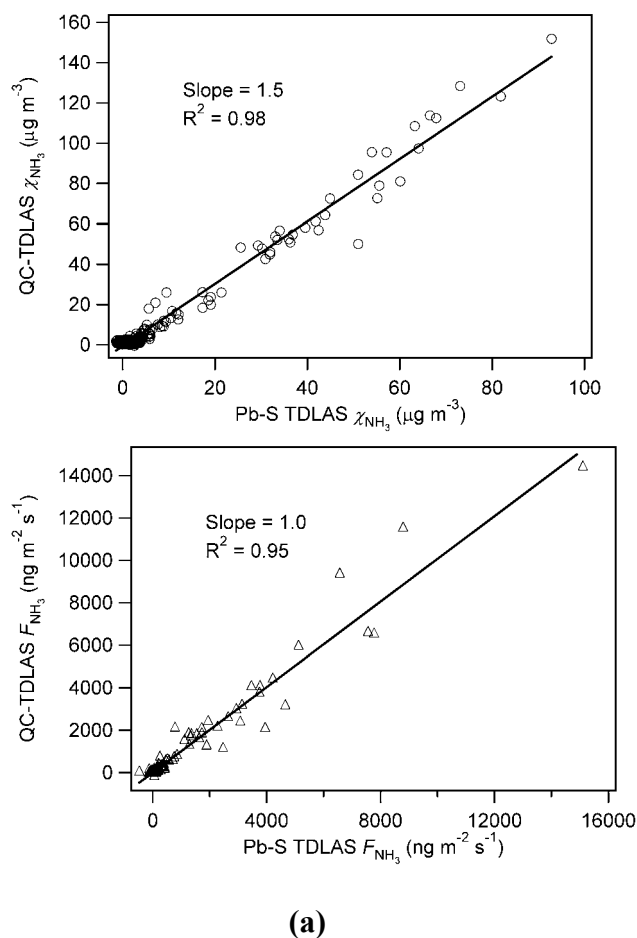


Figure 1.13. Scatter plots showing correlations of: (a) NH_3 concentration and (b) flux between the two TDLAS instruments during the first Easter Bush experiment.

QUANTIFICATION OF NH_3 EXCHANGE

Measurements of surface / atmosphere exchange fluxes of ammonia were made at the Easter Bush field site during more than 120 days, covering the periods 14-Sep to 06-Oct 2004, 28-Mar to 12-May 2005 and 2-Oct to 27-Nov 2006, with application of cattle slurry around 28-Sep 2004 and 28-Apr 2005. The summaries of the concentrations and fluxes measured prior, during and after fertilisation events are presented in Tables 1.2 to 1.5 (Twigg, 2006).

Table 1.2 Summary of the mean NH₃ concentrations at 1 m during the 2004 Easter Bush campaign.

Period	μ_A ($\mu\text{g m}^{-3}$)	σ_A ($\mu\text{g m}^{-3}$)	μ_M ($\mu\text{g m}^{-3}$)	χ_{\min} ($\mu\text{g m}^{-3}$)	χ_{\max} ($\mu\text{g m}^{-3}$)	Data Coverage (%)
Pre-fertilization: 25/09/04 - 28/09/04	1.73	0.66	1.55	0.83	6.05	52.9
During fertilization: 28/09/04 - 30/09/04	17.7	31.5	1.32	0.05	168	93.3
Post fertilization: 30/09/05-05/10/05	1.81	1.54	2.03	0.03	12.1	94.1

Note: No filtering was applied to the data presented. Pre-fertilization: data using the QC-TDLAS and gap-filled with AMANDA data. Fertilization and Post fertilization: Dual TDLAS values unless gap filled with QC-TDLAS and AMANDA data to replace missing values. μ_A - arithmetic mean; σ_A - standard deviation; μ_M - Median.

Table 1.3 Summary of the mean NH₃ concentrations at 1 m during the 2005 Easter Bush campaign.

Period	μ_A ($\mu\text{g m}^{-3}$)	σ_A ($\mu\text{g m}^{-3}$)	μ_M ($\mu\text{g m}^{-3}$)	χ_{\min} ($\mu\text{g m}^{-3}$)	χ_{\max} ($\mu\text{g m}^{-3}$)	Data Coverage (%)
Pre-fertilization: 25/04/05 - 27/04/05	1.98	1.09	1.69	0.60	5.08	63.4
During fertilization: 27/04/05-30/04/05	102.4	152	43.6	0.11	767	98.6
Post fertilization: 30/04/05-06/05/05	5.35	4.37	4.27	0.22	23.7	59.5

Note: No filtering was applied to the data presented. Pre-fertilization: data using the QC-TDLAS data. Fertilization and Post fertilization: Based on dual TDLAS values unless gap filled with QC-TDLAS, with the exception of the 27/04-29/04 which QC-TDLAS data. μ_A - arithmetic mean; σ_A - standard deviation; μ_M - Median.

Table 1.4. Summary of the mean NH₃ fluxes during the 2004 Easter Bush campaign.

Period	μ_A (ng m ⁻² s ⁻¹)	σ_A (ng m ⁻² s ⁻¹)	μ_M (ng m ⁻² s ⁻¹)	χ_{min} (ng m ⁻² s ⁻¹)	χ_{max} (ng m ⁻² s ⁻¹)	Data Coverage (%)
Pre-fertilization: Gap filled and filtered	-3.05	47.2	3.51	-437	100	92.0
During fertilization: General treatment of data and gap filled	680	1827	39.3	-473	15105	99.5
Gap filled and filtered	853	2088	40.6	-132	15105	72.8
Post fertilization: filtered and gap filled data	9.09	11.9	8.14	86.5	-27.2	83.9

Note: All flux values presented are from the dual TDLAS unless gap filled which contains QC-TDLAS or AMANDA data to replace missing values. Gap filling and filtered is dual TDLAS filtered with instrumentation and meteorological filters. QC-TDLAS and AMANDA gap filling was only done under suitable meteorological conditions. Pre-fertilization: 25/09/04 - 28/09/04, During fertilization: 28/09/04 - 30/09/04, Post fertilization: 30/09/05-05/10/05. μ_A - arithmetic mean; σ_A - standard deviation; μ_M - Median.

Table 1.5. Summary of the mean NH₃ fluxes during the 2005 Easter Bush campaign.

Period	μ_A (ng m ⁻² s ⁻¹)	σ_A (ng m ⁻² s ⁻¹)	μ_M (ng m ⁻² s ⁻¹)	χ_{min} (ng m ⁻² s ⁻¹)	χ_{max} (ng m ⁻² s ⁻¹)	Data Coverage (%)
Pre-fertilization: Gap filled	1.23	13.9	2.41	-64.4	42.4	100
During fertilization: General treatment of data and gap filled	5504	10317	1108	-667	58918	100
Gap filled and filtered	5542	10027	1190	-590	49906	69
Post fertilization: Gap filled and filtered	138	249	128	-285	2437	38

Note: All flux values presented are from the dual TDLAS unless gap filled which contains QC-TDLAS data to replace missing values. Gap filling and filtered is dual TDLAS filtered with instrumentation and meteorological filters. QC-TDLAS gap filling was only performed under suitable meteorological conditions. Pre-fertilization: 25/04/05 - 27/04/05 (QC-TDLAS data only), During fertilization: 27/04/05-30/04/05 (Combination data), Post fertilization: 30/04/05-06/05/05(QC-TDLAS data only). μ_A - arithmetic mean; σ_A - standard deviation; μ_M - Median.

2.4. Measurement of aerosol dry deposition rates

Eiko Nemitz, Gavin Phillips and Rick Thomas

BACKGROUND

First estimates of the contribution of aerosol dry deposition to the UK deposition of N and S were presented in the final report of the previous Acid Deposition Processes project (EGP/1/3/166), suggesting country aerosol dry deposition totals of 16.7 kt $\text{NH}_4^+\text{-N}$, 12.9 kt $\text{NO}_3^-\text{-N}$ and 11.1 kt SO_4^{2-} . A large fraction of this deposition was estimated to occur to aerodynamically rough surfaces, i.e. forest. For this initial assessment, dry deposition rates were calculated by combining typical size distributions of these aerosol compounds with size-dependent deposition rates from very few measurements, and these were multiplied with the aerosol concentration fields derived from the UK Nitric Acid Network. New instrumentation now allows dry deposition of these aerosol compounds to be measured directly using micrometeorological techniques. For forest, the old parameterisation used in the initial dry deposition mapping was taken from measurements over a rather mature, 30 m tall Douglas Fir stand in the Netherlands, which is likely to take up particles at a faster rate than average UK forests. In addition, there is the potential of the Dutch measurements being affected by chemical processes, such as NH_4NO_3 aerosol evaporation near the canopy, which can be shown to lead to erroneous fluxes (Nemitz and Sutton, 2004). By contrast, grassland is one of the dominating land cover types in the UK. Hence, new aerosol measurements focussed on grassland and forest.

MEASUREMENTS OVER GRASSLAND

The Aerodyne AMS (Aerosol Mass Spectrometer) and the ECN GRAEGOR (Gradient of Reactive Aerosols and Gases with Online Registration) were installed at the CEH Easter Bush grassland site in Southern Scotland. The early AMS results (Table 1.6) indicate deposition velocities for sulphate of around 0.9 mm s^{-1} , consistent with former aerosol number flux measurements above a Scottish moorland (Nemitz *et al.*, 2001). By contrast, there is indication of net nitrate emission over this agricultural surface, possibly representing aerosol formation above the grassland, as a result of combined emission of NH_3 and HNO_3 . Ammonium, which would be expected to be partly associated with sulphate and partly with nitrate, shows an intermediate net deposition velocity.

Table 1.6. Summary of initial results of flux measurements of aerosol ammonium, nitrate and sulphate at the Easter Bush grassland site.

	Ammonium (m/z 16)	Nitrate (m/z 30)	Nitrate (m/z 46)	Sulphate (m/z 48)	Sulphate (m/z 64)
Median concentration ($\mu\text{g}/\text{m}^2$)	10.1	3.0	2.6	2.4	2.6
Median Flux ($\text{ng m}^{-3} \text{ s}^{-1}$)	-3.5	2.15	0.00	-0.75	-1.4
Median V_d (mm s^{-1})	0.32	-1.43	-0.20	0.64	1.1

The results of the GRAEGOR gradient measurements over grassland were modified by chemistry following slurry application, as presented in more detail below (cf Fig. 1.59). However, during periods of deposition, NO_3^- , SO_4^{2-} and Cl^- were deposited with average deposition velocities of 1.27, 1.70 and 1.43 mm s^{-1} , respectively.

MEASUREMENTS OVER CONIFEROUS FOREST

First forest measurements were made with the Aerosol Mass Spectrometer eddy-covariance system at a Loblolly Pine plantation at Duke Forest, North Carolina. Here sulphate showed a bi-directional behaviour. By contrast nitrate was continuously being deposited at a deposition velocity that increased linearly with the friction velocity (u_*), a measure of turbulence or the speed at which momentum is transferred to the canopy. Values ranged from 2 to 6 mm s^{-1} (Fig. 1.14) and are about a factor of three lower than deposition rates applied in the initial deposition modelling for the UK. While the old parameterisations were derived from particle number flux measurements over a mature, 30 m tall, Douglas fir stand, the new measurements were made above an 18 m tall canopy, possibly more representative of UK plantations.

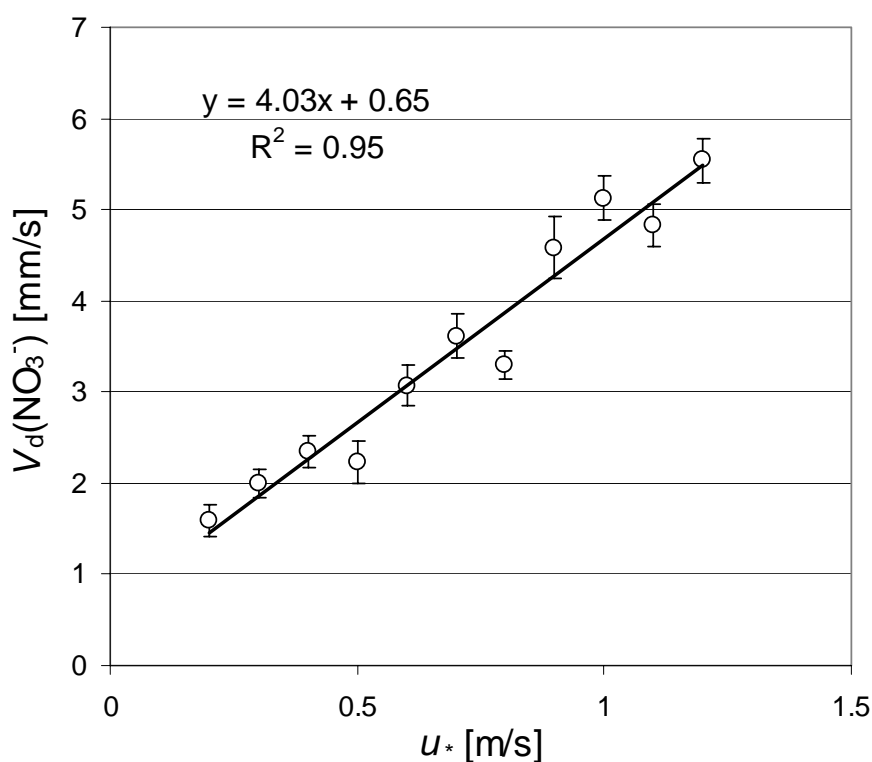


Figure 1.14. Results of the first eddy-covariance measurements of NO_3^- aerosol fluxes above forest.

MEASUREMENTS OF AEROSOL DEPOSITION RATES TO DECIDUOUS OAK FOREST

Measurements of aerosol fluxes were made during the period 27-Jul to 18-Aug 2005 at the oak forest at the Forest Research station at Alice Holt. This initiative included speciated aerosol measurements of NO_3^- , SO_4^{2-} and organic aerosols by AMS and total particle number fluxes by condensation particle counter (CPC). At the same time emissions of volatile organic compounds (VOCs), primarily isoprene and its oxidation products methyl vinyl ketone (MVK) and methacrolein (MACR), were measured with a proton transfer reaction mass spectrometer (ptr-ms) to investigate the potential of primary emissions on aerosol formation and hence its effect on the aerosol fluxes.

The time series of the concentrations (χ_N), fluxes (F_χ) and deposition velocities ($V_d = -F_\chi/\chi$) are shown in Fig. 1.15. Wind speed during this campaign was rather low (typically 0.5 to 4 m s⁻¹), which may have led to reduced fluxes. While the majority of the fluxes shows deposition, with a diurnal pattern in V_d , emission fluxes occur during a substantial part of the time. On average, there is a dependence of V_d on u^* (Fig. 1.16a). The remaining variability can be partially explained with effects of atmospheric stability. Fig. 1.16b shows the relationship of the u^* -normalised deposition velocity (V_d/u^*) on the stability parameter ($1/L$, where L is the Monin-Obukhov length). The results show the expected theoretical behaviour, with a constant value during stable conditions ($1/L > 0$) and an increase for increasingly unstable conditions.

The time series of the aerosol composition of non-refractory PM₁ aerosol as measured with the AMS is shown in Fig. 1.17. There was a consistent elevated background concentration of SO₄²⁻, with episodic higher concentrations, due to long range transport. Nitrate (NO₃⁻) shows a diurnal pattern, with increasing concentrations over night. This is consistent with the temperature dependence of the NH₄NO₃ equilibrium and also with NO₃⁻ formation via nighttime N₂O₅ chemistry, together with dilution in the morning when the boundary layer grows. The overall level of NO₃⁻ differs between days, probably linked to the air mass history.

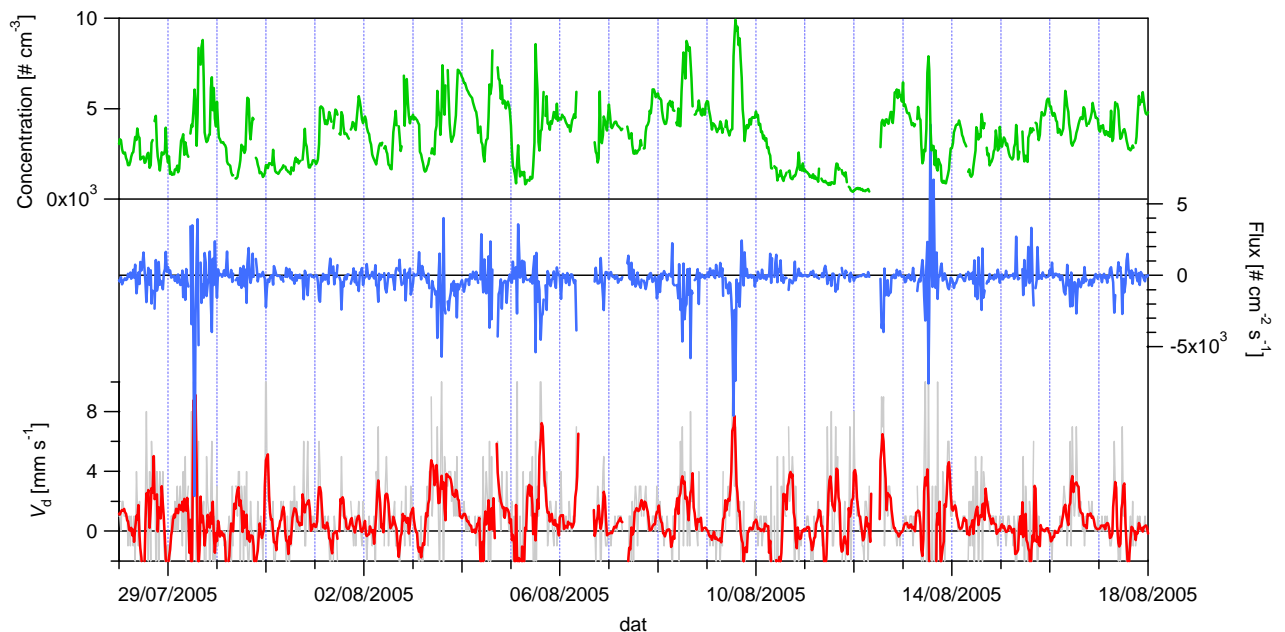


Figure 1.15. Results of total particle number measurements (concentrations, fluxes and deposition velocities, V_d) above the Alice Holt oak forest.

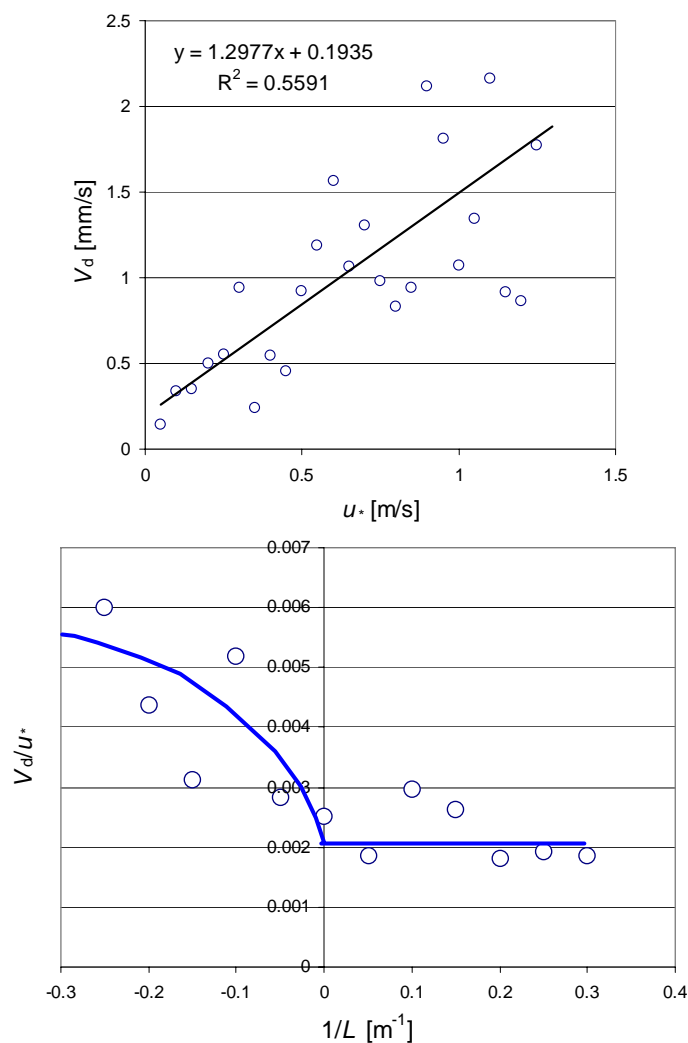


Figure 1.16. Parametrisation of total number aerosol deposition velocity to the Alice Holt oak forest.

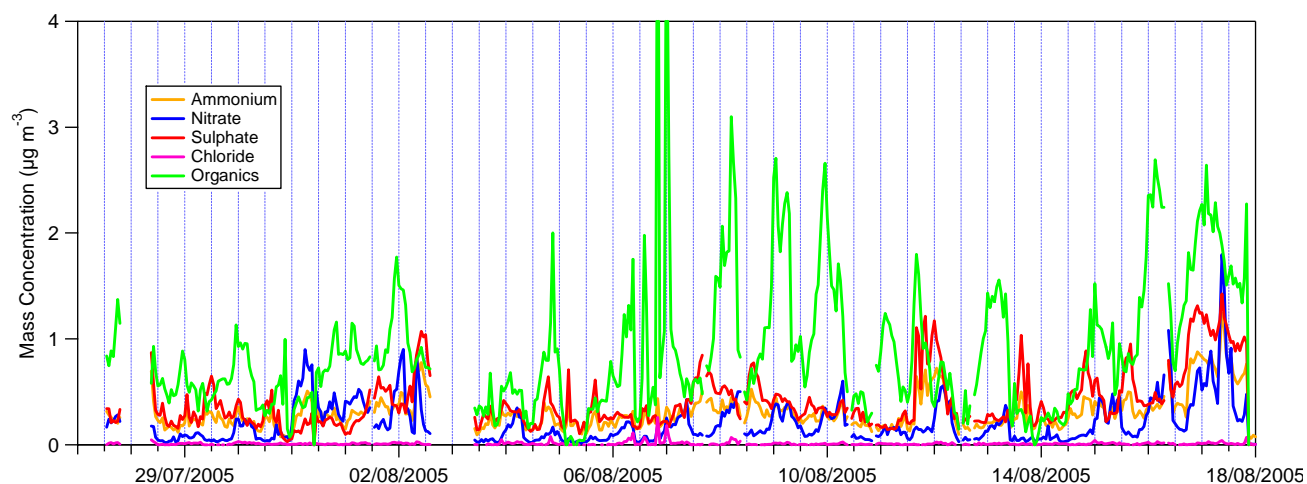


Figure 1.17. Time series of aerosol composition over Alice Holt oak forest as measured with the Aerosol Mass Spectrometer (AMS).

Interestingly, the organic aerosol concentration shows a clear diurnal cycle with night-time maxima, which is particularly pronounced from 8-Aug. This cycling appears to be synchronised with the variability in NO_3^- concentration. It is currently unclear whether this

nocturnal increase is purely the result of anthropogenic emissions, such as (a) the accumulation of combustion derived primary organic aerosol in the contracting nocturnal boundary layer or (b) the increased condensation of anthropogenic precursors at cooler, more humid night-time conditions. Alternatively, the low nocturnal wind speed could have supported the accumulation of biogenically derived secondary organic aerosol (BSOA) in and above the forest.

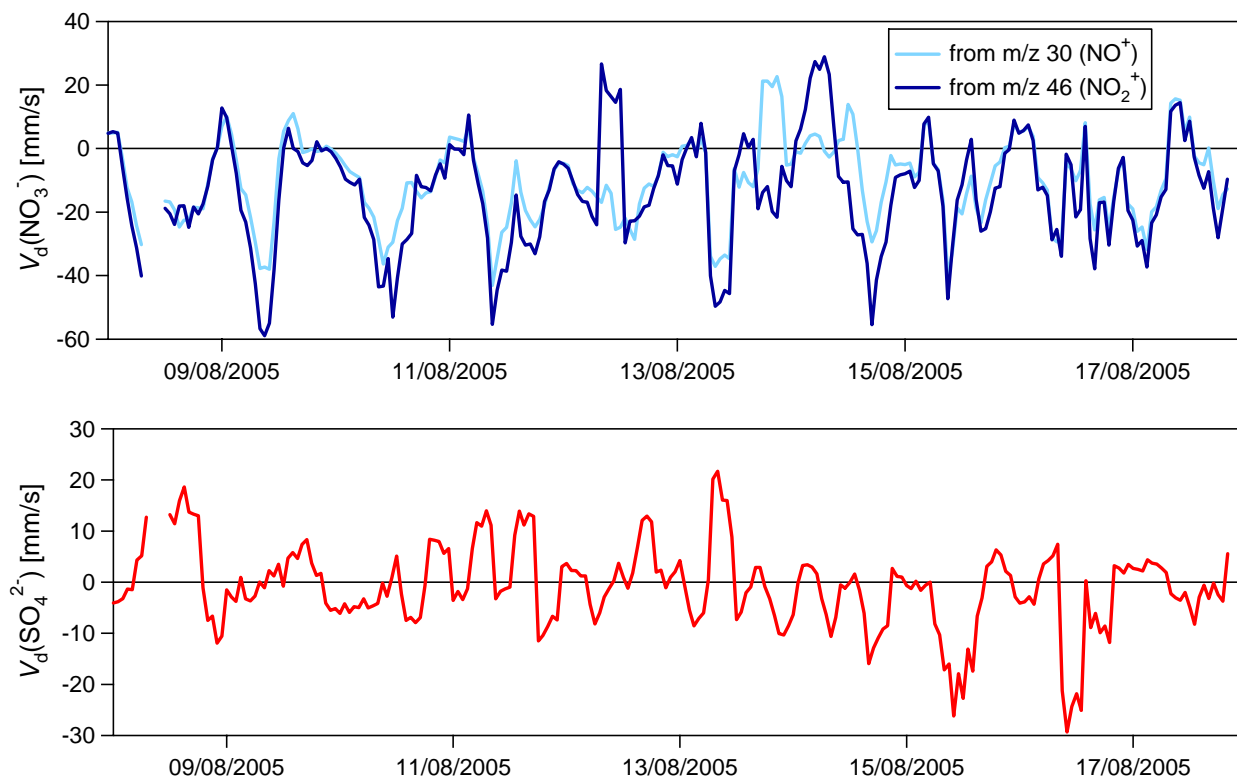


Figure 1.18. Deposition velocities of aerosol nitrate and sulphate measured at Alice Holt oak forest using the Aerosol Mass Spectrometer (AMS).

The compound specific aerosol fluxes were meant to derive compound specific deposition velocities of NO_3^- and SO_4^{2-} . However, the fluxes of NO_3^- show clear diurnal patterns of negative deposition velocities (apparent emission) (Fig. 1.18a), which would indicate production of NO_3^- in or above the canopy and still needs to be understood more fully. The two estimates of the NO_3^- flux are derived from two different fragment ions (NO^+ and NO_2^+). Since only one ion is monitored at a time, the fluxes correspond to different particle populations and are thus (semi-) independent. Thus the good agreement between the two estimates supports that the fluxes are robust (or affected by a common, yet unidentified error). The V_d of SO_4^{2-} was smaller and more variable, with positive and negative values, which did not follow a diurnal cycle and thus probably represent scatter. However, on 8 and 9 August a positive V_d was measured, while on 15 and 15 August negative V_d was derived.

Fluxes of biogenic isoprene emissions and their first generation oxidation products methyl vinyl ketone (MVK) and methacrolein (MACR) are presented in Fig. 1.19. The role of isoprene as a potential precursor for biogenic secondary aerosol (BSOA) formation is currently controversially discussed in the literature. From the comparison between the time series of the organic aerosol loading (Fig. 1.17) and the isoprene emission (Fig. 1.19) it is apparent that organic concentrations were particularly large on days with high isoprene emissions. However, it is currently uncertain that isoprene indeed acts as an aerosol precursor. Alternatively, both measurements may be responding to a third variable, such as temperature or solar radiation.

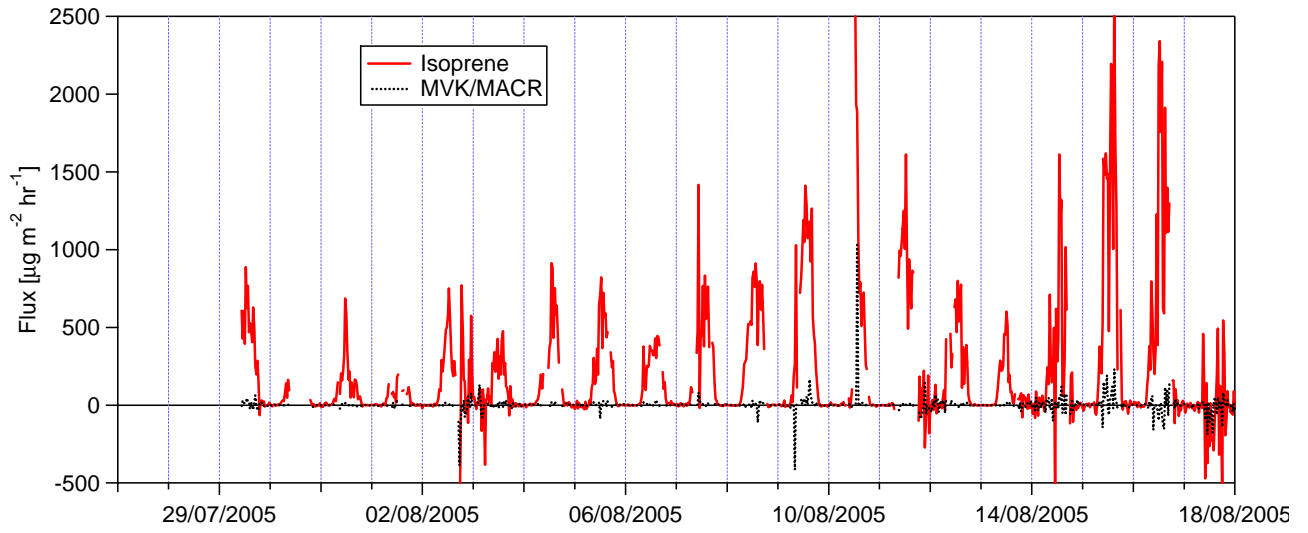


Figure 1.19. Fluxes of volatile organic compounds measured at Alice Holt.

2.5. UK 5km dry deposition maps

Rognvald Smith

MODELLING DRY DEPOSITION OF GASES AND AEROSOLS ACROSS THE UK

Dry deposition is the direct removal of the pollutant gas to vegetation, soils or other surfaces. In the simple cases, the estimate of dry deposition is the product of the air concentration and a deposition velocity.

Dry deposition maps for the UK of sulphur dioxide (SO₂), ammonia (NH₃), nitrogen dioxide (NO₂) and nitric acid (HNO₃) are given in Figures 1.2 (a-c).

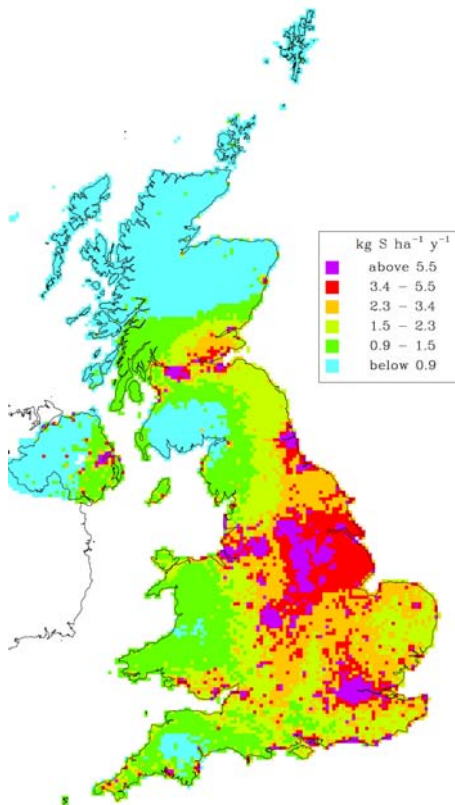
Air concentrations of pollutants are mapped from observational data collected through the year at rural sites in the UK monitoring networks. The initial concentration maps are produced by interpolation between the monitoring sites, usually by a technique called kriging. For some of the gases (SO₂, NO₂ and NH₃), there is extra information on local variability which is added to the interpolated map to increase the concentration close to known sources of the gas. For SO₂ the sources are associated with urban areas, for NO₂ the major extra component is from road traffic and for NH₃ the pattern of high and low concentrations is associated with the agricultural activity within the landscape.

The dry deposition model simulates the transport of gas molecules from the atmosphere directly onto a surface, such as the soil surface or a leaf surface, or into plants through stomatal uptake. A number of processes control this exchange, and rates of deposition are dependent on both the turbulence of the atmosphere and the properties of the surface. For SO₂, for example, the current model requires hourly meteorological data on the wind speed, solar radiation, temperature, and vapour pressure deficit (ideally at 1m to 3m above the canopy surface) as well as vegetation data on canopy height and surface roughness, rates of molecular diffusion close to the vegetation surfaces, parameters to control stomatal opening for the particular species of plant, and the stage of plant development within the growing season including its current leaf area index. The model for NO₂ is similar to that for SO₂, although the uptake is purely through stomata and not onto leaf surfaces. NH₃ is modelled with bi-directional exchange, in other words allowing the possibility of emission of NH₃ from plants as well as deposition to plants for arable and grassland landuse. HNO₃ is deposited to vegetation on the assumption that there is no canopy resistance, so it depends only on the wind speed and the surface roughness of the vegetation. Further details of these models can be found in Smith et al, 2000.

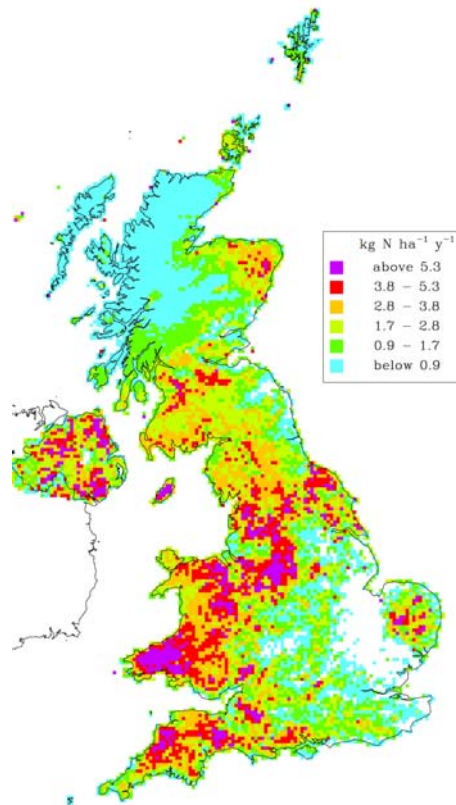
Dry deposition maps for the UK of aerosol sulphate (SO₄²⁻), ammonium (NH₄⁺-N), and nitrate (NO₃⁻-N) are given in Figures 1.3 (a-c), along with dry deposition of non-seasalt calcium (Ca). This estimate of aerosol deposition is a product of concentration, friction velocity (derived from a 30-year average wind field, and so does not yet reflect inter-year variability in wind pattern) and an alpha factor relating to vegetation type and aerosol size. The alpha factors will be revised as more data become available. To maintain consistency over the previous period, base cation deposition (Ca²⁺ and Mg²⁺) is derived from the rain ion concentration maps assuming a wet scavenging ratio of 700 to define an aerosol concentration field and then applying landuse dependent deposition velocities.

Reference

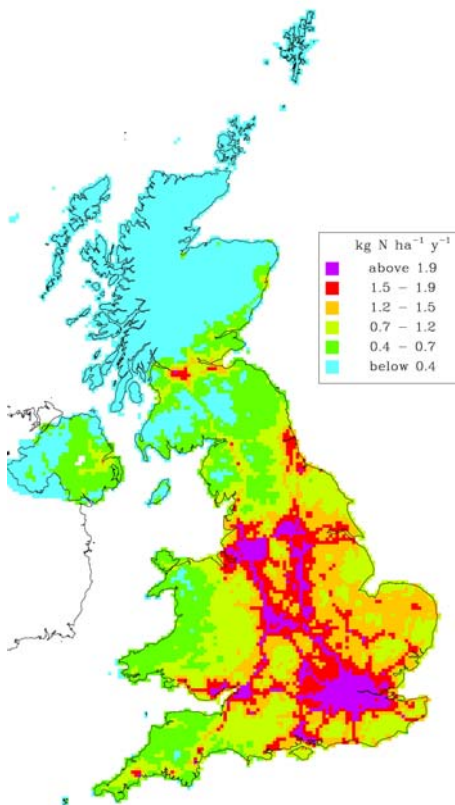
Smith, R.I., Fowler, D., Sutton, M.A., Flechard, C.R. and Coyle, M. 2000. Regional estimation of pollutant gas dry deposition in the UK: model description, sensitivity analyses and outputs. *Atmospheric Environment*, **34**, 3757-3777.



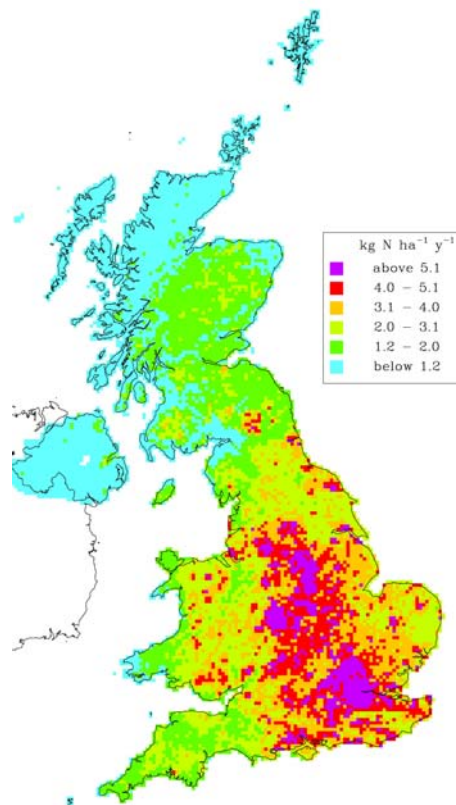
Dry deposition, Sulphur Dioxide, 2002



Dry deposition, Ammonia, 2002

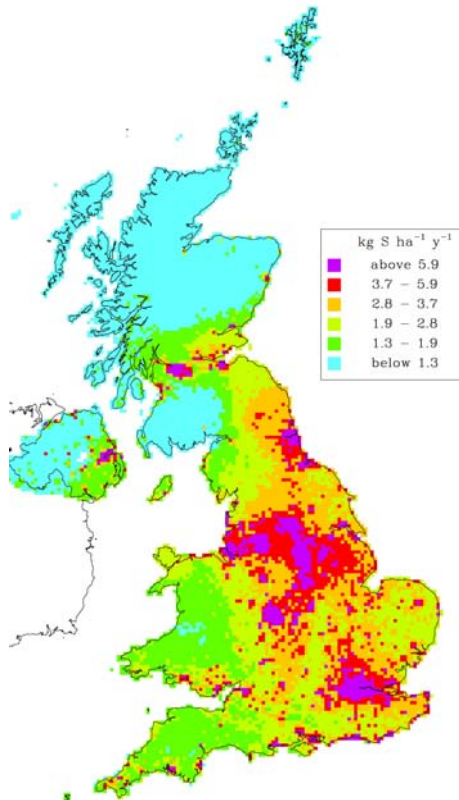


Dry deposition, Nitrogen Dioxide, 2002

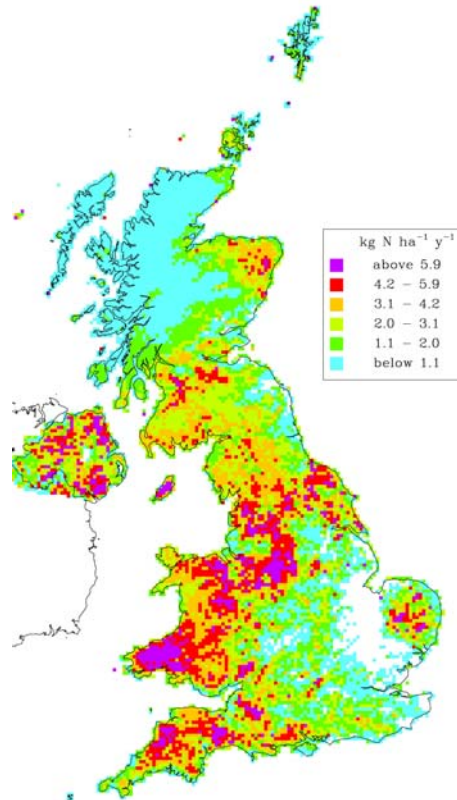


Dry deposition, Nitric Acid, 2002

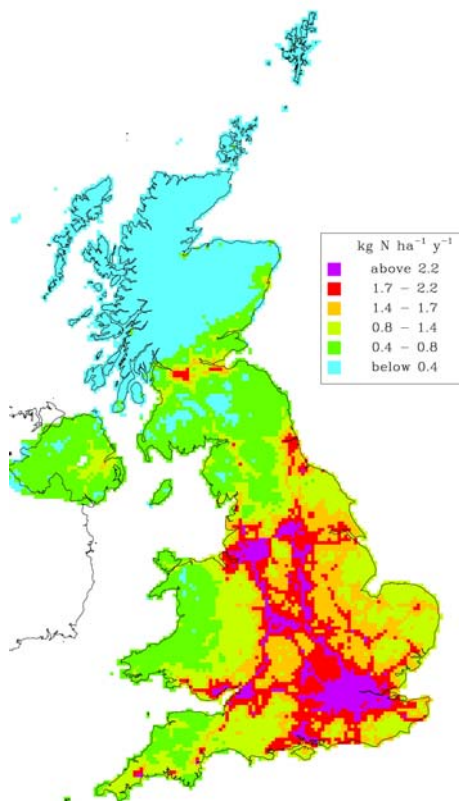
Fig 1.20(a) Maps of dry deposition of sulphur and nitrogen for 2002.



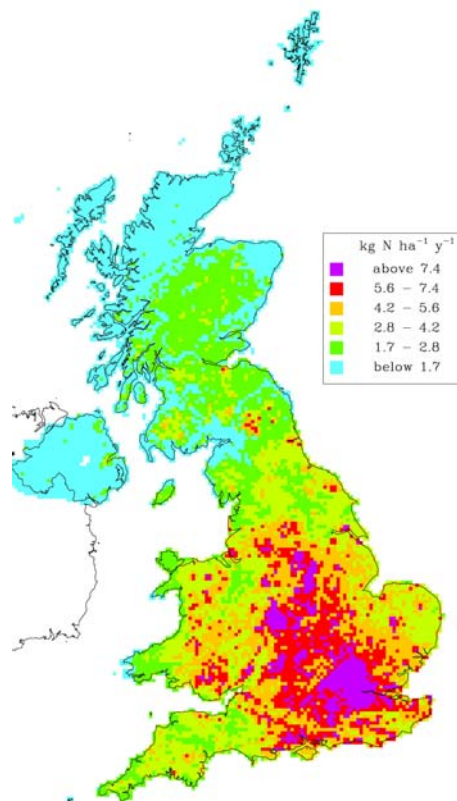
Dry deposition, Sulphur Dioxide, 2003



Dry deposition, Ammonia, 2003

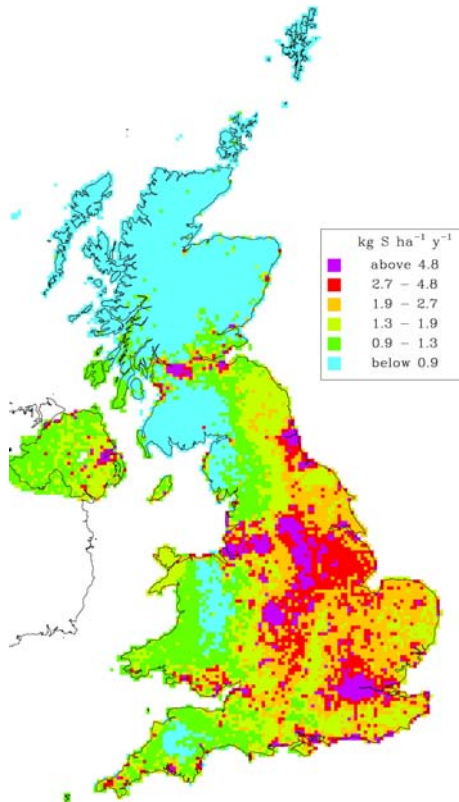


Dry deposition, Nitrogen Dioxide, 2003

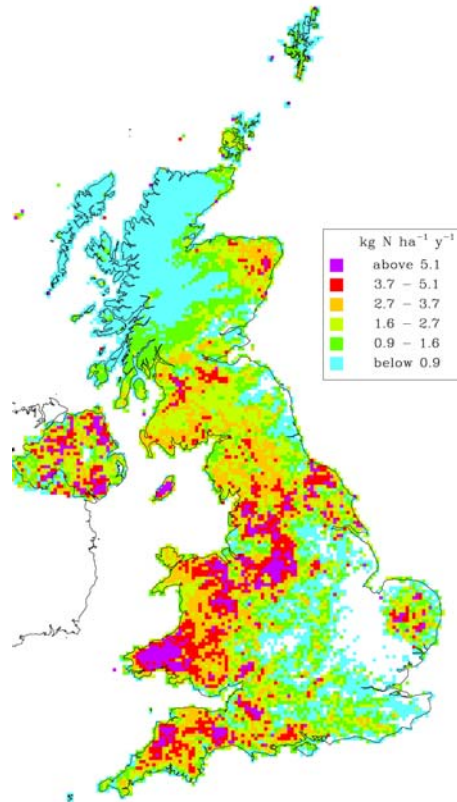


Dry deposition, Nitric Acid, 2003

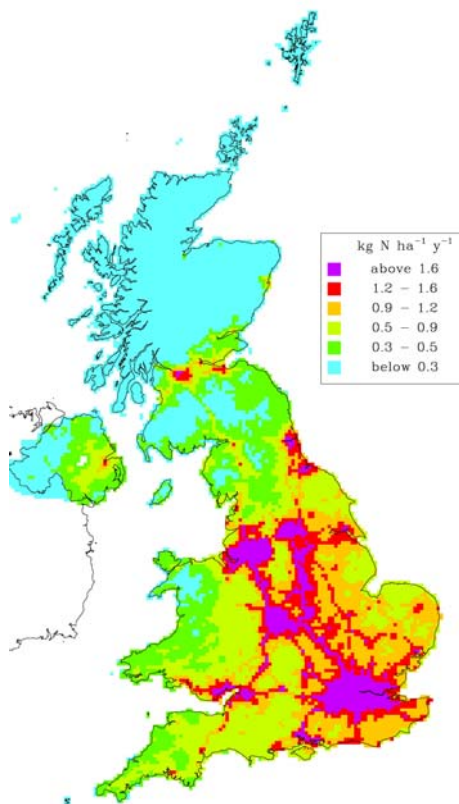
Fig 1.20(b) Maps of dry deposition of sulphur and nitrogen for 2003.



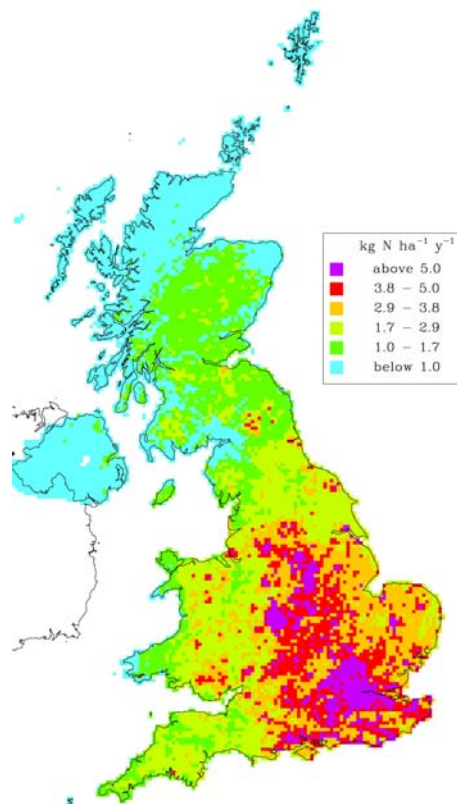
Dry deposition, Sulphur Dioxide, 2004



Dry deposition, Ammonia, 2004

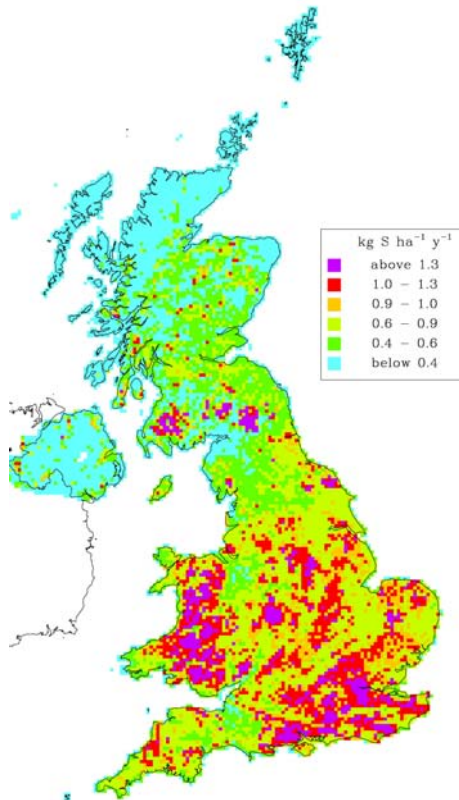


Dry deposition, Nitrogen Dioxide, 2004

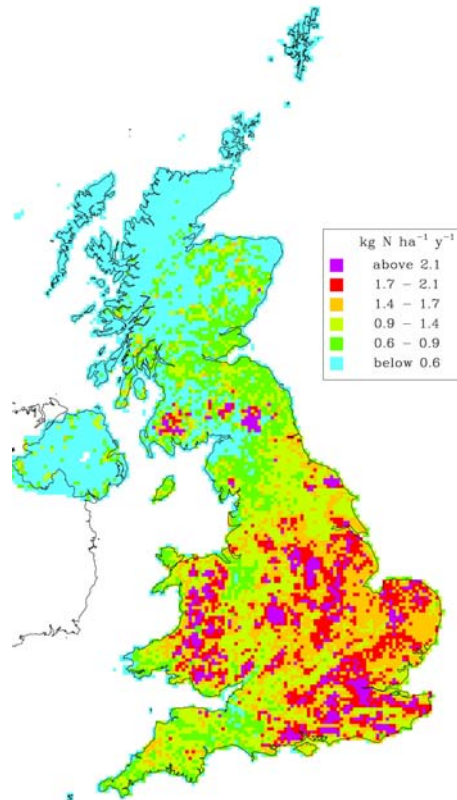


Dry deposition, Nitric Acid, 2004

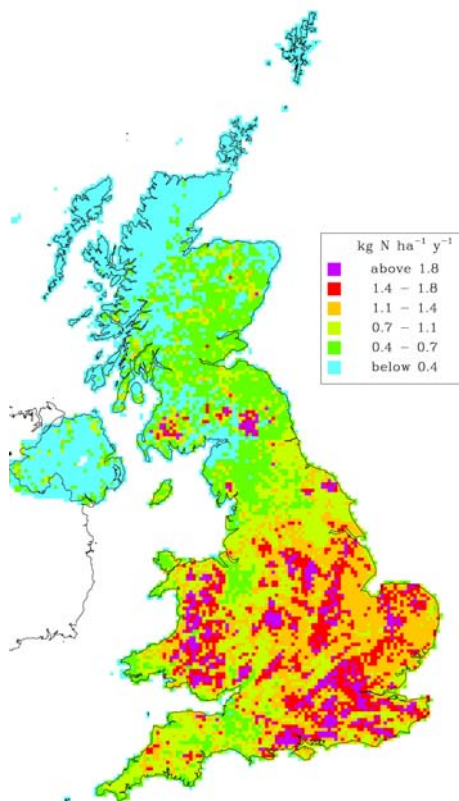
Fig 1.20(c) Maps of dry deposition of sulphur and nitrogen for 2004.



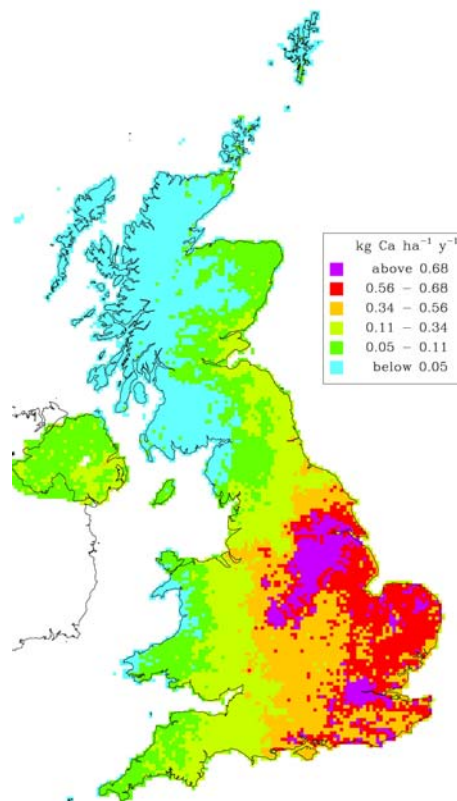
Dry deposition, Sulphate aerosol, 2002



Dry deposition, Ammonium aerosol, 2002

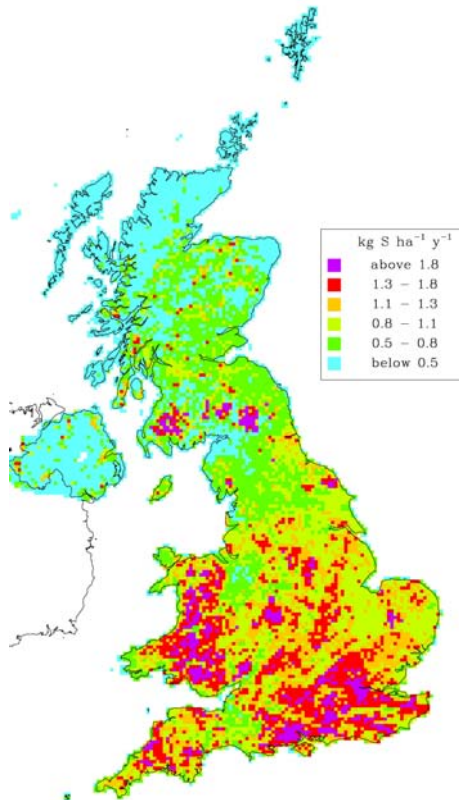


Dry deposition, Nitrate aerosol, 2002

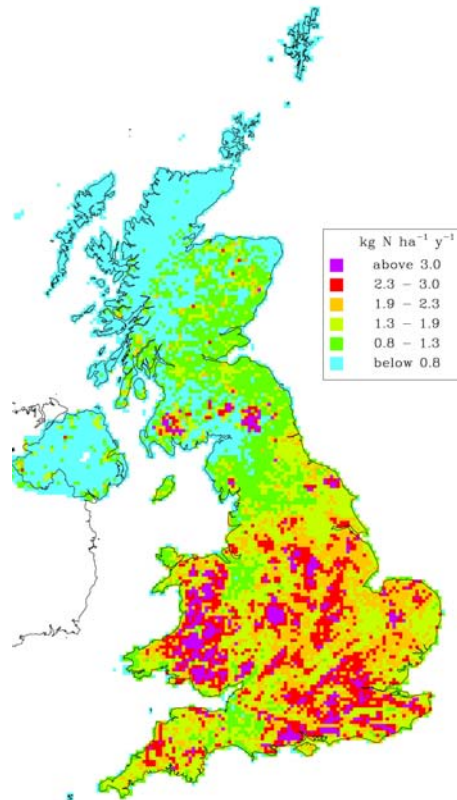


Dry deposition, Non-seasalt Calcium, 2002

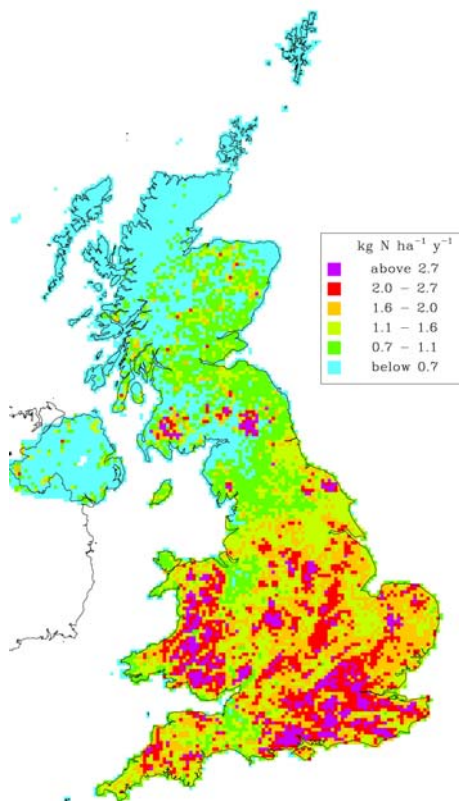
Fig 1.21(a) Maps of dry deposition of aerosols and non-seasalt calcium for 2002.



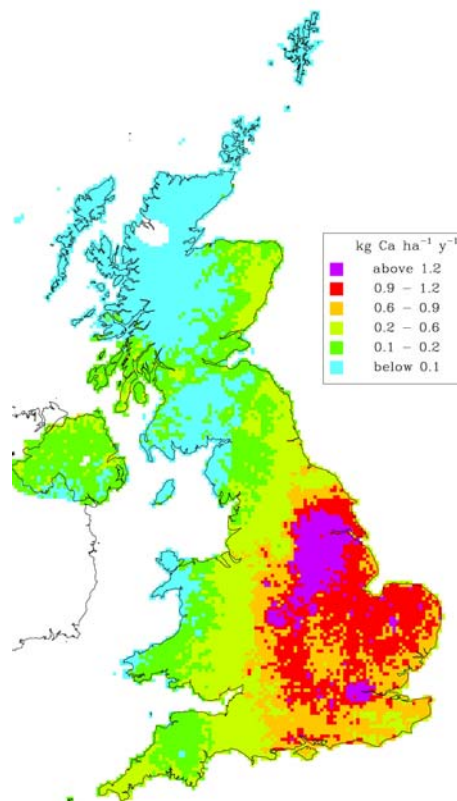
Dry deposition, Sulphate aerosol, 2003



Dry deposition, Ammonium aerosol, 2003

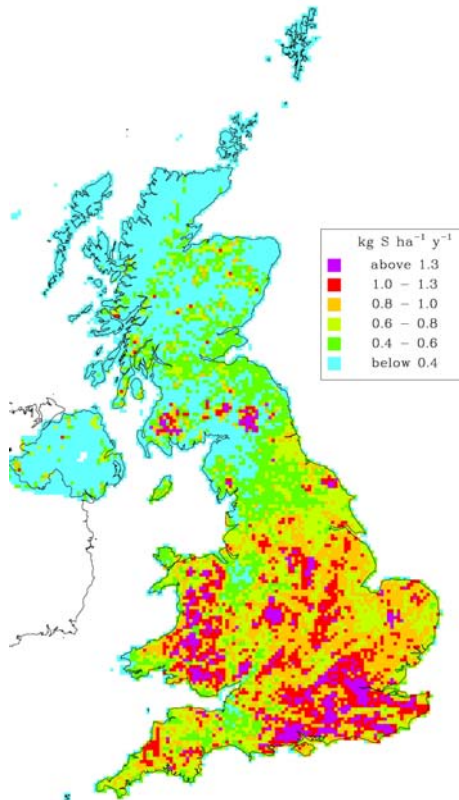


Dry deposition, Nitrate aerosol, 2003

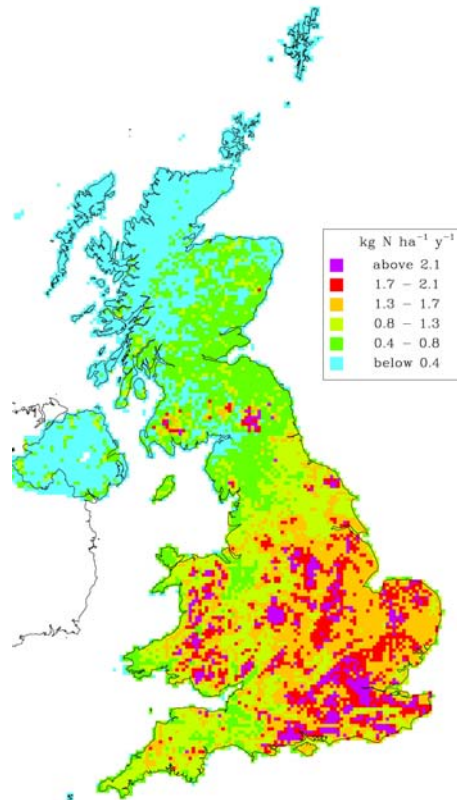


Dry deposition, Non-seasalt Calcium, 2003

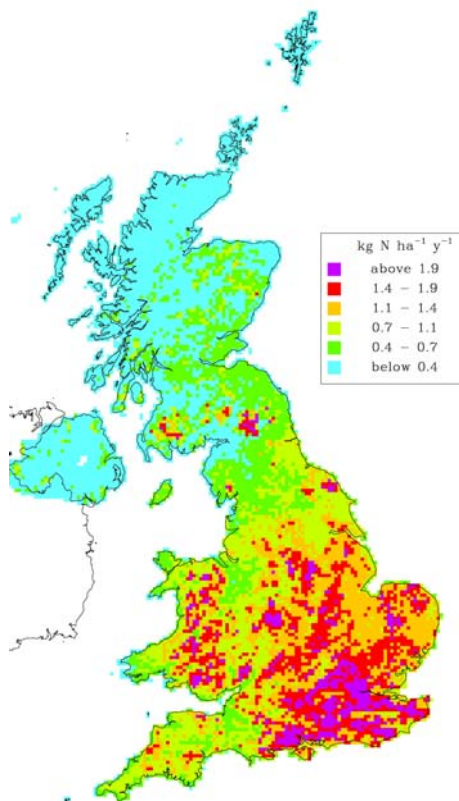
Fig 1.21(b) Maps of dry deposition of aerosols and non-seasalt calcium for 2003.



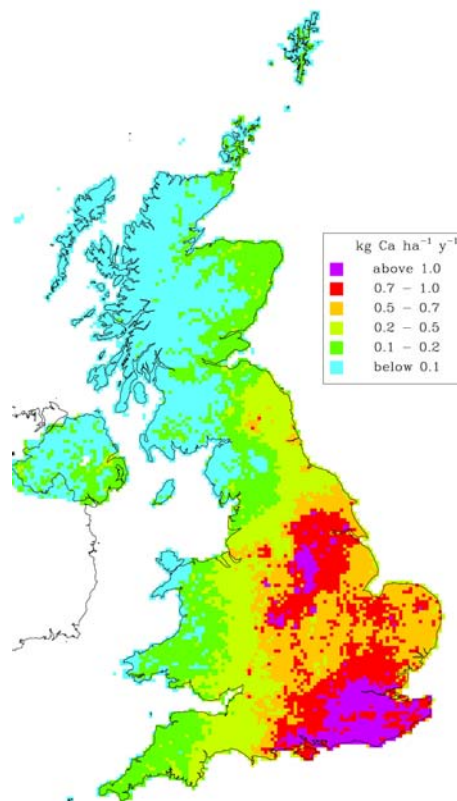
Dry deposition, Sulphate aerosol, 2004



Dry deposition, Ammonium aerosol, 2004



Dry deposition, Nitrate aerosol, 2004



Dry deposition, Non-seasalt Calcium, 2004

Fig 1.21(c) Maps of dry deposition of aerosols and non-seasalt calcium for 2004

2.6. Monitoring and modelling of cloud water deposition

COMPARISON OF BOWBEAT AND DUNSLAIR

J Neil Cape and Alan Crossley

The forest growth adjacent to the Dunslair monitoring site had started to compromise the data collected and as a consequence Bowbeat is now the replacement location for cloud and rain monitoring in the Scottish Southern Uplands. There was a short overlap period between Sept 2003 and May 2004 where samples were collected at both sites.

Venlaw was the lower altitude rainfall collecting site for comparison with the higher altitude sites.

There is some evidence of lower rainfall amounts latterly at Dunslair, especially in comparison with the Bowbeat data (Fig 1.22). Sample 9 at Dunslair was in fact a combination of samples 8 and 9 (due to snow preventing access to the higher altitude site), resulting in the apparent large discrepancy.

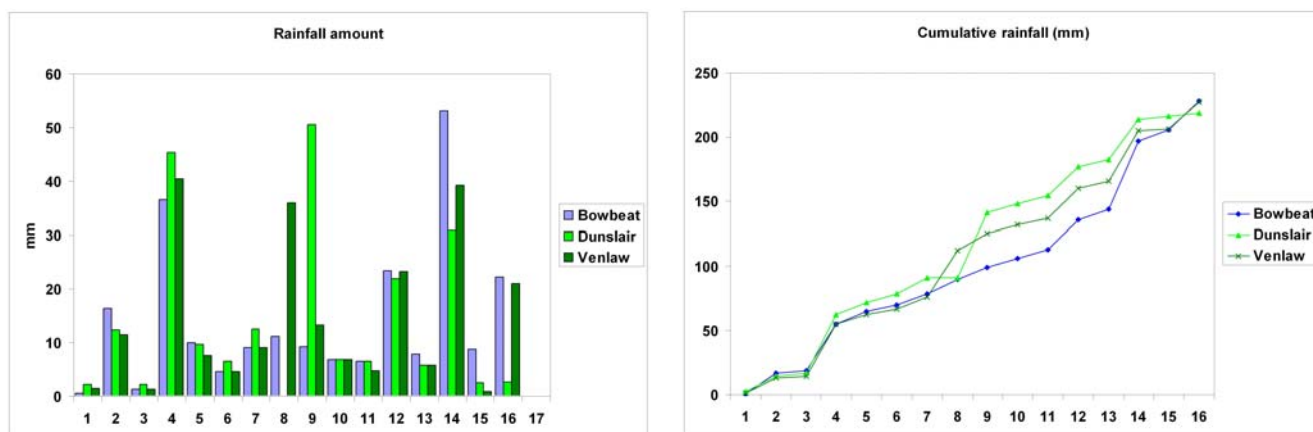


Figure 1.22 Rainfall amount at Bowbeat, Dunslair and Venlaw (left) and cumulative rainfall (right)

The reason for moving the site was that due to interception by the adjacent forest, almost no cloud water was captured at Dunslair, as is clearly illustrated in figure 1.23.

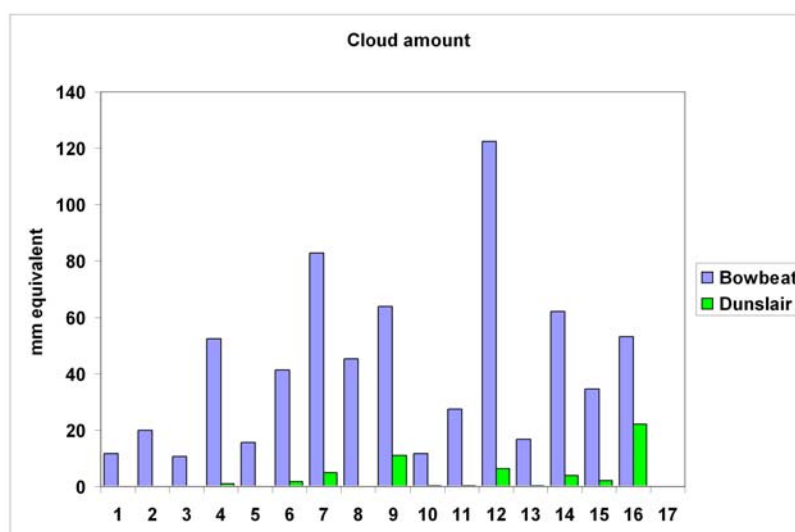


Figure 1.23. Cloud amount at Bowbeat and Dunslair

There was also evidence that Dunslair was capturing less sea-salt, non-sea sulphate and nitrate in rain than either Bowbeat or Venlaw (see Figures 1.24 and 1.25)

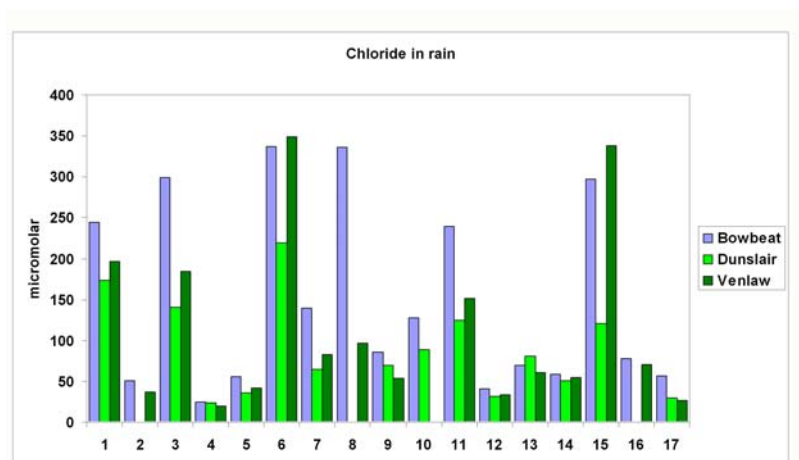


Figure 1.24. Chloride in rain at Bowbeat, Dunslair and Venlaw

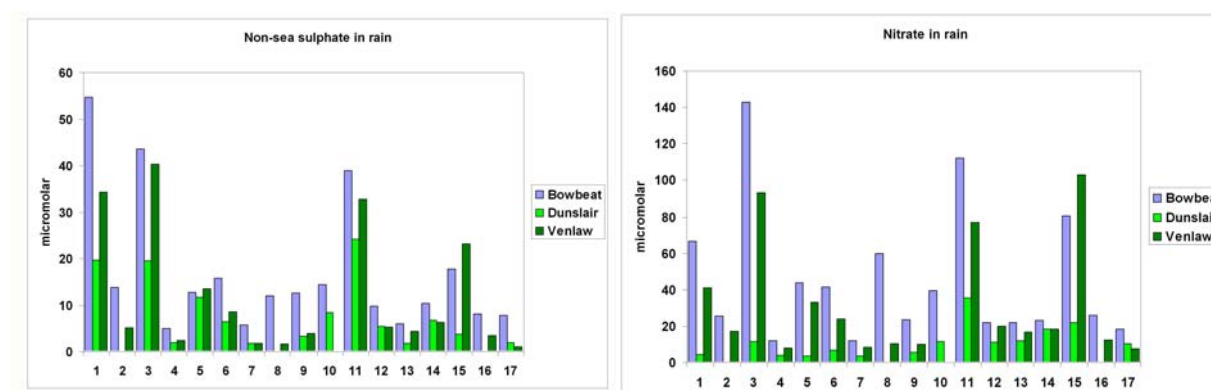


Figure 1.25. Non-sea sulphate (left) and nitrate concentrations (right) in rain at Bowbeat, Dunslair and Venlaw

CLOUD VERSUS RAIN COMPOSITION

The cloud concentrations relative to rain were greater at Dunslair than at Bowbeat. This was due to the combined effect of higher cloud concentrations and lower rain concentrations at Dunslair. The higher cloud concentrations could have been expected as a consequence of the adjacent trees intercepting virtually all but the finest cloud droplets. The lower concentration in the rain collections however has no explanation at this stage of the analysis. Both Chloride and non-sea Sulphate illustrate these observations (see figures 1.26 and 1.27)

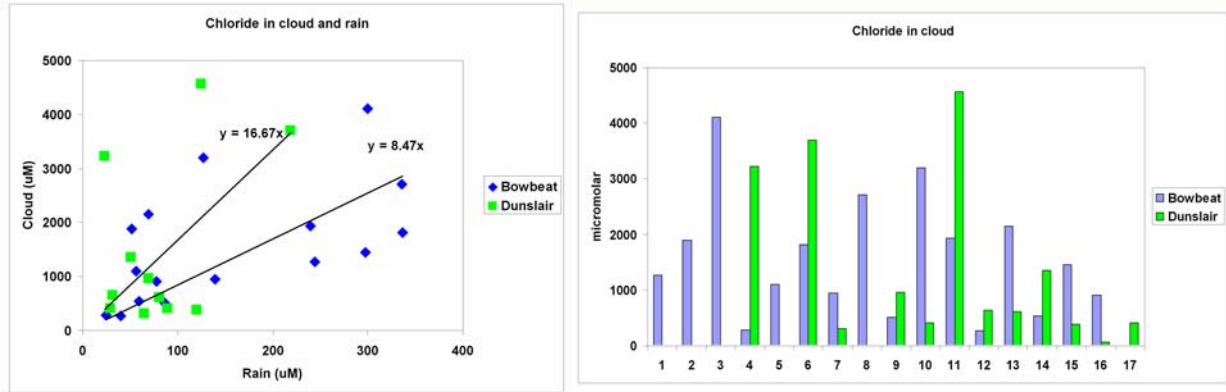


Figure 1.26. Comparison of Chloride in cloud and rain (left) and Chloride concentrations in cloud (right) at Bowbeat and Dunslair

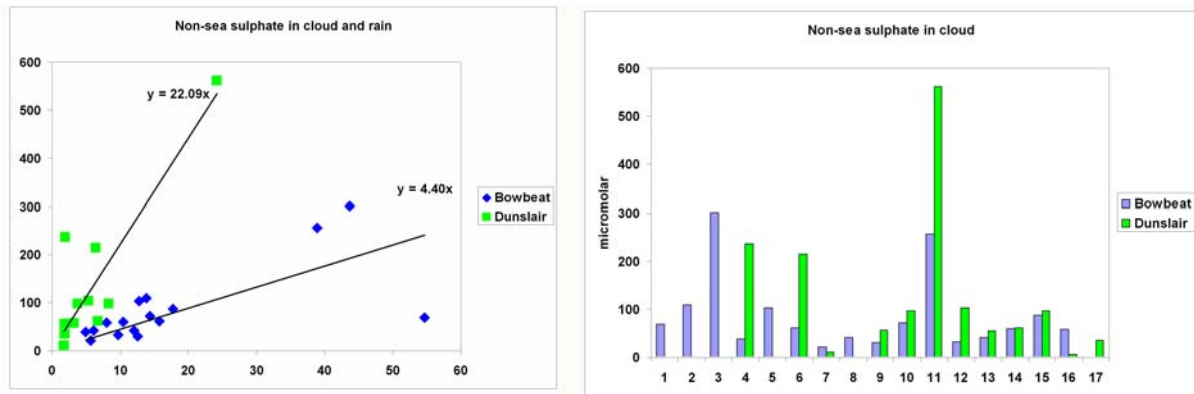


Figure 1.27. Comparison of non-sea sulphate in cloud and rain (left) and non-sea sulphate concentrations in cloud (right) at Bowbeat and Dunslair

LONG-TERM MONITORING OF ION CONCENTRATIONS IN CLOUD AND RAINWATER AT HOLME MOSS FROM 1994 TO 2006

Karl Beswick and Tom Choularton

Background

Long-term monitoring of rain and cloud water has been carried out at a high level site within the urban plume downwind of Manchester in northwest England. Samples have been taken weekly at Holme Moss. The site experiences significant orographic cloud cover, resulting in enhancement of rainfall volume via the seeder-feeder process. Samples are analysed for major ions, with the results being interpreted in the light of the effects of the seeder-feeder enhancement and reductions in UK emissions of pollutants. Rainfall volume enhancement is dependent on the spatial and temporal extent of orographic cloud at the site, with resultant consequences on ionic strength in the samples. Large rainfall amounts are associated with longer cloud duration and lower cloud base. Rain passing through the cloud scavenges proportionately more larger droplets, resulting in relatively lower ionic concentration. Coupled with increased washout upwind, this limits the amount of deposition, with some ions showing a decrease in deposition at high rainfall amounts. Clear downward trends are seen in sulphate concentration in rain and cloud water, with both emissions reduction and the dilution effect of increasing rainfall being responsible. Nitrate concentrations also decreased up until 2002 since when an increase is observed coinciding with a drop in rainfall amount. Deposition at Holme Moss for all ions is dominated by the prevailing, predominantly maritime, southwesterly airflow, although for non-marine ions there are significant contributions from the industrial areas of Yorkshire to the east, and to a lesser extent the Birmingham conurbation to the south.

Holme Moss

The site

Holme Moss lies at an altitude of 525 m within the Peak District in the southern Pennines (OS grid reference 4095 4040), 35km ENE of the Manchester conurbation. Situated downwind of Manchester in the prevailing wind direction, the site is ideal for urban plume studies. In particular, the high prevalence of cloud cover due to altitude allows studies of cloud processing of pollutants and the quantification of the seeder-feeder process of rainfall enhancement.

Automatic weather station (AWS) data is available from 1995, including wind speed, wind direction, temperature, relative humidity, solar radiation, rain amount using a tipping bucket raingauge; cloud amount using a cloud collector connected to a tipping bucket raingauge. A present weather sensor (PWS), model VPF730, manufactured by HSS Incorporated, was installed in late 1996, capable of determining precipitation type and intensity, visibility (distance and extinction coefficient) and presence of cloud or haze.

Comparison with a low altitude site

For the purposes of comparison with a low-level site, data from Holme Moss will be compared to data from Wardlow Hay Cop. This rural background site, run by English Nature, forms part of the UK acid rain monitoring network and is situated 40 km SE of Manchester (OS grid reference 4177 3739). At an altitude of 350 m, the site lies in the southern Pennines 7 km NNE of Bakewell. Although the site does not normally lie within the Manchester urban plume it is expected that the data will be representative of the seeder rain at Holme Moss. Calculated enhancements will therefore be relative to the rural background and not that between Manchester and Holme Moss, particularly with regard to the major

anthropogenically sourced ions. Data from Wardlow Hay Cop were not available for the period 2003- 2005 at the time of writing.

Methodology

Rain is sampled using an 8 inch diameter HDPE funnel mounted at a height of 1.5 m above ground, feeding into a 20 l collecting container. The cloud collector is identical, but with the addition of a conical array of PTFE strings mounted above which collect cloud droplets by interception, with the droplets running down the strings into the collecting funnel. All items are rinsed with deionised water after each sample is taken.

For each weekly sample, total volume is measured, and a sub-sample of 150 ml taken for ion analysis. The cloud collector samples rain with around 90-95% of the efficiency of the rain collector, based on a comparison of identical collectors logged to the AWS, and using the PWS to determine cloud-free periods. The “cloud” sample is therefore contaminated by rainwater of a different ionic strength. If the concentration and amount of the rain sample are known, then the concentration of the “cloud” sample can be corrected to give a more accurate estimation of the true value: this work uses the derived cloud-only concentration.

Samples are analysed by ion chromatography for SO_4^{2-} , NO_3^- , Cl^- , Na^+ , NH_4^+ , Mg^{2+} , K^+ and Ca^{2+} . Concentration of H^+ is unavailable for significant periods and is not discussed. Each sample is analysed twice and an average value taken: repeat analyses agree to within 10%. For periods where H^+ is available, ion balances are mostly consistent with the difference between total cations and anions being within 10% of the total ion count. Concentrations averaged over a period of time are weighted by sample volume. Of most importance in this work is the annual average, since this can be compared with annual emissions data. Additionally, an average of all available data for each month gives a strong indication of seasonal cycles.

Deposition of ions by rainfall is the simple product of ionic strength and sample volume divided by the rain gauge sample area. Total collection for cloud water is calculated in a similar manner, but is not normalised by sample area. This is not equivalent to cloud water deposition to the ground, since the sample volume is a function of the collection efficiency of the cloud collector, not the ground surface. However, the total ion collection is useful for the purposes of comparison between different time periods.

There is no provision to sample only during cloud or wet periods, leading to errors caused by dry deposition of aerosol onto the samplers, with errors likely to be larger for smaller samples. There is no direct method by which this source of uncertainty can be reliably estimated using the available data, although a small sample volume (less than 0.5 l) associated with a significant increase in concentration across all ions is probably due to dry deposition. To estimate this error, an extra dataset is created by removing such periods from the original data to give a “filtered” signal. Since this is a subjective estimate, reference to the original data will always have to be made, representing an upper limit. In the wetter years (1997-2001), the change in volume-averaged rain and cloud concentration is of the order of 0-15%, whilst in the dry years (1994-1996) this rises to 10-30%. For total annual deposition, the differences are larger, with a reduction of 0-20% in rain deposition and 10-40% in cloud collection for the dry years, whilst for the wet years the reduction remains in the 0-15% range for both rain and cloud ion collection. Except where specifically stated, the discussion below refers to the original data. High concentration in small cloud samples can also be associated with smaller cloud droplet size- this is discussed under Seeder-Feeder Rainfall Enhancement.

Non-sea-salt concentrations are calculated in the same manner as Inglis *et al.* (1995), based on standard seawater composition with the assumption that all sodium sampled at Holme Moss is of marine origin.

Meteorological Influences

Wind direction dependence

Aside from changes in emissions, there are a number of factors which are expected to have a major influence on ionic trends at Holme Moss. Wind direction gives a strong indication of the source of the air arriving at Holme Moss. Figure 1 shows wind direction frequency in 10° segments for the period 1996-2001. The predominant wind direction is clearly from the SW, with the 210° to 300° sector accounting for 57% of all data. This direction is dominated by air of marine origin arriving as frontal systems from across the North Atlantic Ocean, but also encompasses the Manchester conurbation. It is therefore expected that ion concentrations at Holme Moss will reflect both marine and urban influences. There is a secondary peak between 40° and 90°, accounting for 16% of all data. Of principal interest in this sector is the presence of large amounts of heavy manufacturing industry and power generation, with samples expected to show high concentrations of anthropogenically sourced ions.

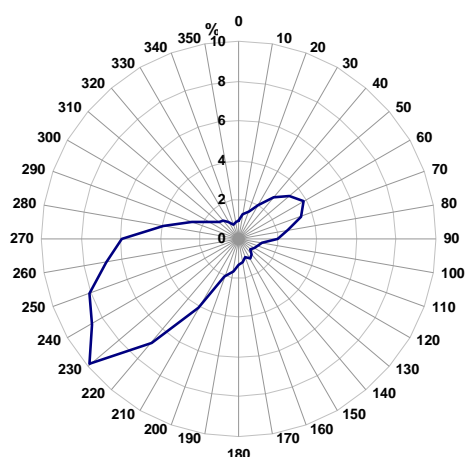


Fig. 1.28 *Wind direction frequency at Holme Moss, 1995-2001*

Wind direction may change significantly within the period of a sample: only data for periods of precipitation or cloud cover are used for comparison with sample concentration. Average ion concentrations or deposition are then calculated for 22.5° sectors. For the period 1996-2001, there were no significant periods of precipitation and/or cloud cover in the NNW and N sectors, although these wind directions are represented in the wind direction rose which uses all wind direction data. Where deposition occurs during two different wind directions within a sample period, the wind direction with the greater amount of deposition is used.

Rain and Cloud Trends

Table 1.7 and figure 1.29 show the annual rainfall at Holme Moss and Wardlow Hay Cop for the years 1994 to 2005, as well as annual cloud volume collection. A clear increasing trend in rainfall amount and cloud collection has been followed more recently by a drop in rainfall and a levelling off in the cloud collection, although it is beyond the scope of this paper to offer explanations of climate trends. Regardless of these patterns, the rain volume enhancement factor between the low and high level sites is an increasing function of cloud and rain amount.

Table 1.7 Summary of rainfall and cloudwater collections at Holme Moss and Wardlow Hay Cop

Year	Wardlow Hay Cop: rainfall (mm)	Holme Moss: rainfall (mm)	Enhancement factor	Holme Moss: original cloud (l)	Holme Moss: cloud- only (l)
1994	977	1496	1.53	140.8	86.7
1995	534	1079	2.02	82.9	53.6
1996	563	1590	2.82	119.2	72.3
1997	852	2276	2.67	158.9	88.7
1998	1010	3091	3.06	209.9	114.7
1999	864	2407	2.79	180.5	107.1
2000	1019	3924	3.85	298.7	177.8
2001	807	3561	4.41	220.3	109.3
2002	875	3979	4.55	233.9	111.6
2003	n/a	1231	n/a	175.4	137.5
2004	n/a	1871	n/a	233.0	179.0
2005	n/a	1687	n/a	160.9	102.3

Sample Volumes

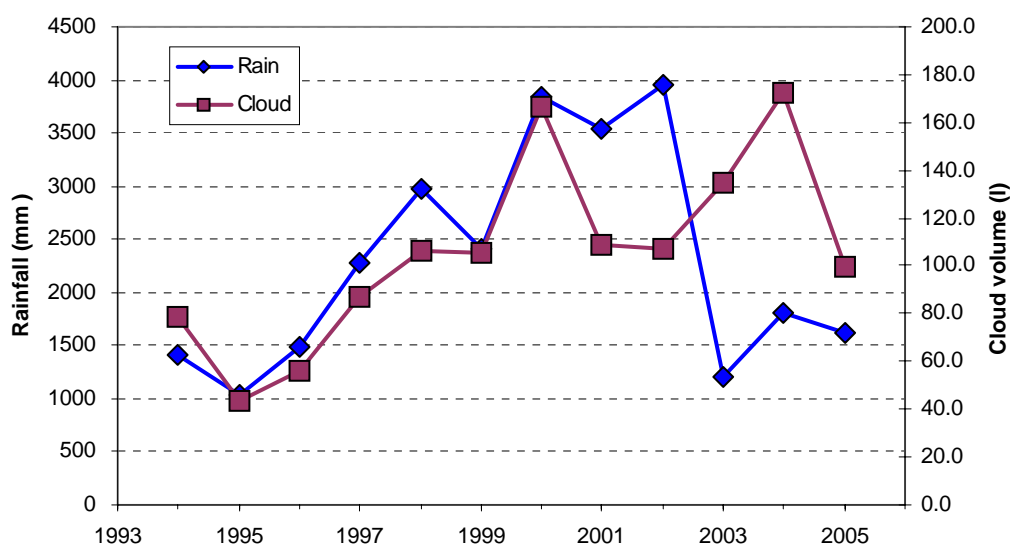


Fig. 1.29 Trends in annual rainfall and cloud collection volumes

The precise impact on the deposition process at Holme Moss of a change in frontal activity cannot be determined in isolation. In the prevailing wind direction, air arriving at Holme Moss has already traversed the Manchester/Liverpool urban area as well as much of North Wales. The mountains of Wales serve to deplete aerosol concentration and rainfall amount, in addition to subjecting aerosol to in-cloud chemical processing. The final impact at Holme Moss will therefore be a complex function of all the processing and scavenging events upwind, but with a probable decrease in ion concentrations due to increased wash-out before air arrives at the site as precipitation and cloudiness increase. This may also be accompanied by a change in cloud base, and this is discussed in more detail below.

Seeder-Feeder Rainfall Enhancement

The substantial enhancement in rainfall with altitude can be largely accounted for with the seeder-feeder enhancement mechanism, whereby rain falling from a higher level cloud layer passes through an orographically-formed “cap cloud” over high terrain such as Holme Moss (e.g. Carruthers and Choularton 1983, Blas et al. 1999). As it passes through the cap cloud, the rain scavenges cloud droplets, adding to the rainfall bulk and ion content. Concentration is enhanced since cloud droplets are much smaller than rain drops and are thus far more concentrated for a given aerosol loading. This process has been confirmed at a number of sites across the United Kingdom (e.g. Choularton et al. 1988, Dore et al. 1992a, Inglis and Choularton 2000).

The influence of changes in cap cloud cover on enhancement are dependent on the droplet spectra at different levels of the cloud. The cloud has the smallest average drop size near cloud base where the drops form by condensation of water vapour onto cloud condensation nuclei. As each droplet is carried upwards over the hill by the airflow, it continues to grow so that for any point above the hill the smallest average drop size remains at the hill surface. The larger droplets will be more dilute in their ionic strength, resulting in an ion concentration gradient within the cloud.

If the cloud base remains stable, but the depth of the cap-cloud increases, the path length of a rain droplet through the cloud is increased and the raindrop will be disproportionately affected by larger volume cloud droplets. If the cloud base lowers, the path length of a rain droplet above any given point on the hill will not be significantly altered, but will be higher relative to the cloud base. Once again the raindrop will be disproportionately affected by larger cloud droplets. In both cases enhancement of ion concentration may be expected to be reduced, given the same concentration in the seeder rain. By a converse argument, if the cloud base rises, or the depth of the cloud reduces, it may be expected that the enhancement of ion concentration in rainfall may be increased. The data shown in Table 1 strongly suggest an increase in cloud cover with time, with a possible lowering of cloud base. It would therefore be expected that for the wetter, cloudier years, smaller absolute enhancements and lower concentration will be observed, although relative enhancements are a more complicated function of upwind concentration and the seeder-feeder mechanism.

The ion content of a cap-cloud tends to reflect local sources of pollution, since it forms in boundary-layer air which has been more influenced by locally sourced aerosol, with the higher level seeder cloud more representative of sources on a much larger, often synoptic, scale. This is particularly so at Holme Moss, where in the prevailing wind direction the distance from major sources of anthropogenic pollutants in the Manchester conurbation is insufficient to allow mixing and modification in significant quantities at the rain-production level.

Assuming that the seeder-feeder mechanism is the only rainfall volume enhancement process, if the rainfall amounts and ion concentrations are known at the upwind and high-level sites then the concentration in scavenged cloud water required to account for the difference in rainwater ion concentration can easily be inferred. The scavenged cloud concentration is smaller than the ground-measured cloud concentration, since the ground-based collector captures cloud droplets which are smaller, and therefore more concentrated in their ion content, than droplets higher up in the bulk of the cloud.

The scavenged cloud concentration, c_s , is expected to be a more stable parameter, reflecting properties of the bulk of the cloud, and is used to calculate an enhancement parameter, as used in models to predict pollutant deposition to high level sites. Specifically, c_s is divided by the rainfall ion concentration at the upwind low level site, c_l , to give the parameter c_s/c_l . At present, this factor is fixed at the value 2.0 for all ions in the models used for mapping pollutant deposition in the United Kingdom (Dore et al. 1992b, Metcalfe et al. 2001). This is a best-fit approximation, necessitated by the lack of studies on the seeder-feeder process, and

may not be valid for all ions under all circumstances. In particular, the value seems to be an underestimate for major marine ions (Dore et al. 2001, Inglis et al. 2001).

Ion trends at Holme Moss

The trends in concentration and deposition for each ion will be described separately. The trends for all ions share many major features: these and their exceptions will be fully considered in the Discussion.

Nitrate

Rain Table 1.8 gives a summary of the concentration and deposition of NO_3^- ions in rain and cloud water at Holme Moss. For the year 2000 the filtered data are used, due to distortion of the full dataset by a single contaminated sample. There had been an apparent downward trend in NO_3^- concentration from 1996 to 2002, disturbed only by an increase in 1999. Over the past few years, however, there has been an increase in the measured NO_3^- concentrations (Fig. 1.30). This is probably associated with the reduction in rainfall seen over the same period. For rainfall amounts above about 2000 mm y^{-1} concentration declines with increasing rainfall. Similarly, the deposition data peaks at around $1.5 \text{ g m}^{-2} \text{ y}^{-1} \text{ N}$ for a rainfall amount of around 3000 mm y^{-1} (Fig. 1.31). Thus, despite increasing rainfall amount at the time, there has been a downward trend in deposition from 1998 to 2005 with a slight increase between 2003 and 2005. Concentration is highest in rain coming from the S and E sectors (Fig. 1.32), reflecting the expected industrial contributions, whilst deposition is dominated by the prevailing wind in the SW-WSW sectors (Fig. 1.33). The strong sources to the south probably represent longer-distance transport from the Birmingham conurbation.

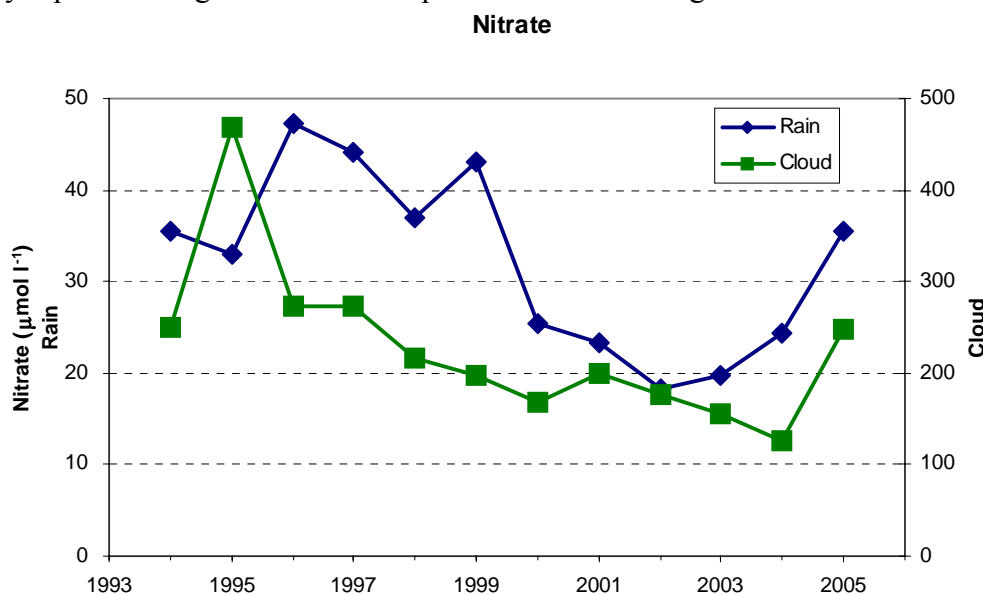


Fig. 1.30 Time-series showing trends in annual concentrations of NO_3^- in rain and cloudwater (using the filtered data)

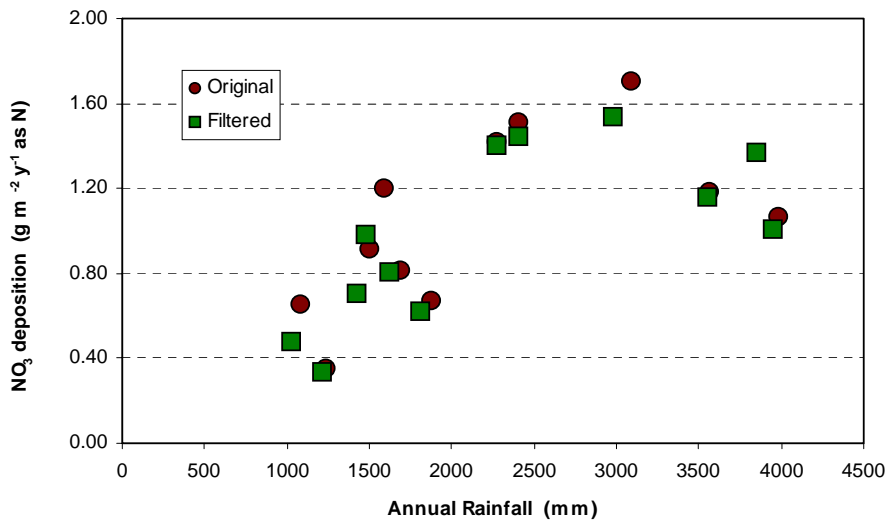


Fig. 1.31 NO_3^- rain deposition as a function of rainfall amount for Holme Moss, showing decrease in deposition at high rainfall volume

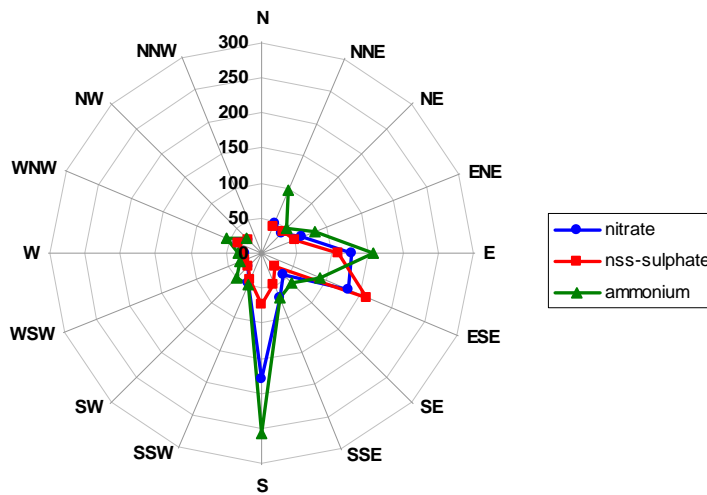


Fig. 1.32 Wind direction dependence of ion concentration in rain water. Units are : $mol\ l^{-1}$

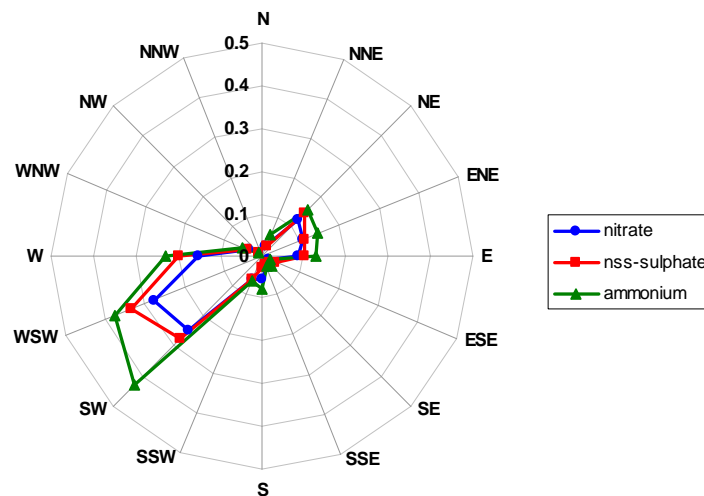


Fig. 1.33 Direction dependence of ion deposition in rainwater. Units are $g\ m^{-2}\ y^{-1}$ (as N for nitrate and ammonium, and as S for sulphate)

Cloud There has been a steady decrease in nitrate concentration in cloud water since the peak in the dry year of 1995 (Fig. 1.30). The peak suggests exposure to smaller, higher concentration cloud droplets. Concentration in 2001 shows an increase but remains consistent with the effects of an increase in cloud duration and associated lowering of the cloud base. The decline in nitrate concentration has been offset by the increase in cloud collection, resulting in no significant trend in collection. Concentration of nitrate in cloud water shows considerably less variation with direction than for rainwater (Fig. 1.34), although as with rain deposition collection is dominated by the SW-W sectors (Fig. 1.35).

Scavenged cloud Trends in scavenged cloud concentration are very similar to that of Holme Moss rain concentration. Of more importance is the upward trend in the value of c_s/c_l , although the large increase in precipitation volume in 2000 and the associated drop in concentration of rain and cloud water resulted in a drop in the value of c_s/c_l .

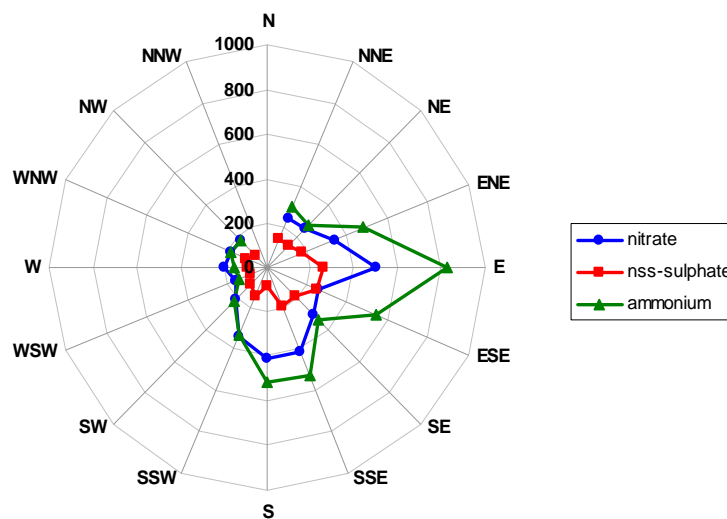


Fig. 1.34 Direction dependence of ion concentration in cloud water (units are $\mu\text{mol l}^{-1}$)

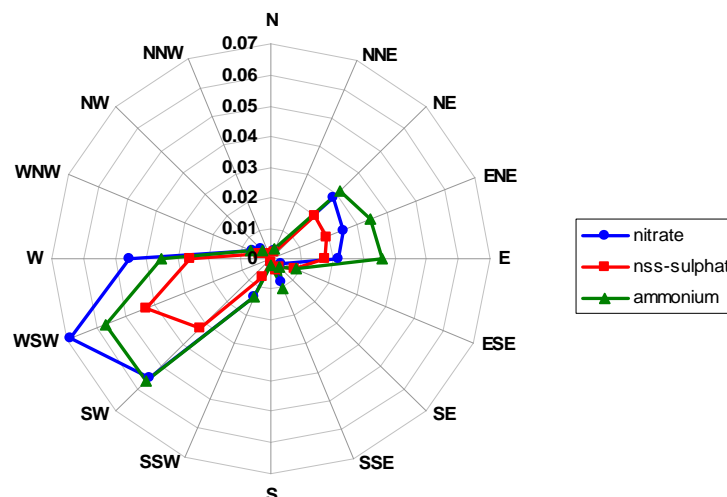


Fig. 1.35 Direction dependence of ion collection in cloud water. Units are $\text{g m}^{-2} \text{y}^{-1}$ (as N for nitrate and ammonium, and as S for sulphate)

Non-sea-salt sulphate

Total sulphate at Holme Moss can be split into two components i.e. sea-salt derived sulphate and non-sea-salt sulphate assumed to be of anthropogenic origin. The sea-salt component follows closely the trends of sodium and chloride (see below) and will not be considered in detail here.

Rain Table 1.9 gives a summary of the concentration and deposition of nss SO_4^{2-} ions in rain and cloud water at Holme Moss. Trends are somewhat less complicated than for nitrate with a steady decline in concentration at Holme Moss since 1996 (Fig. 1.36). Unlike nitrate, no increase in nss SO_4^{2-} concentration is seen since the onset of the current relatively dry period. In terms of deposition, the reduction in concentration was more than compensated for by the increase in rainfall amount over the wet period, resulting in an increase in deposition peaking in 2000, the wettest year.

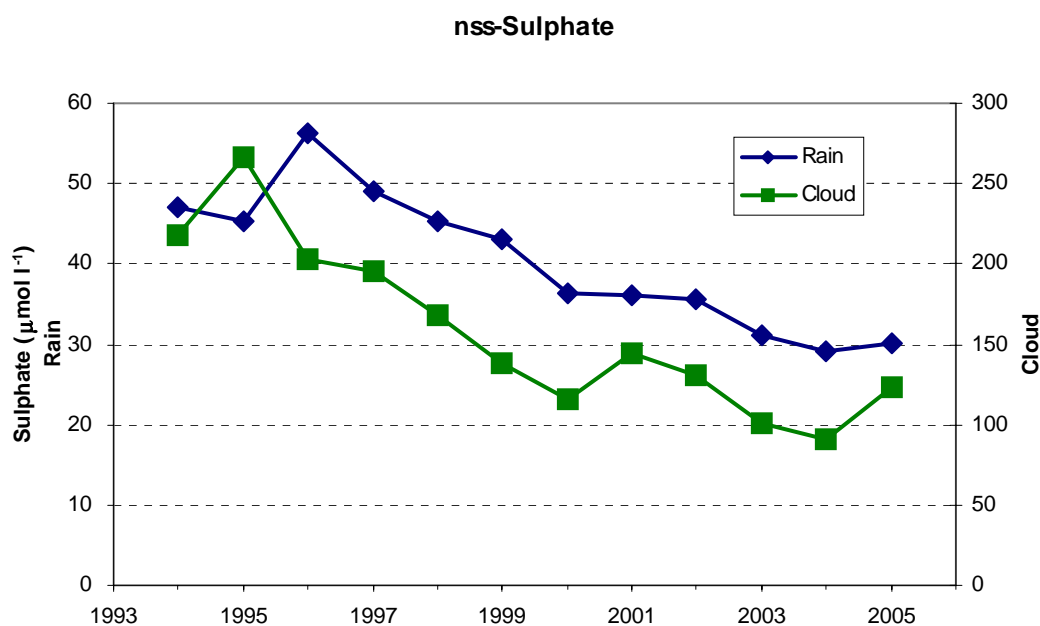


Fig. 1.36 Time-series showing trends in annual concentrations of nss- SO_4^{2-} in rain and cloudwater (using the filtered data)

Deposition in rain is dominated by the SW-W sectors (Fig. 1.33), and volume-averaged concentration peaks to the south and east (Fig. 1.32), reflecting the higher density of anthropogenic sources in those directions. This is also an indication of the greater distance available between source and sink for the processing of sulphur emissions into sulphate aerosol in these wind directions compared to those for the Manchester conurbation. However, for nss- SO_4^{2-} the percentage of deposition in the E-NE sectors is considerably greater than for total sulphate, as it constitutes a much greater proportion of total SO_4^{2-} in an easterly flow. Whilst this may be partly due to the longer time available for incorporation of pollutants into the rain, the major influence is the industrial and power-generating areas of Yorkshire in this sector.

Cloud Concentration of nss-sulphate in cloud water at Holme Moss shows a clear downward trend over the period of measurements, strongly suggesting that the anthropogenic source strength of sulphate has declined over the measuring period. Collection of nss-sulphate in cloud water is determined largely by the cloud amount, with the upward trend in sulphate collection matching the increase in total cloud collection. nss- SO_4^{2-} provides around 70% of the total sulphate ion collection in the NE-N sectors, compared to around 30% in the SW-W sectors (Fig. 1.35).

Scavenged cloud In line with the decrease seen in the ground-measured cloud, scavenged cloud concentration shows a clear downward trend at Holme Moss. The values of c_s/c_l for nss-sulphate are slightly less than for total sulphate, for which the value is close to the value of 2 used in wet deposition mapping models, but both show a small but steady rise over the measurement period.

Sodium, Chloride

Rain As the constituent ions of sea-salt, and with no significant anthropogenic source, sodium and chloride are expected to have the same marine source in relation to concentration and deposition at Holme Moss, and will therefore be discussed together. Tables 1.10 and 1.11 give summaries of the concentration and deposition of Na^+ and Cl^- ions in rain and cloud water at Holme Moss. The concentration trends are shown in figures 1.37 and 1.38, respectively.

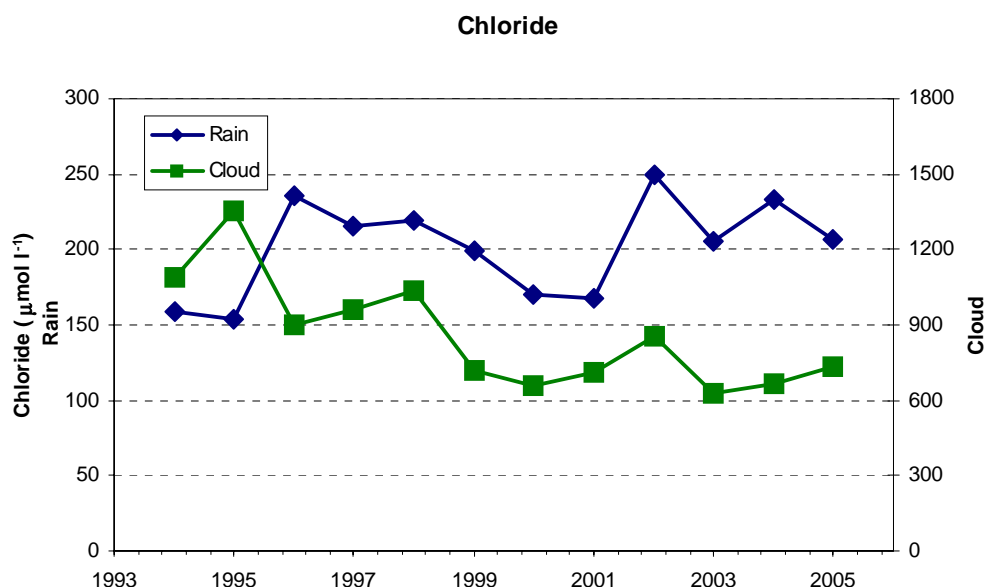


Fig. 1.37 Time-series showing trends in annual concentrations of Cl^- in rain and cloudwater (using the filtered data)

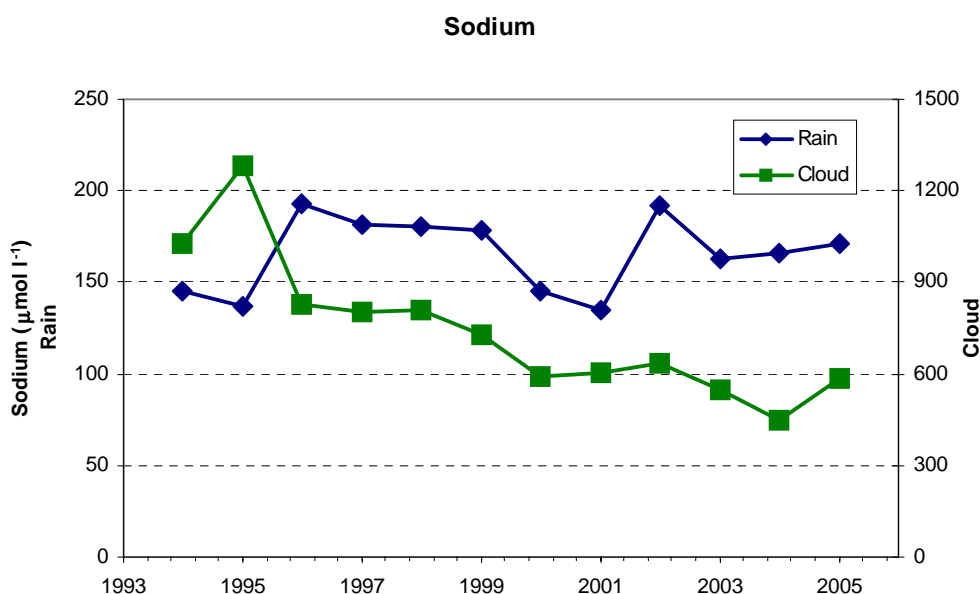


Fig. 1.38 Time-series showing trends in annual concentrations of Na^+ in rain and cloudwater (using the filtered data)

Overall, there has been little change in the concentration of sodium and chloride in rain at Holme Moss. Since they are almost entirely marine-sourced, the concentration at Holme Moss will be largely determined by the wind direction. For both ions there is a broad and even distribution of concentration from S to NW, covering all directions likely to be marine-influenced.

An upward trend in deposition of sodium and chloride in rainwater from the start of measurements until 2002 can be entirely attributed to the general increase in rainfall amount over the same period (this has reversed with the decline in rainfall since then). In common with the concentration, deposition begins to tail off with higher rainfall amounts. Total deposition of sodium and chloride in rainwater is almost entirely dominated by the SW-W sectors, confirming that marine air masses are the primary source for these ions.

Cloud Concentrations of sodium and chloride in cloud water have shown steady rates of decrease over the measurement period whilst collection of sodium and chloride in the cloud water is determined largely by the amount of cloud. Again, collection in cloud water is almost entirely accounted for by the SW-W sectors, with concentration being high in a broad band from SSW-NW.

Scavenged cloud The enhancement factor c_s/c_l shows a steady rise over the measurement period for both ions, although the concentration of the scavenged cloud water shows smaller trends than for nitrate and nss-sulphate. The rise in enhancement is therefore primarily influenced by the rain concentration at Wardlow Hay Cop, which shows a downward trend.

Ammonium

Rain Table 1.12 gives a summary of the concentration and deposition of NH_4^+ ions in rain and cloud water at Holme Moss. In common with most of the other ions, NH_4^+ in rain mostly shows a downward trend in concentration from 1996 onwards, although it appears to have levelled off since 2002, probably due to lower rainfall (Fig. 1.39). Regression analysis shows that this trend, although not statistically significant due to high year-on-year variation, mirrors that of the other anthropogenically sourced ions. This implies that there has probably been a reduction in emissions during the measurement period.

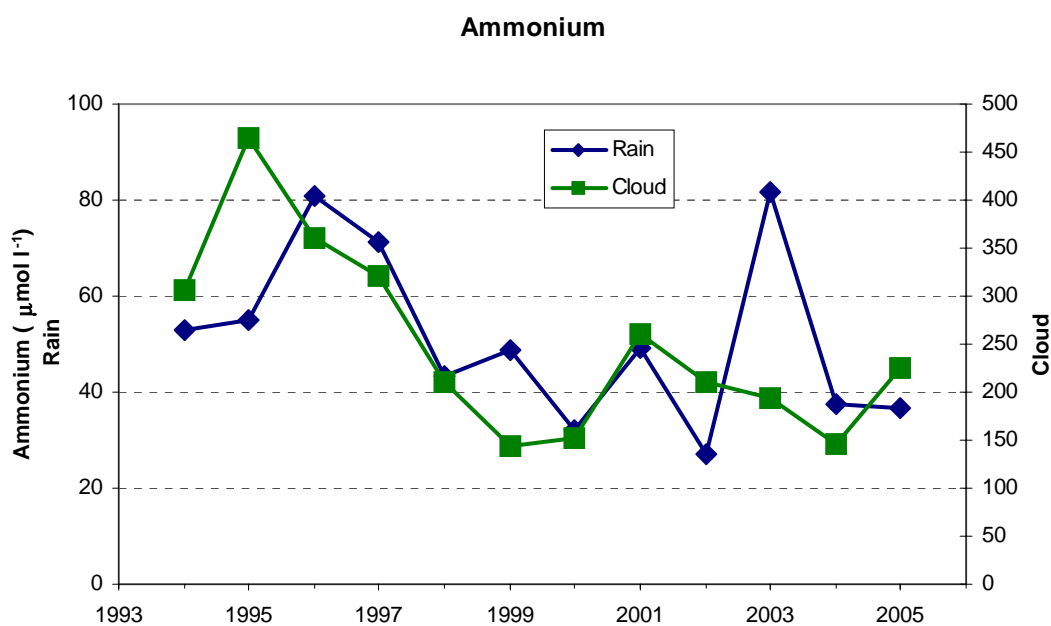


Fig. 1.39 Time-series showing trends in annual concentrations of NH_4^+ in rain and cloudwater (using the filtered data)

In contrast to the behaviour of the other ions, deposition of ammonium via rainwater does not show an increasing trend over the wet period (with the exception of 2001), with the reduction in concentration far outweighing the influence of increasing rainfall volume. Once again, this strongly indicates a real reduction in concentration brought about by reduced emissions. However, since NH_4^+ is expected to be mainly local in origin, year-to-year variation in mean wind direction may also account for some variation in NH_4^+ concentration.

The highest volume-weighted concentrations for ammonium in rain are to be found in the E and S sectors (Fig. 1.32), indicating predominantly agricultural land use, although because of the prevailing wind direction deposition is dominated by the SW-W sectors. There is a substantial secondary deposition peak in the NE-E sectors (Fig. 1.33), again indicating that the strongest sources for this ion are anthropogenic.

Cloud The behaviour of cloud concentration of ammonium is similar to that for rain, with a marked downward trend, again strongly suggesting that there has been a decrease in emissions. Because of the sharp fall in concentration, collection of ammonium in cloud water has only a weak relationship with rainfall and cloud amount, with the increase in cloud amount only partially offsetting the decline in concentration.

The directional dependence of ammonium in cloudwater (Fig. 1.34) shows some important differences compared to that in rainwater. Volume-weighted concentration is high in a broad range from NNE-SSW, peaking in the E and SSE sectors. For total collection, although the peak is once again in the SW-W sectors, there is a substantial contribution from the NE-E sectors. These distributions confirm the agricultural and industrial source of ammonium, but also highlight the fact that the cloud is more likely to reflect local sources.

Scavenged cloud Scavenged cloud concentration shows a clear downward trend since the dry year of 1996, following the trends in rainfall and ground-level cloud water. The c_s/c_l ratio also declines during the measurement period, since concentrations in rainwater at Wardlow Hay Cop do not reduce by the same proportion as at Holme Moss. However, it must be remembered that by its nature, ammonium is likely to be locally sourced, and that the concentration at Wardlow Hay Cop may not be representative of the seeder input at Holme Moss.

Other ions

Concentrations of Mg^{2+} and K^+ measured in rain and cloudwater at Holme Moss are generally quite low, and so will not be discussed in great detail. Overall, no significant trends in the concentrations of K^+ could be found (Fig. 1.40). An apparent downward trend in the cloudwater concentration of Mg^{2+} is probably related to the increased cloud collection volumes. It appears to have recovered slightly in recent years, although not to the levels seen during the last dry period (Fig. 1.41).

Values of Ca^{2+} are considered unreliable due to the effects of local quarrying (Beswick *et al.*, 2003). Over the measurement period, however, there has been a downward trend in the ratio of the cloudwater Ca^{2+} concentrations to those of rainwater, which may be an indication of a reduction in local quarrying activity (see Fig. 1.42 for concentration trends).

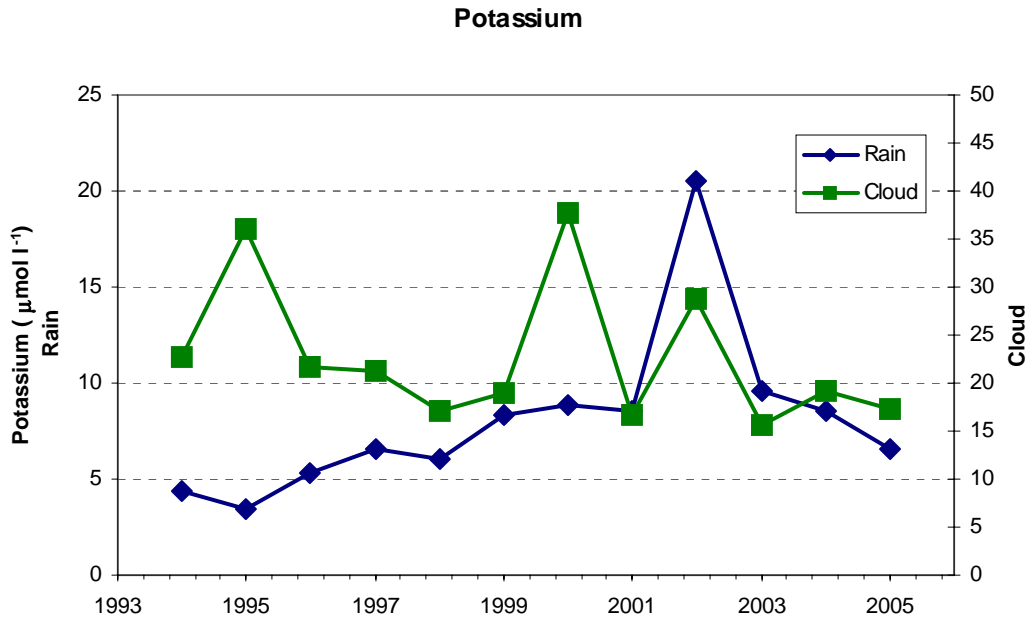


Fig. 1.40 Time-series showing trends in annual concentrations of K^+ in rain and cloudwater (using the filtered data)

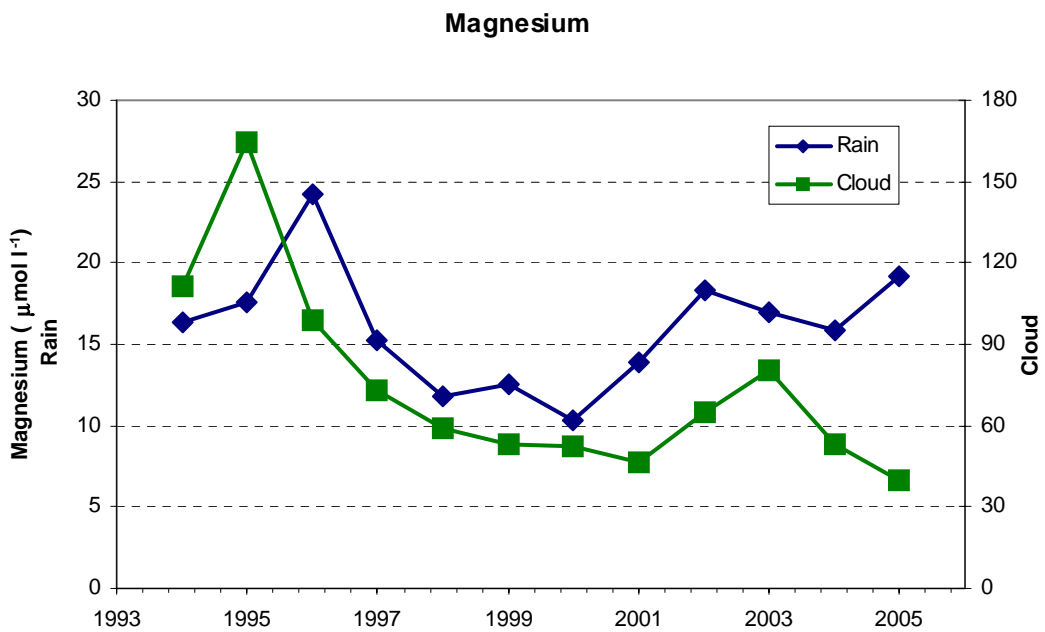


Fig. 1.41 Time-series showing trends in annual concentrations of Mg^{2+} in rain and cloudwater (using the filtered data)

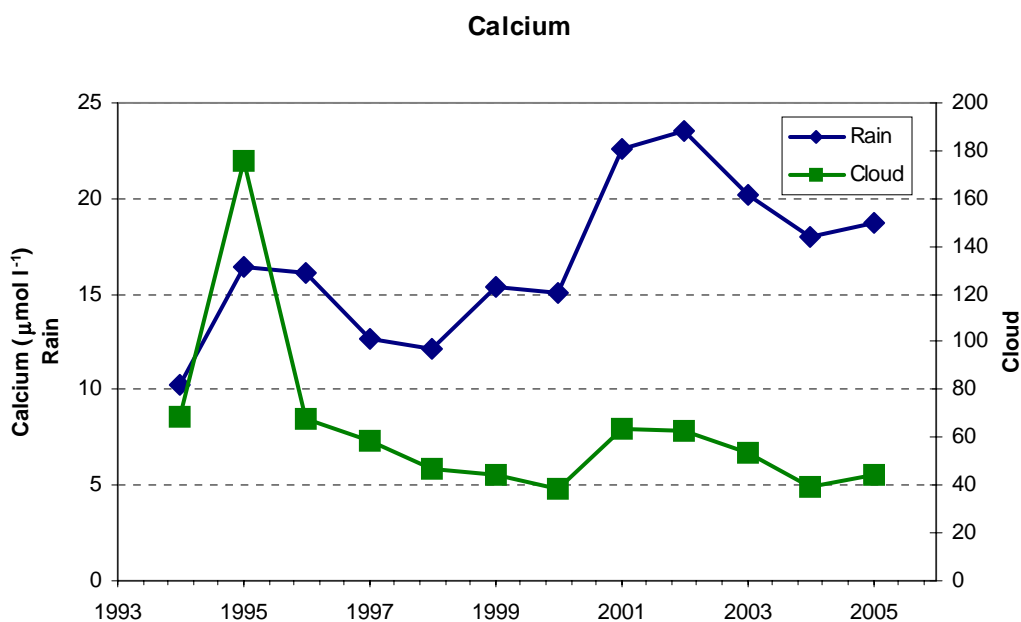


Fig. 1.42 Time-series showing trends in annual concentrations of Ca^{2+} in rain and cloudwater (using the filtered data)

Discussion

It is clear that the concentration and deposition of most ions at Holme Moss are determined largely by the relative volumes of rain and cloud water, which in turn are heavily influenced by the seeder-feeder enhancement process. In drier years such as 1995 the incidence of cloud and rain is low and the seeder-feeder process operates less often, resulting in only a small enhancement of rain volume and concentration. Cloud water in these years is more concentrated due to smaller cloud droplets. In wetter years such as 2000 and 2001 with a high incidence of cloud, the rainfall is substantially enhanced in volume, with the rain composition being more closely related to the feeder cloud. The increased rainfall volume also results in more dilute concentrations of ions, since the scavenged cloud droplets are larger on average. Furthermore, increased rainfall also results in enhanced washout of aerosol upwind of Holme Moss (as shown by the inverse relationship between rainfall volume and concentration at Wardlow Hay Cop), reducing the amount available to the cap cloud. With all these processes combined, for the majority of ions there is a “trade-off” between concentration and deposition: as rainfall and cloud incidence increases, cloud and rain water ionic strengths decrease, which in turn limits potential deposition. In general, maximum deposition and minimum concentration occur in the wetter years, whilst minimum deposition and maximum concentration occur in the dry years. The main corollary of this is that any decrease in emissions may ultimately be offset by enhanced deposition in the wet years.

The seeder-feeder process also determines to a large extent the seasonal variations in concentration and deposition. Both cloud and rain volume peak in February, with a second peak in late autumn between October and November. This dictates much of the annual cycle of rain deposition for nitrate, sulphate (total and nss), sodium and chloride. As with the annual data, concentrations are mostly anti-correlated with the rain and cloud amount for nitrate and sulphate (Fig. 1.43). However, sodium and chloride concentrations follow the wet deposition cycle, indicating that the bulk of these ions arrive with frontal systems during the autumn and winter months. The cycles for ammonium concentration and deposition are more complicated, both having peaks in spring and autumn. This is due to the interaction of agricultural practices with the wet event cycle.

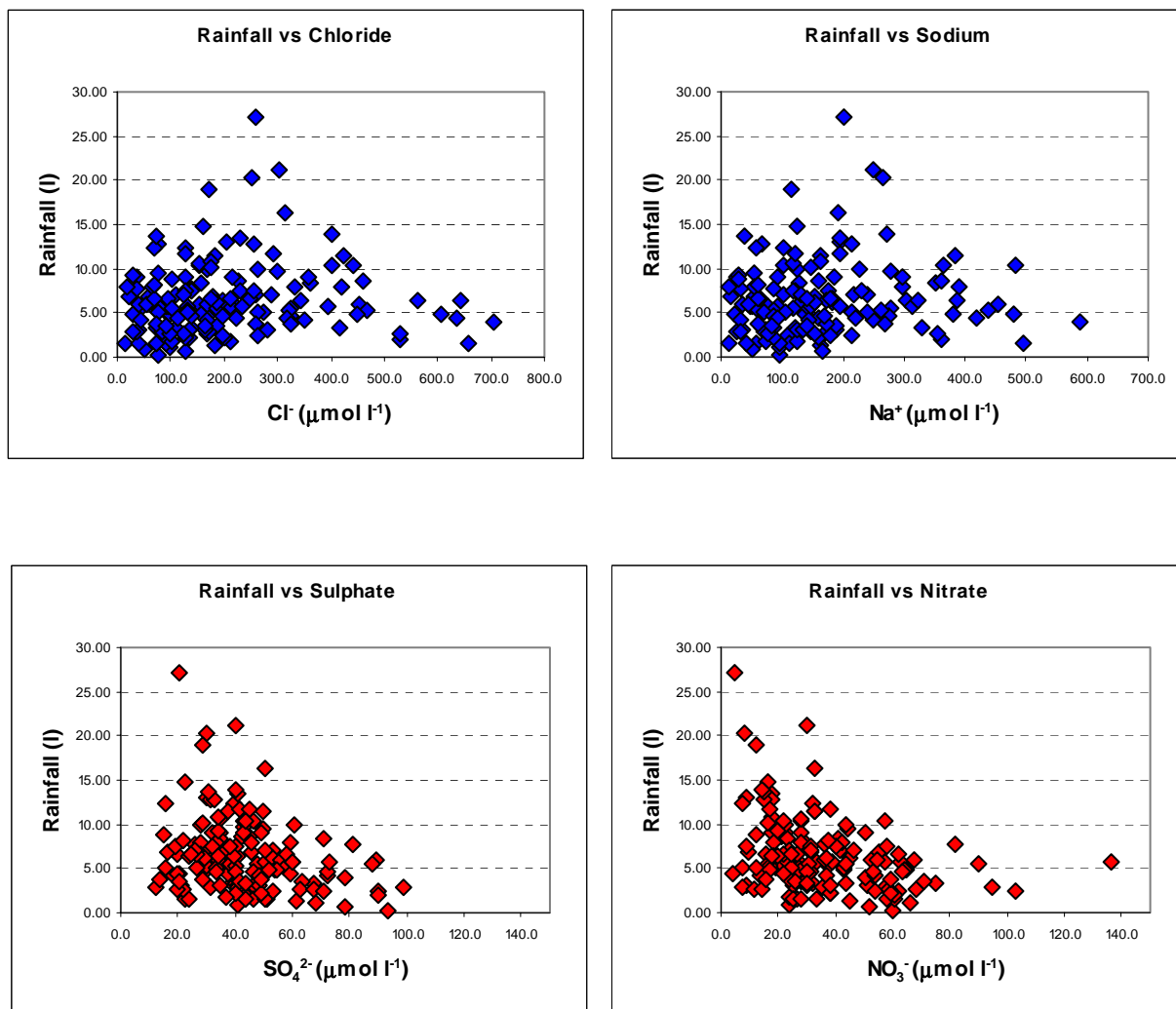


Fig. 1.43 Scatter plots of monthly concentration data showing the inverse relationship between the anthropogenically produced ions (SO_4^{2-} , NO_3^-) and rainfall, in contrast to the relationship between the marine ions (Cl^- , Na^+) and rainfall

There are some deviations from the general pattern described above. For nitrate, there is some evidence for a source-limiting effect on deposition, which decreases with increasing rain and cloud volume at high rain/cloud volume. The principal source of nitrate at Holme Moss is from vehicle emissions in the Manchester conurbation. These do not have enough time to be incorporated into the seeder cloud, and only a fraction will be incorporated into the feeder cap cloud at Holme Moss. For high volumes of rain and cloud, this supply will consequently be more easily exhausted. A converse argument applies to Na^+ and Cl^- : these have an abundant supply in the seeder rain in the prevailing wind direction, with the result that concentration actually increases with increasing rain amount until very high annual rain volume.

A further exception is the behaviour of ammonium, which showed unusually elevated concentration in 2001, mainly due to higher than normal concentrations between September and December. This seems to have brought about by enforced restrictions on animal movements as a result of foot and mouth disease, with free movement only being possible from the end of September. There were still abnormally high numbers of animals in the area until late November/early December.

The second major influence on trends has been the reduction in emissions of major pollutants brought about through international protocols designed to reduce the area experiencing critical load exceedance. It is difficult to specify exactly to what extent emission reduction has resulted in downward trends in concentration because of the effects of the natural variations in rainfall and cloud amount. However, if the assumption is made that the source strength for the marine ions remains largely unchanged over the measurement period, then any trends in those ions could be ascribed to meteorological factors, including the seeder-feeder process. Trends in other ions which differ significantly from trend in the marine ions might therefore be attributable to changes in source strength.

In the case of nss-sulphate and nitrate the downward trends in concentration in rain are greater than for the marine ions, suggesting that they are responding to emissions reduction. This is consistent with the national trends outlined in the NEG-TAP report which shows that between the years 1994-2000, emissions of sulphur reduced on average by 10% of the 1994 value per year. The reduction in rainwater concentration of nss-sulphate of around $3 \mu\text{eq l}^{-1} \text{y}^{-1}$ averaged over the east midlands, Yorkshire and the southeast of England (the "group 1" area), is equivalent to around 5% reduction per year on the 1994 level. Regression analysis shows that at Holme Moss nss-sulphate concentration has been reducing by around 6 % per year (statistically significant at the 95% confidence level), or of the order of $5.8 \mu\text{eq l}^{-1} \text{y}^{-1}$, although it must be remembered that the Holme Moss data is for a single high level site which is known to experience higher concentrations due to the seeder-feeder effect. Reduction in total sulphate is around 5 % per year, but this is almost entirely due to the reduction in nss-sulphate, confirming that the fall is most likely due to reductions in anthropogenic emissions. For nitrate the NEG-TAP report shows reductions of nitrogen emissions of 5% per year, again for the "group 1" region, leading to concentration reductions of around $1 \mu\text{eq l}^{-1} \text{y}^{-1}$ (a 2% reduction per year based on the 1994 concentration). Rain concentration of nitrate at Holme Moss had reduced on average by around 5 % per year up to 2001, equivalent to around $3.1 \mu\text{eq l}^{-1} \text{y}^{-1}$ (statistically significant). However, the recent increase in NO_3^- concentrations, coinciding with the decline in rainfall, implies that the increase in rainfall prior to 2001 was a significant factor in the observed reduction in NO_3^- concentrations. Furthermore, in terms of deposition, Holme Moss departs radically from the data in the NEG-TAP report, which reports a decrease in deposition of both sulphur (42% between 1986-1999) and nitrogen (16% between 1986-1999). At Holme Moss there has been a general upward trend in deposition, brought about mainly due to rainfall volume enhancement through the seeder-feeder process. Ammonium concentration also shows a downward trend in excess of that for the marine ions, which although not statistically significant due to large year-on-year variations, points to a response to reduction in emissions.

At Holme Moss changes in cloudwater concentration of pollutants are larger than for rainwater. These cannot be compared directly with national trends, but may be expected to be more closely related to emissions reduction, since Holme Moss is downwind of a major urban conurbation which produces much of the pollutant aerosol on which cloud at Holme Moss forms. Non-sea-salt-sulphate concentration reduced by 8% per year based on the 1994 value (equivalent to around $30 \mu\text{eq l}^{-1} \text{y}^{-1}$, statistically significant), with a similar proportional reduction for nitrate (8% per year, $33 \mu\text{eq l}^{-1} \text{y}^{-1}$, statistically significant). Trends in scavenged cloud concentration for nss-sulphate and nitrate match those for ground-measured cloudwater, although for nitrate the trend is not significant at the 95% confidence level.

Of significance to the wet deposition mapping modelling is the change in the values of c_s/c_l at Holme Moss. For most ions this ratio is not constant, increasing with increases in rain and cloud volume. This is a consequence of the relatively larger fall in concentration at the low level Wardlow Hay Cop site as the rainfall increases. Thus, although concentration may decrease in absolute terms, the enhancement factor at the high level site actually increases because of the scavenging of ions from the feeder cloud. Also of importance is the fact that

c_s/c_l has different values for different ions, with the marine ions in general having larger enhancement factors.

The large year-on-year variation in ionic constitution of rain and cloud water at Holme Moss inevitably leads to the conclusion that long-term studies such as this are crucial in determining the true effects of reductions in emissions. This is particularly so at high level sites where the effects of the seeder-feeder process serve to mask other trends. Modelling studies would also be of great benefit in this respect.

References

Beswick, K.M., Choularton, T.W., Inglis, D.W.F., Dore, A.J. and Fowler, D. (2003) Influences on long-term trends in ion concentration and deposition at Holme Moss. *Atmospheric Environment*, 37, 1927-1940

Blaś, M., Dore, A.J. and Sobik, M., 1999. Distribution of precipitation and wet deposition around an island mountain in south-west Poland. *Quarterly Journal of the Royal Meteorological Society*, 125, 253-270

Carruthers, D.J. and Choularton, T.W., 1983. A model of the feeder-seeder mechanism of orographic rain including stratification and wind-drift effects. *Quarterly Journal of the Royal Meteorological Society*, 109, 575-588

Choularton, T.W., Gay, M.J., Jones, A., Fowler, D., Cape, J.N. and Leith, I.D., 1988. The influence of altitude on wet deposition at Great Dun Fell and the predictions of a seeder-feeder model. *Atmospheric Environment*, 22 (7), 1363-1371

Dore, A.J., Choularton, T.W., Brown, R. and Blackall, R.M., 1992a. Orographic rainfall enhancement in the mountains of the Lake District and Snowdonia. *Atmospheric Environment*, 26A (3), 357-371

Dore, A.J., Choularton, T.W. and Fowler, D., 1992b. An improved wet deposition map of the United Kingdom incorporating the seeder-feeder effect over mountainous terrain. *Atmospheric Environment*, 26A (8), 1375-1381

Dore, A.J., Choularton, T.W. and Inglis, D.W.F., 2001. Monitoring studies of precipitation and cap cloud chemistry at Holme Moss in the southern Pennines. *Journal of Water Air and Soil Pollution: Focus*, 1 (5-6), 381-390

Inglis, D.W.F., Choularton, T.W. and Wicks, A.J., 1995. The effect of orography on wet deposition in an industrial area. *Quarterly Journal of the Royal Meteorological Society*, 121, 1575-1588

Inglis, D.W.F., Beswick, K.M., Dore, A.J., Choularton, T.W., Fowler, D., Crossley, A. and Leith, I.D., 2001. Verification of procedures for estimating the contribution of hill fog to wet deposition in the UK. In: *Proceedings of the Conference on Fog and Fog Collection*, St. Johns, Canada, 15-20 July 2001, 157-160

Inglis, D.W.F. and Choularton, T.W., 2000. Fine scale spatial variations in wet deposition. *Journal of Atmospheric Research*, 55, 139-157

Metcalf, S.E., Whyatt, J.D., Broughton, R., Derwent, R.G., Finnegan, D., Hall, J., Mineter, M., O'Donoghue, M. and Sutton, M.A., 2001. Developing the Hull Acid Rain Model: it's validation and implication for policy makers. *Environment Science and Policy*, 4, 25-37

National Expert Group on Transboundary Air Pollution, 2001. *Transboundary Air Pollution: Acidification, Eutrophication and Ground-Level Ozone in the UK*. ISBN 1 870393 61 9

Table 1.8 Summary of NO₃⁻ concentration, deposition and enhancement. Figures in italics indicate filtered data.

	Year	1994	1995	1996	1997	1998	1999	2000	2001	2002	2003	2004	2005	Volume Average
Holme Moss		43.9	43.3	53.8	44.5	39.3	44.8	48.2	23.7	19.1	20.7	25.5	34.3	35.6
Rain Concentration (µmol l⁻¹)		35.5	33.0	47.3	44.0	36.9	43.0	25.4	23.4	18.2	19.6	24.4	35.5	30.7
Holme Moss		0.92	0.65	1.20	1.42	1.70	1.51	2.65	1.18	1.07	0.36	0.67	0.81	1.38
Rain deposition (g m⁻² y⁻¹ N)		0.71	0.48	0.98	1.40	1.54	1.45	1.37	1.16	1.01	0.33	0.62	0.80	1.12
Holme Moss		334	469	294	293	235	222	179	206	202	175	136	261	226
Cloud Concentration (µmol l⁻¹)		249	467	299	280	238	198	168	202	176	156	127	248	205
Scavenged		59.6	53.8	61.2	53.7	46.5	54.3	56.4	20.7	16.1	n/a	n/a	n/a	n/a
Cloud Concentration (µmol l⁻¹)		35.6	33.5	51.6	53.0	43.3	51.5	25.5	20.2	14.9	n/a	n/a	n/a	n/a
Cloud Collection (g)		0.41	0.35	0.30	0.36	0.38	0.33	0.45	0.31	0.32	0.34	0.34	0.37	0.36
(as nitrogen)		0.28	0.29	0.24	0.35	0.37	0.29	0.39	0.31	0.26	0.29	0.31	0.35	0.31
Wardlow Hay Cop														
Rain Concentration (µmol l⁻¹)		35.5	32.6	40.3	29.1	24.3	28.0	25.1	34.0	29.6	n/a	n/a	n/a	30.3
Scavenged cloud / Upwind Rain		1.68	1.65	1.52	1.84	1.91	1.94	2.24	0.61	0.54	n/a	n/a	n/a	1.81
c_s/c_i		1.00	1.03	1.28	1.82	1.78	1.84	1.02	0.59	0.50	n/a	n/a	n/a	1.31

Table 1.9 Summary of nss-SO₄²⁻ concentration, deposition and enhancement. Italics indicate filtered data.

	Year	1994	1995	1996	1997	1998	1999	2000	2001	2002	2003	2004	2005	Volume Average
Holme Moss		44.2	44.3	49.5	37.7	34.6	33.2	29.3	28.1	24.4	21.4	19.1	18.6	30.3
Rain Concentration (µmol l⁻¹)		37.8	36.7	44.1	37.5	33.8	31.9	27.3	27.7	23.6	20.7	18.8	19.2	28.7
Holme Moss		1.06	0.77	1.26	1.38	1.72	1.28	1.85	1.60	1.56	0.42	0.57	0.50	1.39
Rain deposition (g m⁻² y⁻¹ S)		0.86	0.61	1.05	1.37	1.62	1.23	1.68	1.58	1.50	0.40	0.55	0.50	1.30
Holme Moss		182	208	156	151	122	100	89.8	108	103	71.7	65.4	89.4	108
Cloud Concentration (µmol l⁻¹)		154	186	161	147	124	92.8	79.1	107	91.3	65.7	62.3	85.9	98.6
Scavenged		55.8	55.8	55.6	42.8	39.3	38.0	32.5	28.7	25.2	n/a	n/a	n/a	n/a
Cloud Concentration (µmol l⁻¹)		37.3	41.0	47.7	42.4	38.4	36.1	29.8	28.2	24.2	n/a	n/a	n/a	n/a
Cloud Collection (g)		0.25	0.18	0.18	0.21	0.22	0.17	0.26	0.19	0.18	0.16	0.19	0.15	0.20
(as sulphur)		0.19	0.13	0.15	0.21	0.22	0.16	0.21	0.19	0.16	0.14	0.17	0.14	0.18
Wardlow Hay Cop														
Rain Concentration (µmol l⁻¹)		38.1	32.6	38.3	29.3	24.9	24.6	20.3	26.0	21.6	n/a	n/a	n/a	27.4
Scavenged cloud / Upwind Rain		1.47	1.71	1.45	1.46	1.58	1.54	1.60	1.11	1.17	n/a	n/a	n/a	1.45
c_s/c_i		0.98	1.26	1.24	1.45	1.54	1.47	1.47	1.09	1.12	n/a	n/a	n/a	1.25

Table 1.10 Summary of Na⁺ concentration, deposition and enhancement. Italics indicate filtered data.

	Year	1994	1995	1996	1997	1998	1999	2000	2001	2002	2003	2004	2005	Volume Average
Holme Moss		168	154	225	182	183	187	150	136	197	170	200	166	173
Rain Concentration ($\mu\text{mol l}^{-1}$)		<i>145</i>	<i>137</i>	<i>193</i>	<i>181</i>	<i>181</i>	<i>178</i>	<i>145</i>	<i>135</i>	<i>192</i>	<i>163</i>	<i>166</i>	<i>171</i>	<i>165</i>
Holme Moss		5.8	3.8	8.2	9.5	13.0	10.4	13.6	11.2	18.0	4.8	8.6	6.4	11.3
Rain deposition ($\text{g m}^{-2} \text{y}^{-1}$)		<i>4.7</i>	<i>3.2</i>	<i>6.6</i>	<i>9.5</i>	<i>12.4</i>	<i>9.8</i>	<i>12.8</i>	<i>11.0</i>	<i>17.5</i>	<i>4.6</i>	<i>6.9</i>	<i>6.4</i>	<i>10.7</i>
Holme Moss		1563	1261	898	824	781	775	578	623	712	582	498	597	734
Cloud Concentration ($\mu\text{mol l}^{-1}$)		<i>1024</i>	<i>1285</i>	<i>912</i>	<i>794</i>	<i>790</i>	<i>728</i>	<i>590</i>	<i>606</i>	<i>633</i>	<i>550</i>	<i>448</i>	<i>585</i>	<i>671</i>
Scavenged		306	241	304	255	241	253	189	162	235	n/a	n/a	n/a	n/a
Cloud Concentration ($\mu\text{mol l}^{-1}$)		<i>259</i>	<i>213</i>	<i>261</i>	<i>254</i>	<i>240</i>	<i>239</i>	<i>183</i>	<i>160</i>	<i>229</i>	<i>n/a</i>	<i>n/a</i>	<i>n/a</i>	<i>n/a</i>
Cloud Collection (g)		3.12	1.55	1.49	1.68	2.06	1.91	2.36	1.57	1.83	1.84	2.05	1.40	1.99
		<i>1.86</i>	<i>1.30</i>	<i>1.22</i>	<i>1.61</i>	<i>2.02</i>	<i>1.76</i>	<i>2.26</i>	<i>1.52</i>	<i>1.56</i>	<i>1.70</i>	<i>1.77</i>	<i>1.34</i>	<i>1.75</i>
Wardlow Hay Cop		93.6	65.4	81.6	60.0	65.0	69.9	39.5	50.4	62.3	n/a	n/a	n/a	64.6
Rain Concentration ($\mu\text{mol l}^{-1}$)		3.28	3.69	3.72	4.24	3.71	3.62	4.79	3.20	3.77	n/a	n/a	n/a	3.58
Scavenged cloud / Upwind Rain		<i>2.77</i>	<i>3.27</i>	<i>3.20</i>	<i>4.24</i>	<i>3.70</i>	<i>3.42</i>	<i>4.62</i>	<i>3.16</i>	<i>3.68</i>	<i>n/a</i>	<i>n/a</i>	<i>n/a</i>	<i>3.24</i>
c_s/c_i														

Table 1.11 Summary of Cl⁻ concentration, deposition and enhancement. Italics indicate filtered data.

	Year	1994	1995	1996	1997	1998	1999	2000	2001	2002	2003	2004	2005	Volume Average
Holme Moss		184	177	279	215	222	218	181	170	264	214	295	200	215
Rain Concentration ($\mu\text{mol l}^{-1}$)		<i>159</i>	<i>154</i>	<i>236</i>	<i>215</i>	<i>220</i>	<i>200</i>	<i>171</i>	<i>168</i>	<i>250</i>	<i>206</i>	<i>233</i>	<i>206</i>	<i>201</i>
Holme Moss		9.8	6.8	15.7	17.4	24.3	18.6	25.2	21.5	37.3	9.3	19.6	12.0	21.8
Rain deposition ($\text{g m}^{-2} \text{y}^{-1}$)		<i>8.0</i>	<i>5.6</i>	<i>12.4</i>	<i>17.3</i>	<i>23.2</i>	<i>17.0</i>	<i>23.3</i>	<i>21.1</i>	<i>35.0</i>	<i>8.9</i>	<i>15.0</i>	<i>11.8</i>	<i>20.3</i>
Holme Moss		1711	1356	989	984	1004	775	652	730	941	662	785	746	876
Cloud Concentration ($\mu\text{mol l}^{-1}$)		<i>1091</i>	<i>1351</i>	<i>985</i>	<i>952</i>	<i>1018</i>	<i>720</i>	<i>661</i>	<i>711</i>	<i>853</i>	<i>628</i>	<i>668</i>	<i>736</i>	<i>796</i>
Scavenged		319	266	375	300	291	295	227	202	317	n/a	n/a	n/a	n/a
Cloud Concentration ($\mu\text{mol l}^{-1}$)		<i>260</i>	<i>227</i>	<i>317</i>	<i>300</i>	<i>293</i>	<i>267</i>	<i>214</i>	<i>200</i>	<i>300</i>	<i>n/a</i>	<i>n/a</i>	<i>n/a</i>	<i>n/a</i>
Cloud Collection (g)		5.26	2.58	2.53	3.09	4.08	2.94	4.11	2.83	3.72	3.23	4.98	2.70	3.74
		<i>3.05</i>	<i>2.10</i>	<i>2.03</i>	<i>2.98</i>	<i>4.01</i>	<i>2.68</i>	<i>3.91</i>	<i>2.75</i>	<i>3.24</i>	<i>3.00</i>	<i>4.08</i>	<i>2.61</i>	<i>3.25</i>
Wardlow Hay Cop		113	86.3	104	73.8	77.4	80.7	50.3	59.6	75.2	n/a	n/a	n/a	78.8
Rain Concentration ($\mu\text{mol l}^{-1}$)		2.82	3.09	3.61	4.06	3.77	3.65	4.51	3.40	4.22	n/a	n/a	n/a	3.45
Scavenged cloud / Upwind Rain		<i>2.31</i>	<i>2.63</i>	<i>3.05</i>	<i>4.06</i>	<i>3.79</i>	<i>3.30</i>	<i>4.26</i>	<i>3.35</i>	<i>3.99</i>	<i>n/a</i>	<i>n/a</i>	<i>n/a</i>	<i>3.08</i>
c_s/c_i														

Table 1.12 Summary of NH₄⁺ concentration, deposition and enhancement. Italics indicate filtered data.

	Year	1994	1995	1996	1997	1998	1999	2000	2001	2002	2003	2004	2005	Volume Average
Holme Moss		59.4	64.6	90.2	71.8	46.9	48.6	35.4	49.6	27.4	81.7	37.9	35.6	48.5
Rain Concentration (µmol l⁻¹)		52.9	55.1	80.9	71.2	43.4	48.6	32.1	49.3	27.2	81.6	37.6	36.5	46.4
Holme Moss		1.25	0.98	2.01	2.29	2.03	1.64	1.95	2.48	1.53	1.41	0.99	0.84	1.80
Rain deposition (g m⁻² y⁻¹ N)		<i>1.05</i>	<i>0.80</i>	<i>1.68</i>	<i>2.27</i>	<i>1.81</i>	<i>1.64</i>	<i>1.73</i>	<i>2.45</i>	<i>1.51</i>	<i>1.39</i>	<i>0.96</i>	<i>0.83</i>	<i>1.70</i>
Holme Moss		380	518	398	335	246	158	201	263	237	211	149	244	249
Cloud Concentration (µmol l⁻¹)		306	465	395	328	252	143	153	262	211	194	146	226	221
Scavenged		82.1	82.1	109	91.9	53.5	55.3	37.5	51.5	24.4	n/a	n/a	n/a	n/a
Cloud Concentration (µmol l⁻¹)		65.2	<i>64.1</i>	95.8	90.9	48.5	53.3	33.0	51.1	24.1	n/a	n/a	n/a	n/a
Cloud Collection (g)		0.46	0.39	0.40	0.42	0.39	0.24	0.50	0.40	0.37	0.41	0.37	0.35	0.40
(as nitrogen)		<i>0.34</i>	<i>0.29</i>	<i>0.32</i>	<i>0.41</i>	<i>0.39</i>	<i>0.21</i>	<i>0.36</i>	<i>0.40</i>	<i>0.32</i>	<i>0.37</i>	<i>0.35</i>	<i>0.32</i>	<i>0.34</i>
Wardlow Hay Cop														
Rain Concentration (µmol l⁻¹)		47.3	46.8	56.5	38.3	33.2	36.7	29.5	43.1	38.0	n/a	n/a	n/a	39.9
Scavenged cloud / Upwind Rain		1.74	1.76	1.92	2.40	1.61	1.50	1.27	1.19	0.64	n/a	n/a	n/a	1.59
c_d/c_i		<i>1.38</i>	<i>1.37</i>	<i>1.70</i>	<i>2.37</i>	<i>1.46</i>	<i>1.50</i>	<i>1.12</i>	<i>1.18</i>	<i>0.64</i>	<i>n/a</i>	<i>n/a</i>	<i>n/a</i>	<i>1.38</i>

MODELLING CLOUD DROPLET DEPOSITION ACROSS THE UK

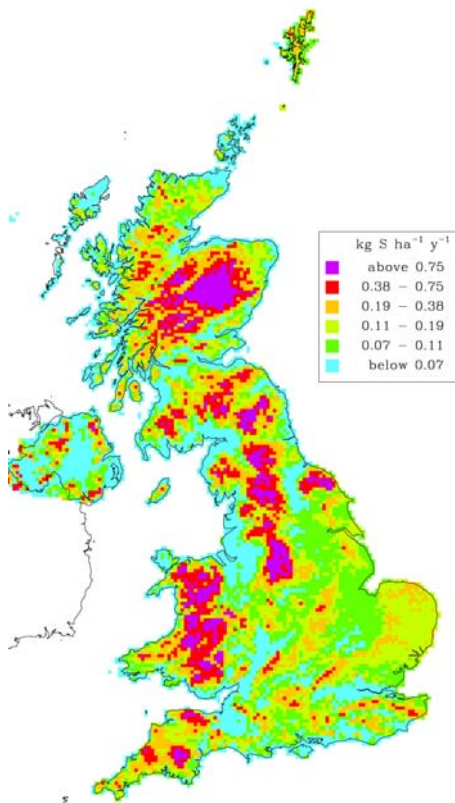
Rognvald Smith

Annual maps of cloud droplet deposition for non-seasalt sulphate, non-seasalt calcium, ammonium and nitrate are shown in Figure 1.44 (a-c). The methodology for producing these maps is described in the Fourth Report of the Review Group on Acid Rain: Acid Deposition in the United Kingdom 1992-1994.

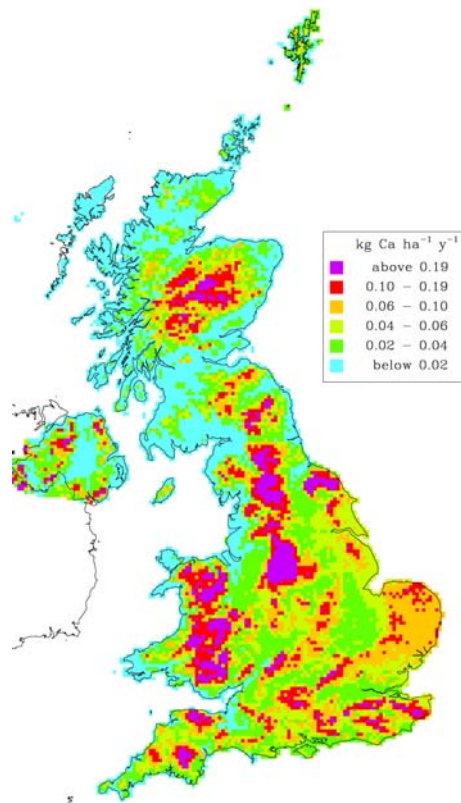
Cloud ion concentrations are derived from the rainfall ion concentration map (See Section 2.1) by assuming that cloud ion concentrations are a factor of 5 greater than the rainfall ion concentrations. From Tables 1.8 to 1.12, the annual ratio of cloud concentration to rain concentration at Holme Moss varies considerably from typically 3 to 9, with non-seasalt sulphate having a shorter range of between 3 and 5. Therefore, except possibly for non-seasalt sulphate, the use of a factor 5 for all ions is not unreasonable.

Cloud droplet deposition assumes a rate of deposition very similar to momentum transfer for the droplet size range 4 to 20 μm (radius), and can be estimated directly from the roughness length and wind velocity over the vegetation. In practice, the conditions associated with cloud interception over the uplands of the UK are not those in which significant corrections for atmospheric stability are necessary. The remaining factor in estimating cloud droplet deposition is the duration of orographic cloud over the UK derived from cloud base statistics.

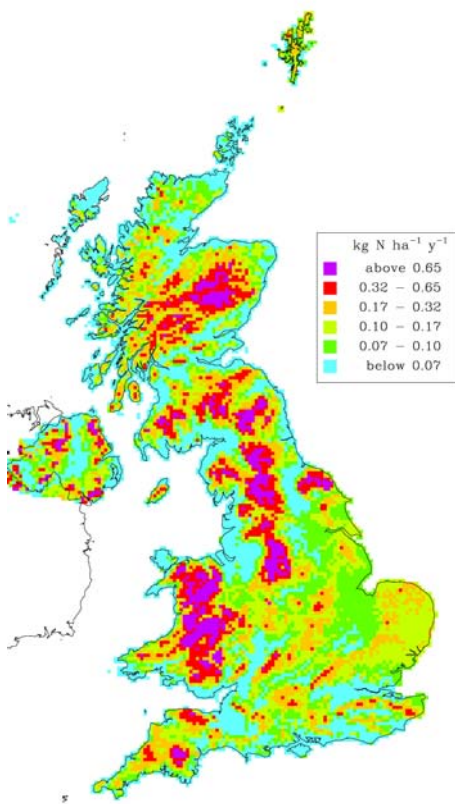
There are a few locations in the UK where estimated cloud droplet deposition exceeds 20% of seeder-feeder enhanced wet deposition, in 2004 it was 1.3% of all UK 5km squares, and the median cloud droplet deposition for 5km squares in 2004 was 3% of the wet deposition. The principal areas where cloud droplet deposition can be important are the Cairngorm Mountains, mid Wales, and the parts of the north Pennines.



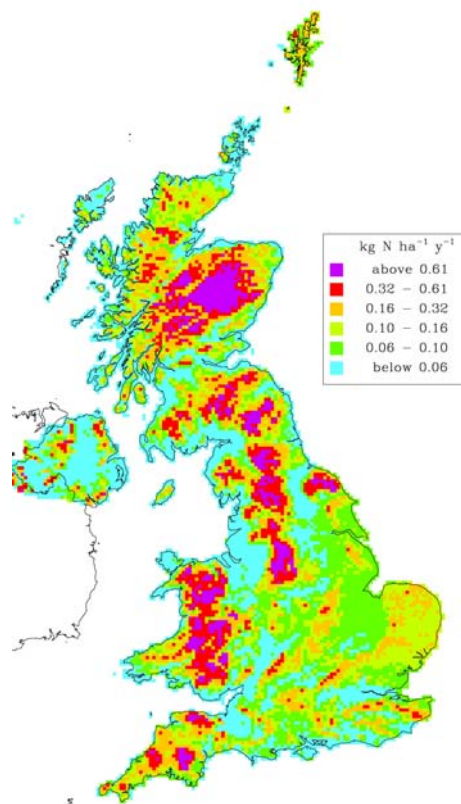
Cloud deposition, non-seasalt Sulphur, 2002



Cloud deposition, non-seasalt Calcium, 2002

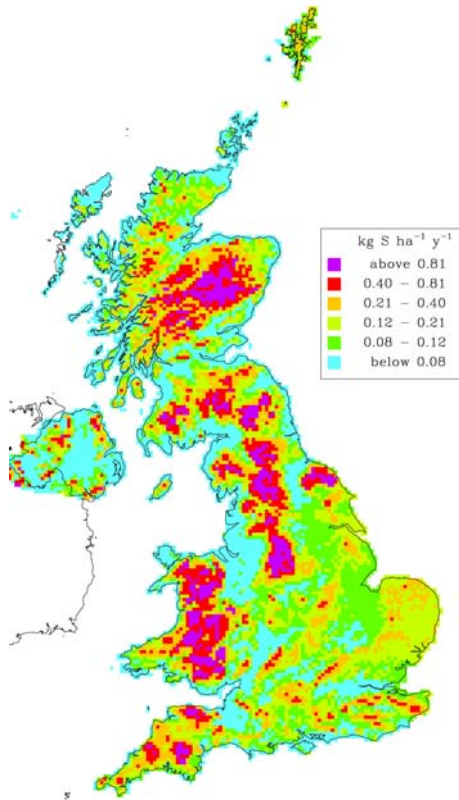


Cloud deposition, Ammonium, 2002

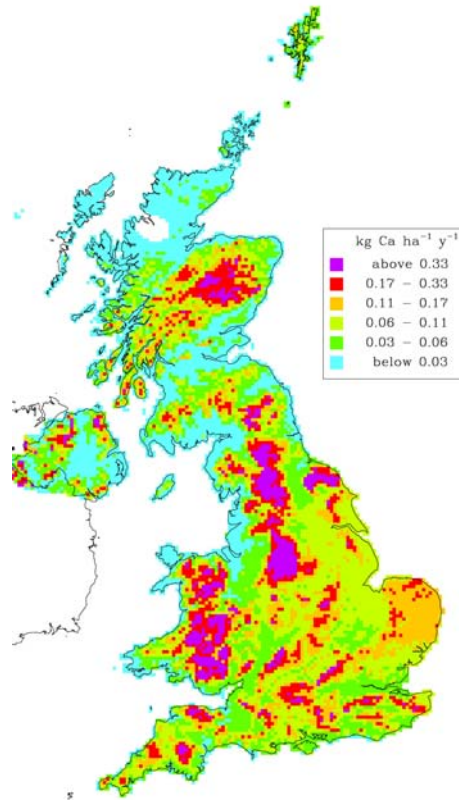


Cloud deposition, Nitrate, 2002

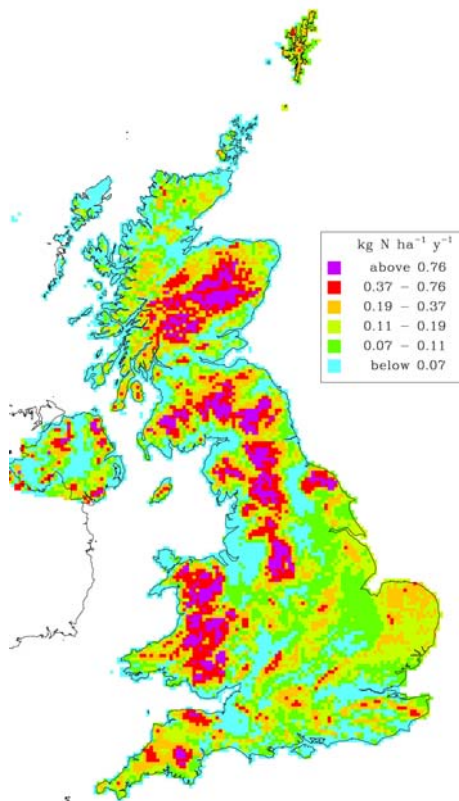
Fig 1.44(a) Maps of cloud droplet deposition for 2002.



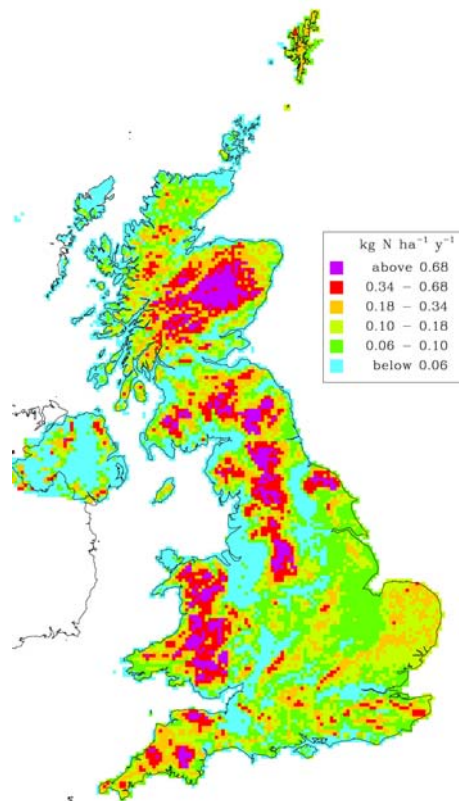
Cloud deposition, non-seasalt Sulphur, 2003



Cloud deposition, non-seasalt Calcium, 2003

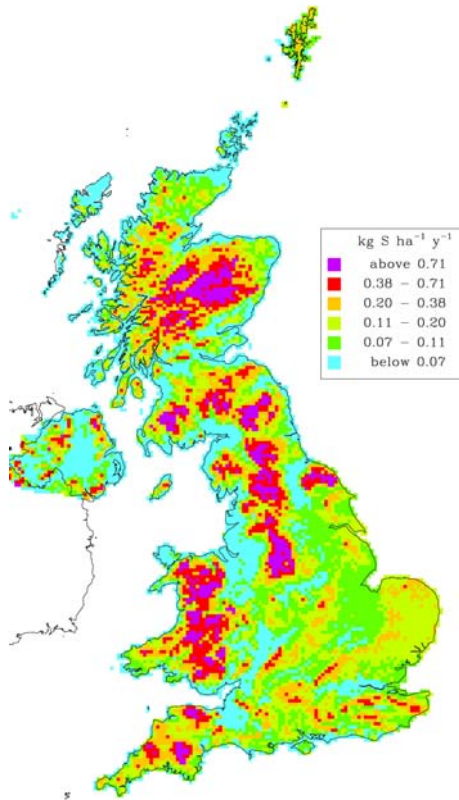


Cloud deposition, Ammonium, 2003

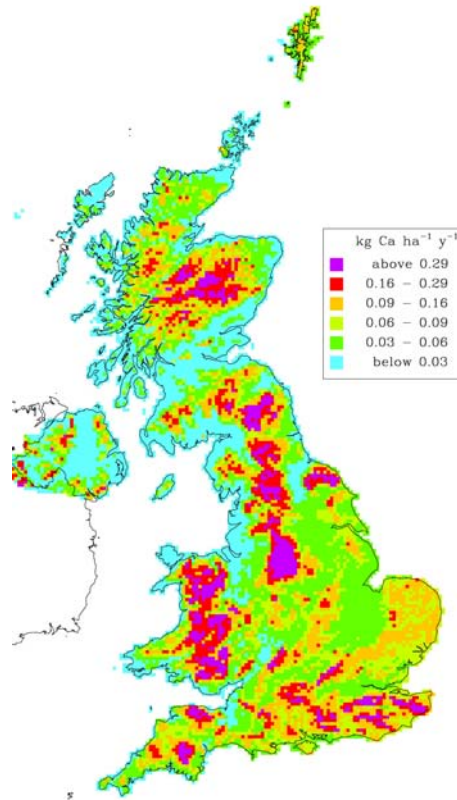


Cloud deposition, Nitrate, 2003

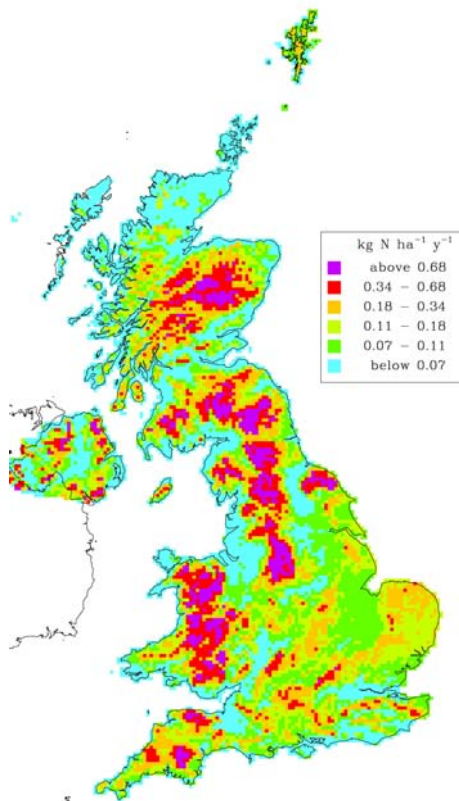
Fig 1.44(b) Maps of cloud droplet deposition for 2003.



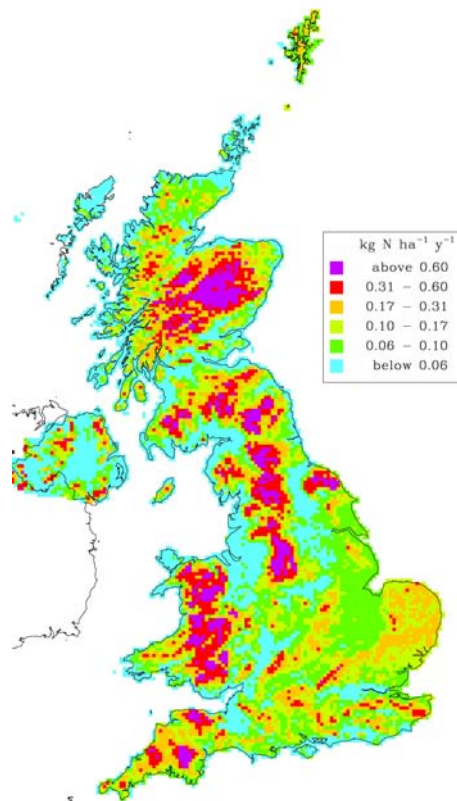
Cloud deposition, non-seasalt Sulphur, 2004



Cloud deposition, non-seasalt Calcium, 2004



Cloud deposition, Ammonium, 2004



Cloud deposition, Nitrate, 2004

Fig 1.44(c) Maps of cloud droplet deposition for 2004.

2.7. Bi-directional exchange in UK dispersion modelling of reduced nitrogen

Tony Dore and Massimo Vieno

INTRODUCTION

In the standard version of the FRAME model, ammonia dry deposition is calculated using the canopy resistance model where the three resistances connected in series are the atmospheric surface layer resistance (R_a), the molecular sub layer resistance (R_b) and the surface resistance (R_c), where R_c is land-cover dependent (Sutton et al., 1994). Six land-cover categories are currently considered in FRAME: forest, moor-land, grassland, arable, urban and water. The flux of material to the surface is calculated by multiplying the ammonia surface concentration by the reciprocal of the sum of the three resistances (equation (1)). The reciprocal of the sum of R_a , R_b and R_c is known as the deposition velocity (V_d). This approach only allows one-way exchange (from the atmosphere to the surface), however vegetation is known to have a bi-directional exchange.

$$FLUX(NH_3) = \frac{\chi}{R_a + R_b + R_c} \quad (1)$$

Introducing the bi-directional exchange of ammonia will mostly affect areas of low ammonia emissions. Ammonia surface concentration is generally underestimated in such areas by the FRAME model and the cause is thought to be the missing process of ammonia emissions through leaf stomata.

NEW PARAMETERISATION OF BI-DIRECTIONAL EXCHANGE OF AMMONIA

The new parameterisation introduced into FRAME is the single-layer canopy compensation point model as suggested by Sutton (1995) where the canopy model is extended introducing stomata and leaf cuticle resistances connected in parallel as shown in Figure 1.45.

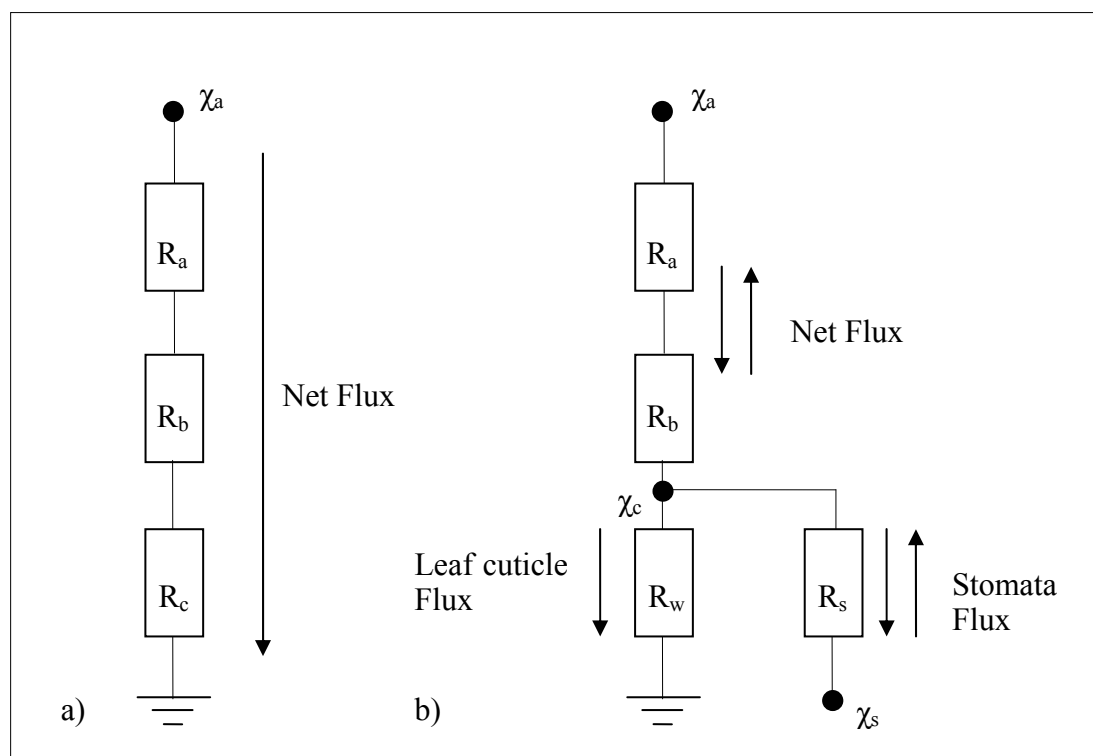


Figure 1.45 a) Canopy model. b) The single-layer canopy compensation point resistance model according to Sutton et al. (1995c). R , resistance; The subscripts are: a, aerodynamic; b boundary layer; w, leaf cuticle and s, stomata. χ_a , NH_3 concentration in air, χ_c and χ_s stomata and canopy compensation points.

The value of R_c for each land-use used in the canopy model is directly derived from measurements (Sutton et al., 1994) where in the single-layer canopy resistance model R_w and R_s are explicitly calculated using equations 2 and 3 respectively.

$$R_w = \min(R_{wMax}, R_{wMin} \exp(\alpha_3 D)) \quad (2)$$

$$R_s = \min(R_{sMax}, R_{sMin} \left(1 + \frac{\alpha_1}{R_s}\right)) \quad (3)$$

Where $R_{wMax} = 5000 \text{ s m}^{-1}$, $R_{wMin} = 35 \text{ s m}^{-1}$, $\alpha_3 = 30 \text{ kPa}^{-1}$, $R_{sMax} = 5000 \text{ s m}^{-1}$, $D = 0.324 \text{ kPa}$ (Water pressure deficit), $R_{sMin} = 1 \text{ s m}^{-1}$, $\alpha_1 = 180 \text{ W m}^{-2}$ and R_s is the global solar radiation expressed in W m^{-2} . The values used here are the same as used in Nemitz et al., (2000) and are intended to be used in the preliminary work on bi-directional exchange of ammonia with the aim to check the necessary numerical stability when a bi-directional exchange of ammonia is applied to the FRAME model. The new deposition module can use either the canopy resistance or the single-layer canopy model so that bi-directional exchange is a model option. This upgrade of the model provides the necessary platform to explicitly calculate all relevant parameters for the bi-directional exchange of ammonia. Moreover the new deposition scheme may be extended for other species such as SO_2 . In the medium term the main goal is to have one resistance equivalent deposition scheme for all species used in the FRAME model.

The stomata compensation point χ_s shown in equation 4 is related to the pH and $[\text{NH}_4^+]$ concentration in the apoplast by Henry's law and the dissociation equilibrium for NH_3 and NH_4^+ . The parameterisation used here is valid for a surface pressure of 1 atm (Nemitz et al., 2000). Canopy compensation point χ_c formulation is shown in equation 5 where T is the temperature and the ratio between the concentrations of $[\text{NH}_4^+]$ and $[\text{H}^+]$ is often referred as Γ_s .

$$\chi_s = \frac{161500}{T} \exp\left(-\frac{10380}{T}\right) \frac{[\text{NH}_4^+]}{[\text{H}^+]} \quad (4)$$

$$\chi_c = \frac{\chi_a (R_a + R_b)^{-1} + \chi_s R_s^{-1}}{(R_a + R_b)^{-1} + R_s^{-1} + R_w^{-1}} \quad (5)$$

RESULTS OF MODELLING BI-DIRECTIONAL EXCHANGE OF AMMONIA WITH FRAME

The 1999 emissions simulation year has been used to test the effect of bi-directional exchange of ammonia onto the NH_3 surface air concentration. Figure 1.46 illustrates the ratio of NH_3 concentrations for a standard FRAME run (using the canopy resistance model) compared to those for a simulation with the canopy compensation point routine included. The figure shows that in the remote upland areas where emissions and concentrations of ammonia are low, the inclusion of the canopy compensation point parameterisation leads to an increase in ammonia concentrations, which is typically 20%. In the lowland areas where ammonia concentrations are higher, use of the compensation point results in a reduction of ammonia concentrations of up to 50%.

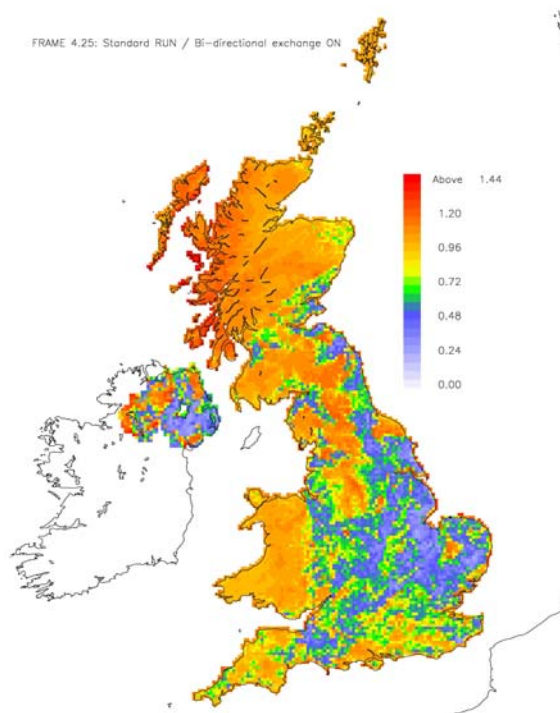


Figure 1.46 Map of the ratio of ammonia concentrations modelled with canopy compensation point to those modelled without

A second experiment has been made to investigate the seasonal effect of the single-layer canopy compensation point at specific geographical locations. Two observation sites were chosen to represent very low and very high ammonia concentrations. Inverpolly, north of Scotland (NC187088 GB National Grid reference), was chosen to be representative of sites of very low ammonia concentrations, where Bedingfield, East Anglia (TM173684 GB National Grid reference), was chosen to be representative of sites with high ammonia concentrations. The FRAME model currently underestimates the surface concentration at the Bedingfield site.

Twelve 1999 FRAME runs were made, one for each month of the year. The FRAME model has been initialised using monthly meteorological parameters such as temperature and humidity representative of the Inverpolly observation site. As they are similar to the default values used in the FRAME model they are thought to be representative of the Bedingfield site. Moreover the main focus is to investigate the net emissions of ammonia which is expected to be negligible at the Bedingfield site; therefore the temperature assumptions made earlier are relatively unimportant. The FRAME model superimposes a diurnal temperature cycle to the monthly mean temperatures as shown in Figure 1.47.

For this experiment the 1999 annual average emissions are divided by twelve and used for each month run.

Figure 1.48 shows monthly predictions of the FRAME model for concentrations at Inverpolly observation site for the year 1999. The FRAME model with the single-layer canopy compensation point was able to capture the seasonal variation in ammonia concentrations, however for two months, April and July, the ammonia concentration was much larger than the concentration predicted by the FRAME model. This is probably due to small spatial scale variations in ammonia emissions which may not be captured by the FRAME model (e. g. wild animals).

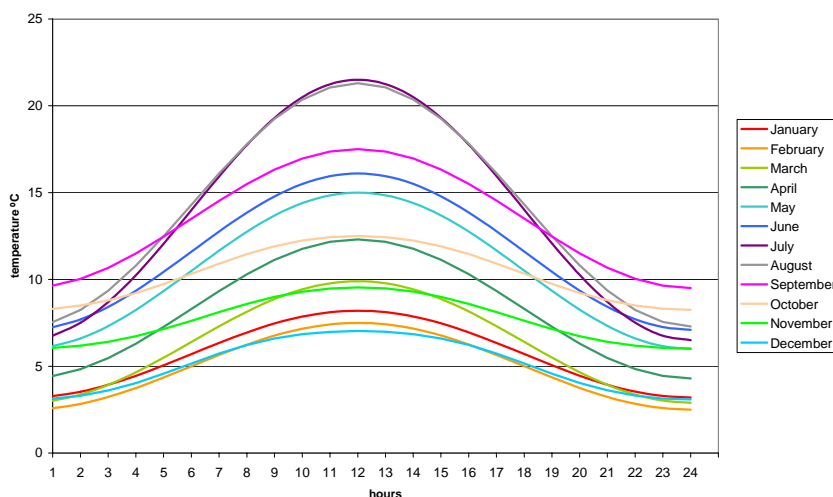


Figure 1.47 : FRAME model hourly temperature profile. The FRAME model uses a monthly average temperature to calculate a diurnal temperature profile. Units are °C.

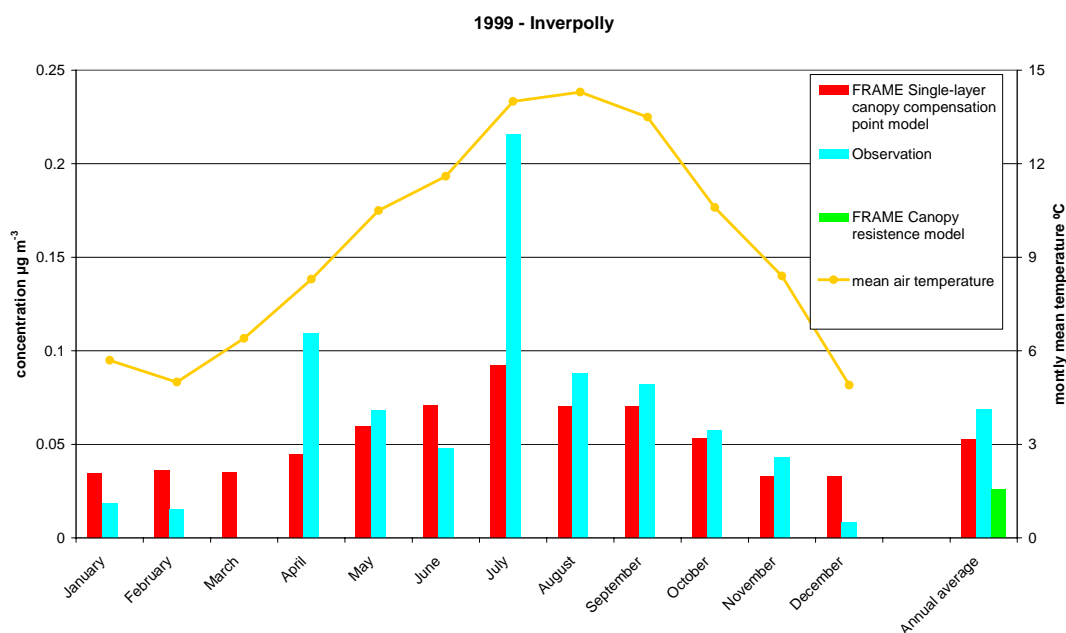


Figure 1.48 : Inverpolly 1999 ammonia concentrations. Observation (Blue). FRAME model prediction: (Red) monthly predictions of single-layer canopy compensation point model, (Green) annual average canopy resistance model. The yellow line is the monthly mean temperature representative of Inverpolly observation site.

The new deposition scheme also increases the annual average surface air concentration of ammonia from $\sim 0.02 \mu\text{g m}^{-3}$ to $\sim 0.05 \mu\text{g m}^{-3}$. The stomata emission is the mechanism which increases the ammonia surface air concentration in this situation.

Figure 1.49 shows the monthly prediction of the FRAME model for surface ammonia concentration at Bedingfield observation site for the year 1999. In contrast to the predicted concentrations at Inverpolly observation site the concentrations vary little through the months of the year. It also appears that the FRAME model does not capture the monthly variations in concentrations. This observation site is located in a mixed agricultural area where ammonia concentrations are strongly influenced by anthropogenic emissions from manure spreading or animal management. To be able to capture the monthly variations of the ammonia concentrations a detailed monthly emissions inventory is required.

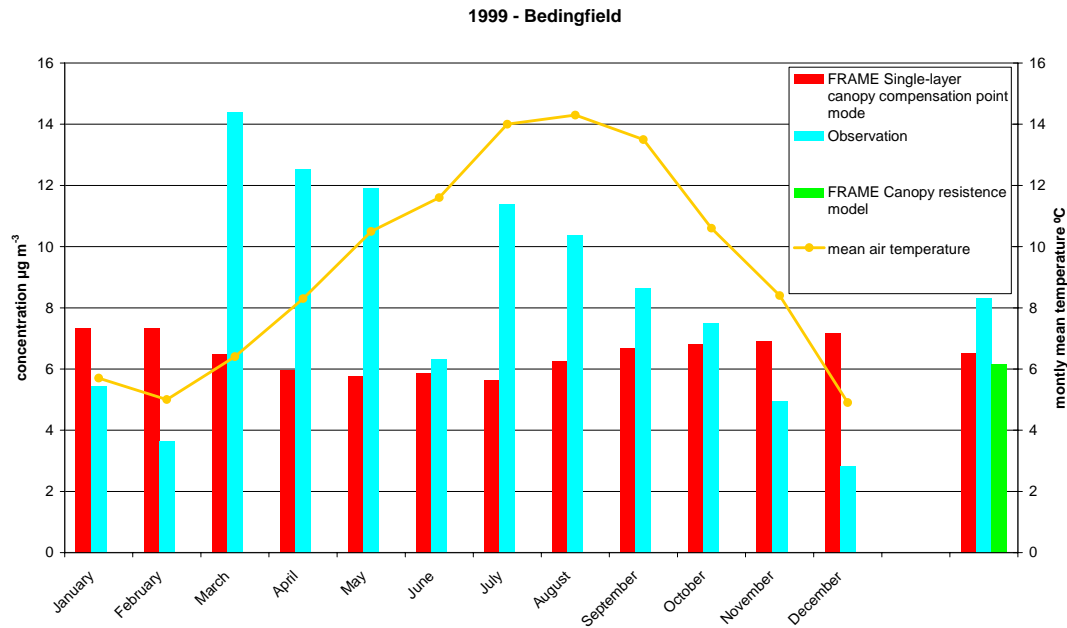


Figure 1.49 : Bedingfield 1999 ammonia concentration. Observations (Blue). FRAME model predictions: (Red) monthly predictions of single-layer canopy compensation point model, (Green) annual average canopy resistance model. The yellow line is the monthly mean temperature representative of Inverpolly observation site.

References

- Nemitz E., Sutton M.A., Schjoerring, J.K., Husted S, Wyers G.P., 2000. Resistance modelling of ammonia exchange over oilseed rape. *Agricultural and Forest Meteorology* 105 405-425.
- Sutton M.A., Asman, W.A.H., Schjoerring, J.K., 1994. Dry deposition of reduced nitrogen. *Tellus* 46B, 255-273
- Sutton M.A., Schjoerring, J.K., Wyers, G.P., 1995 Plant-atmosphere exchange of ammonia. *Phil. Trans. R. Soc. London A* 351, 261-278

2.8 Integrated Deposition monitoring

Eiko Nemitz, Mark Sutton, Daniela Famulari, Chiara di Marco, Robert Storeton-West, Sim Tang, David Fowler

The time-averaged gradient technique (TAG) is being developed as a relatively cost effective solution for measuring long-term dry deposition to ecosystems. Under the previous Acid Deposition Processes contract, a TAG system was developed and tested for NH₃ and SO₂. That system measured fortnightly averaged vertical gradients at three heights, using long-term denuders similar to those deployed within the UK Ammonia Monitoring Network. Air was sampled conditionally through these denuders, depending on meteorological conditions: the sampling pump was switched off during highly stable and unstable atmospheric conditions and when the wind direction was obstructed by buildings or limited fetch. The principal findings were that (a) the data quality depends crucially on the quality of the chemical analysis of the concentration measurements and (b) more than three heights are needed to quantify the quality of the gradient measurement and for outlier identification.

As part of the current project the TAG system at Auchencorth Moss was expanded (a) to measure at five heights, (b) to measure over an extended height range and (c) to measure the full suite of gases and aerosol compounds that are currently measured in the UK Nitric Acid Monitoring Network (i.e. NH₃, HNO₃, HCl, SO₂, NH₄⁺, NO₃⁻, Cl⁻, SO₄²⁻, Na⁺, K⁺, Mg²⁺, Ca²⁺). In order to cope with the increased analytical requirements, the time resolution was relaxed to monthly sampling. For the other aerosol species very small fluxes with deposition velocities of 0 to 5 mm s⁻¹ would be expected. Such small gradients are extremely difficult to detect with current analytical techniques and it is therefore vital to maximize the concentration differences, by increasing the height range compared with the old NH₃ TAG system. For this purpose the TAG system was implemented on a purpose-built 9-m tower as shown in Figure 1.50.



Figure 1.50. Expanded tower at Auchencorth Moss, with TAG samplers.

Figure 1.51-1.52 shows the results so far, while the measurements and chemical analysis are ongoing. Initially, data quality of the aerosol samples was compromised by leaks in the filter packs and very low aerosol concentrations ($< 0.1 \mu\text{g m}^{-3}$ of NH_4^+). A decision was made not to analyse these samples for ions in order to save costs for analysis later in the project.

For NH_3 the results look extremely encouraging, with robust fluxes and deposition velocities derived for most of the period. With the exception of two points, the error in the flux, derived from the scatter in the log-normal profile is good, reflecting the experience now gained in running TAG for NH_3 . Large error bars are associated with the two emission events observed (Jun 2005 and Dec 2006), and is therefore likely that deposition occurred throughout the measurement period. There is some disagreement between the concentrations derived with the TAG system as compared with the continuously sampling DELTA denuder of the UK Ammonia Monitoring Network, which suggests that the conditions excluded from the TAG sampling (very stable & unstable conditions, low wind speeds) significantly modify the concentration.

While the error bars on the NH_4^+ fluxes are similar to those of NH_3 , the magnitude of the fluxes is much smaller. This results in large error bars for the deposition velocities of NH_4^+ . Hence, despite the increase in the measurement range, the current system still struggles to provide values of V_d that are significantly different from 0.

Analysis for the other ions only started when the system was thought to be sampling robustly (Feb 2006) and some of the data are still awaiting processing. From the results so far, measurements of HNO_3 and HCl lie within the expected range, while the other aerosol compounds show similar features as NH_4^+ , with large scatter on the gradients. The scatter is not reflected in the variability of the blanks of the filters used for the aerosol measurements and must thus be introduced during sampling or filter handling. More tests are required to

improve the performance of the TAG system for the robust measurement of long-term aerosol gradients. Possibly, even more heights, or replicate sampling at several heights, would need to be implemented to obtain statistically significant fluxes of aerosol.

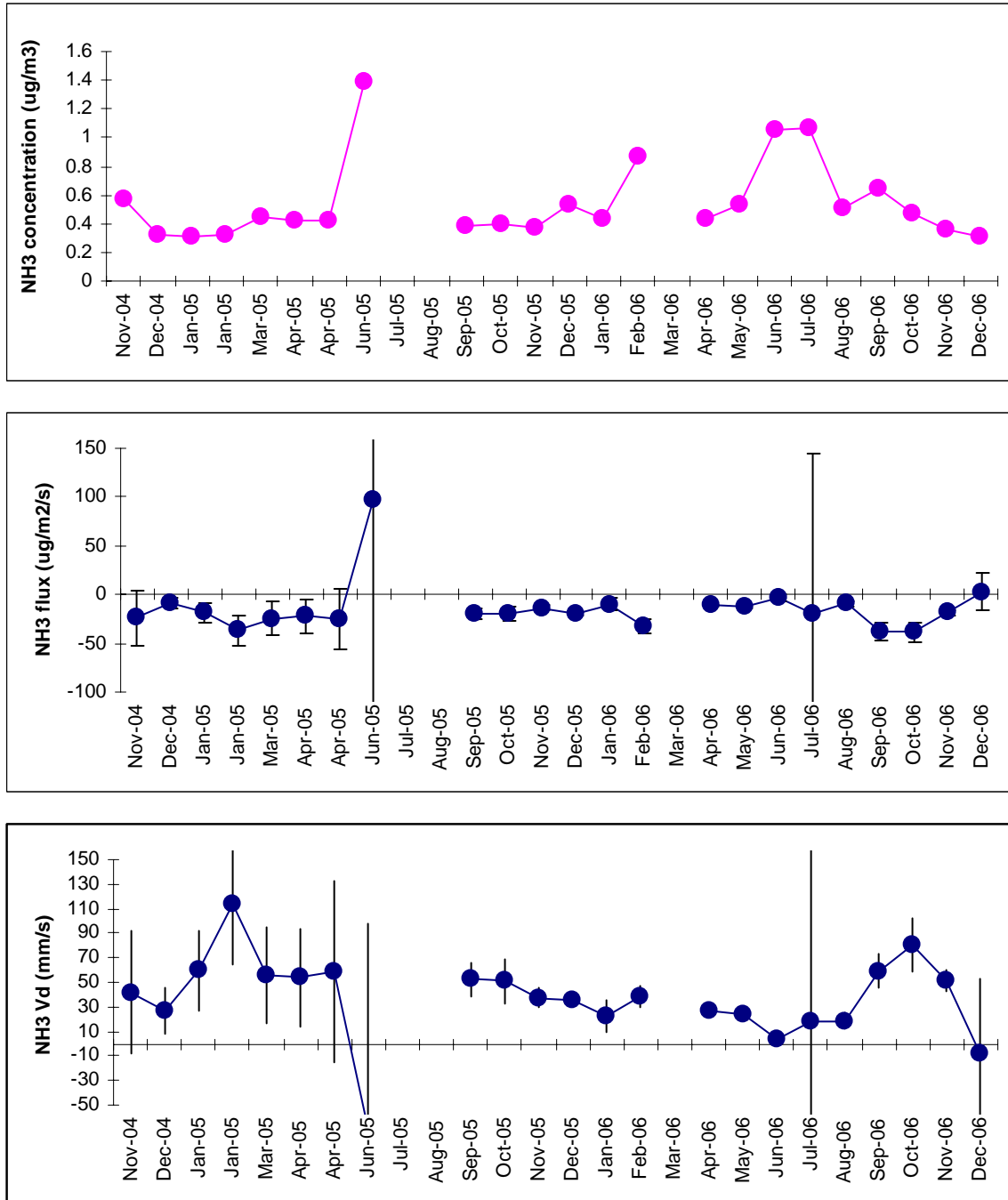


Figure 1.51. Results (concentrations, fluxes and deposition velocities) from the extended TAG system for integrated deposition monitoring for NH_3 .

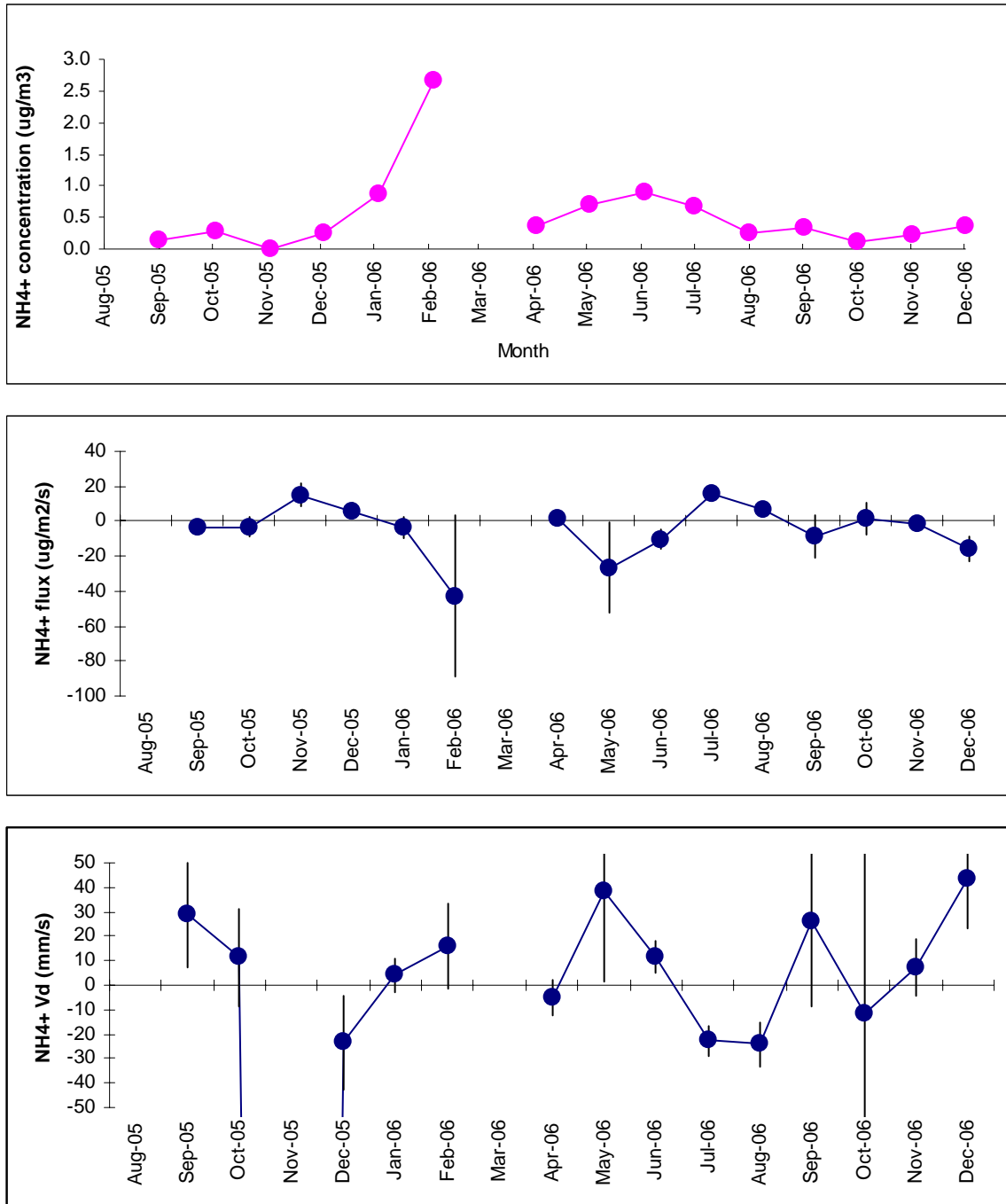


Figure 1.52. Results (concentrations, fluxes and deposition velocities) from the extended TAG system for integrated deposition monitoring for aerosol NH_4^+ .

2.9 Investigation of primary nitric acid emissions from agricultural activities

Eiko Nemitz, Marsailidh Twigg, Daniela Famulari, Rick Thomas, Tony Dore, Emily House, Neil Cape, Mark Theobald, Mark Sutton

Over the past 10 years several observations have indicated that nitric acid is not always deposited at the maximum rate allowed by turbulence, but that deposition can be significantly reduced, and even emission from animal wastes has been indicated by former CEH experiments. In particular, measurements during the 1995 Burrington Moor experiment under the MAFF funded ADEPT project, indicated that HNO_3 concentrations were elevated downwind of a slurry strip. The increase in HNO_3 lagged that of NH_3 by about 1 hour. During these measurements HNO_3 was measured with a wet-chemistry rotating batch denuder technique, in which the liquid samples were stored for typically 3 weeks prior to chemical analysis by anion chromatography. The potential of slurry to emit HNO_3 was confirmed in 1999 during first chamber experiment, again using the batch denuder.

Currently, the FRAME model underpredicts both HNO_3 and NO_3^- aerosol, compared with the measurements from the UK Nitric Acid Network, and here agricultural emissions of HNO_3 , not currently included in any emission inventories, would provide a possible explanation. In this contract variation, agricultural emissions of HNO_3 were investigated for the first time in a coherent manner, using two state-of-the-art instruments (GRAEGOR and TDL-AS). Three lines of enquiry were followed:

- a) Combined NH_3 and HNO_3 concentration measurements at farm yards at high temporal resolution,
- b) Laboratory (cuvette) measurements of slurry emission,
- c) Measurements of emissions from slurry application in the field.

Former observation of HNO_3 emissions were inferred with wet-chemistry systems, which could be sensitive to other gaseous forms of N that, once in solution, form NO_3^- which would be indistinguishable from HNO_3 . By contrast, tunable diode laser absorption spectroscopy (TDL-AS) is highly specific to HNO_3 . The GRAEGOR, although based on similar wet denuder technology and ion chromatography analysis as the batch denuder, enables online analysis without the need to store the samples.

These were the first measurements of HNO_3 made with the TDL-AS approach, several teething problems were encountered. For example, in the analysis of the earlier measurements, it was later found that the spectral absorption line chosen for the HNO_3 measurement overlapped with a very weak NH_3 line, which caused interference. While this interference would not have been significant for ambient measurements, it turned out to be important for measurements under the extreme situations of agricultural emissions, where the TDL-AS needs to detect 1000 ppb of NH_3 at the same time as 5 ppb of HNO_3 . This observation invalidates earlier results reported in a progress report for this project. In addition, the laser diode for HNO_3 failed during the measurements and had to be replaced and re-characterised. These problems limited progress with this work within the allocated project resources. To compensate, the overall research effort addressing HNO_3 emissions could be extended significantly through additional inputs from three studentships at CEH and a clearer picture of the emission process is now emerging.

MEASUREMENTS OF NH_3 AND HNO_3 AT FARMYARD LOCATIONS

The TDL-AS was operated at three farms (a cattle farm at Easter Howgate, Midlothian; a sheep farm at Dean Head, South Lanarkshire, and a poultry farm Earlston, Scottish Borders). Operation for HNO_3 was not only affected by the interference described above, but it was also noisy and showed significant negative values, especially after refilling of the cryogenic dewar. Although the measurements are not good enough to quantify ambient HNO_3

concentrations accurately, it could nevertheless be established that HNO_3 concentrations on the farmyards were $< 10 \mu\text{g m}^{-3}$, while NH_3 concentrations of several $100 \mu\text{g m}^{-3}$ were observed (Fig. 1.53). Hence an emission ratio of HNO_3/NH_3 from livestock wastes of several per cent, as indicated by the early measurements, is unlikely. The measurements also allowed a new photo-acoustic NH_3 sensor (NitroLux-100, Proanalytica, USA) to be compared with the TDL-AS at a poultry installation, covering a large range of concentrations (Fig. 1.53). The measurements show good agreement, with slightly larger concentrations indicated by the Nitrolux. The AMANDA system was operated at a slightly different location, with respect to the vent of the poultry house and the measurements are thus not entirely comparable. However, the slower response time of the AMANDA monitor compared with the other two instruments is clearly visible.

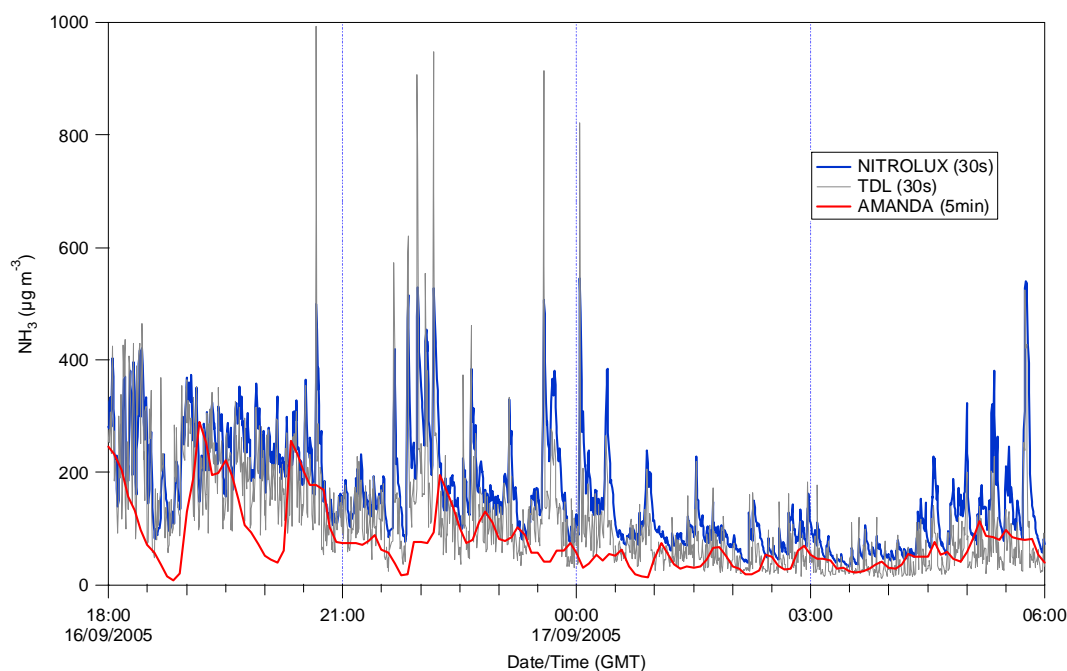


Figure 1.53. Measurements of ammonia concentrations next to a chicken farm.

LABORATORY BASED CUVETTE MEASUREMENTS OF HNO_3 EMISSION FROM SLURRY

As a next step, an attempt was made to confirm HNO_3 emissions from livestock wastes in the laboratory, using this new, improved technique. Slurry was placed in a cuvette in the laboratory and air was passed through the cuvette at a flow rate of 10 l min^{-1} and subsequently analysed for NH_3 and HNO_3 using TDL-AS or QCL-AS (Fig. 1.54). A total of five cuvette runs were conducted as summarised in Table 1.13. For the first experiment, a rather thick layer of slurry was placed in a dynamic flow-through cuvette (Fig. 1.54), which, even after 25 days, had not fully dried out, and probably more resembled the behaviour of a drying cow pad. Subsequent applications were much shallower and dried in at least 4 days.

During selected experiments a proton transfer reaction mass spectrometer (ptrms; Ionicon) was used to measure the emission of selected organic compounds, an infra-red gas analyser (IRGA; LiCor model 7000) was used to measure CO_2 and H_2O , or the GRAEGOR instrument was used to provide additional measurements of HNO_3 and HONO.



Figure 1.54. Photograph of the cuvette setup used to quantify HNO₃ emission from slurry under semi-controlled conditions.

Table 1.13 Summary of the cuvette runs to quantify HNO₃ emission from slurry emissions, indicating what compounds were measured with which instrumentation.

Run	Date	Duration [days]	NH ₃	HNO ₃	CO ₂ /H ₂ O	VOCs	HONO	Comments
I	28/07/05	25	TDL	TDL				NH ₃ interference on HNO ₃
II	11/04/06	3	TDL	TDL	IRGA	ptrms		Noisy HNO ₃
III	14/04/06	2.2	TDL	TDL	IRGA	ptrms		Noisy HNO ₃
IV	11/12/06	1.3	QCL,PA	GRAEGOR,QCL			GRAEGOR,QCL	
V	13/12/06	1.3	QCL,PA	GRAEGOR,QCL			GRAEGOR,QCL	
VI	15/12/06	2	QCL,PA	GRAEGOR,QCL			GRAEGOR,QCL	Slurry spiked with NH ₄ NO ₃

Figure 1.55 shows the time series in the NH₃ concentration at the outlet of the cuvette as measured with the TDL-AS, while Figure 1.56 shows the cumulative emission flux for the first three experiments. The results show that, while during experiments II and III emission had virtually stopped at the end of the campaign, experiment I had to be aborted although emission had not full subsided.

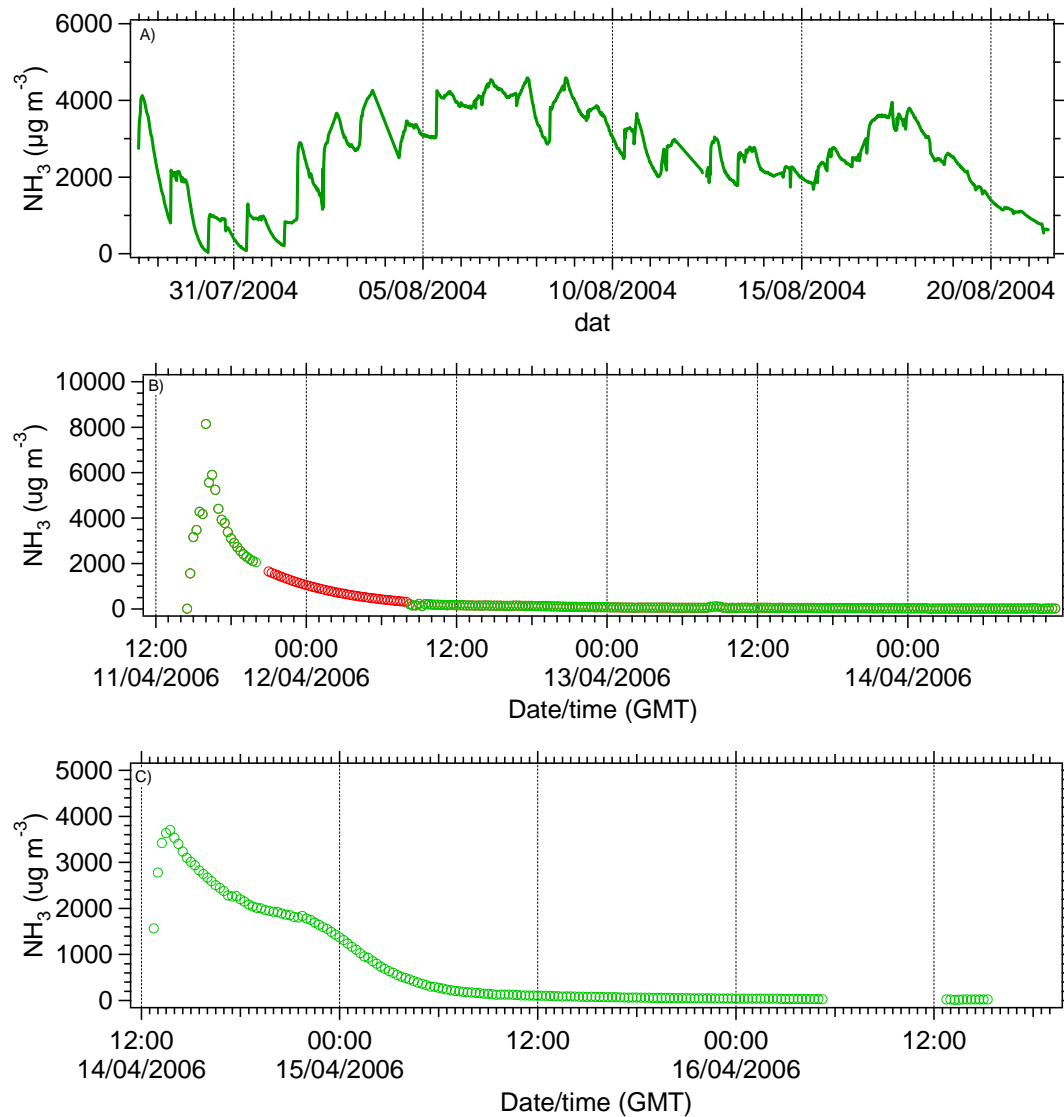


Figure 1.55. NH_3 concentrations (15 minute averages) measured from the cuvette during A) Experiment I, B) Experiment II, C) Experiment III. (The red markers in B) are estimated values which were determined through the exponential fitting, during a period where the dual TDLAS was not operational.)

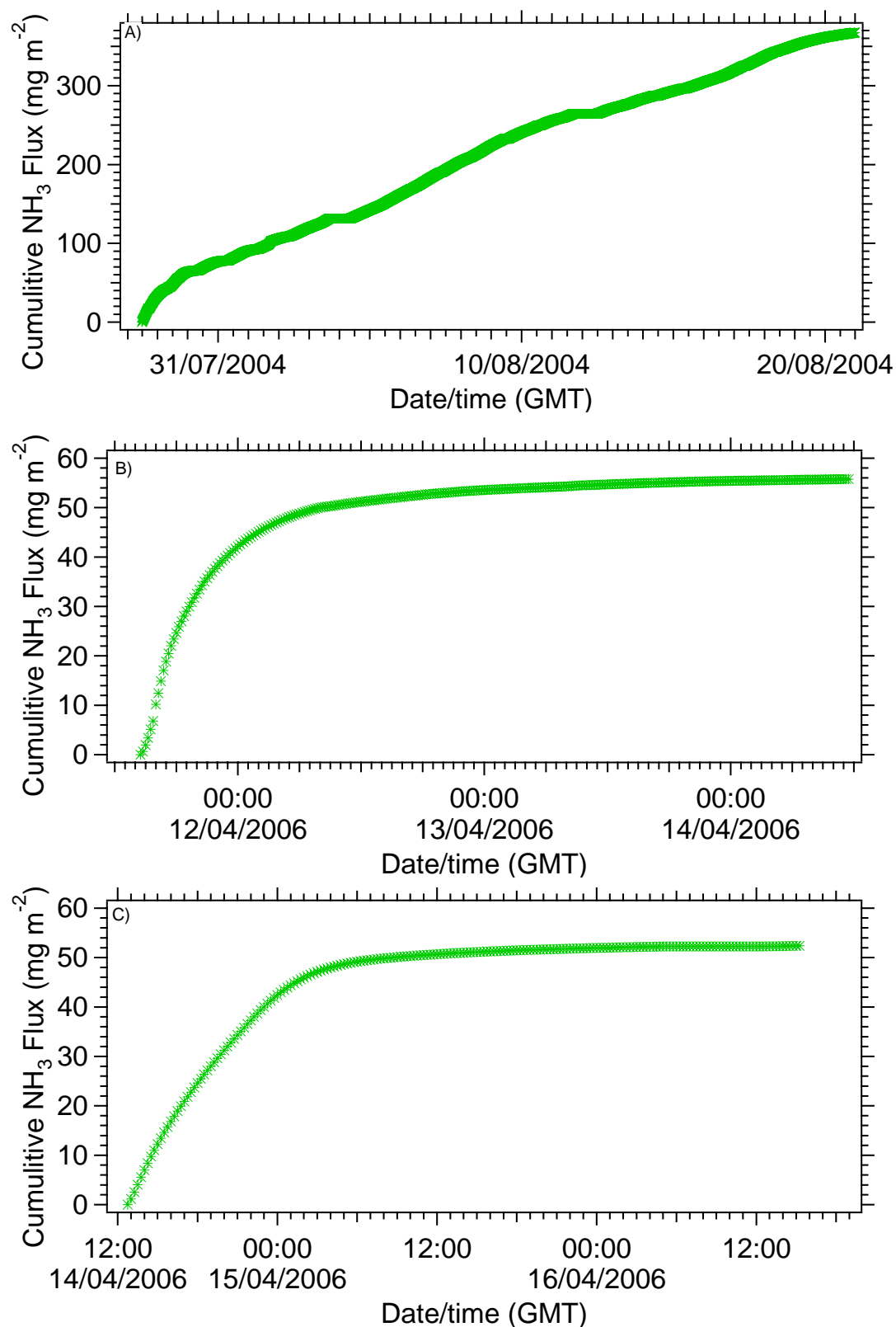


Figure 1.56. Cumulative NH_3 flux (based on 15 minute averages) during A) Experiment I, B) Experiment II, and C) Experiment III.

During experiment I, the HNO_3 was affected by the NH_3 interference described above and the measurements are therefore not useful. During experiments II and III a different absorption line was used, but the measurement was noisy, especially after refills of the dewar with liquid nitrogen (an automated refill every 3 hours). The filtered concentrations (excluding periods

during and after refill) ranged from -33.8 to $35.6 \mu\text{g m}^{-3}$, with an average of $3.03 \mu\text{g m}^{-3}$ during Experiment II. In Experiment II the concentration ranged from -11.6 to $12.1 \mu\text{g m}^{-3}$, with an average concentration of $0.52 \mu\text{g m}^{-3}$ (Fig. 1.57). Excluding the data after refill, these measurements nevertheless allow an upper estimate of the concentrations and hence emissions of the HNO_3 from the slurry cuvette.

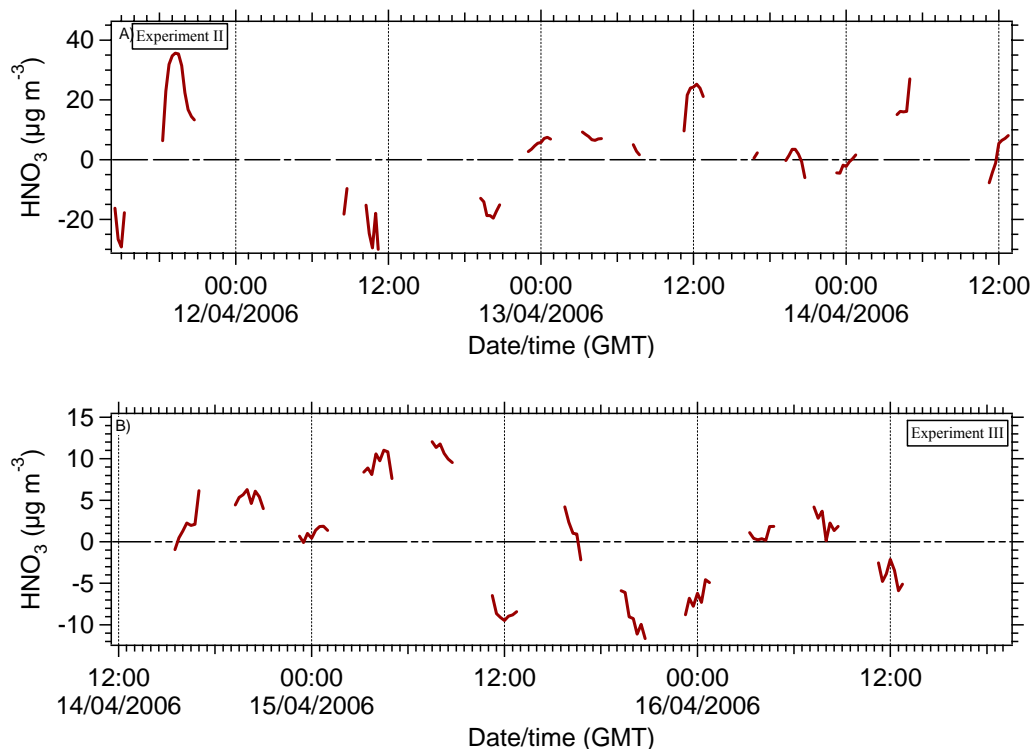


Figure 1.57. Measured HNO_3 concentration at the cuvette outlet during experiments II and III.

Figure 1.58 provides an overview of the fluxes of the VOCs (and nitric acid) in relation to the flux of NH_3 during experiments II and III, which illustrates the relative magnitude but, importantly, also the temporal sequence of the emissions (note the logarithmic scales). It is noted that a range of organic compounds is released from the slurry, but that the peak in the emission differs between compounds. In particular, significant emission of acetic acid was observed, but this emission peaked typically 8 hours after the peak in the ammonia emission. The measurements also indicate emission of organic N compounds (notably trimethylamine) from the slurry, which occurs at the same time as the NH_3 emission and amounts to 7.4 % of the NH_3 emission (in terms of nitrogen).

Following the observation of HONO emissions during the field experiment in 2005 (see below), three more cuvette experiments (Experiments IV to VI) were performed in December 2006, during which an attempt was made to measure HNO_3 and HONO by QCL and with the GRAEGOR instrument. Early results indicate that there was indeed HONO emission, but the data are still being analysed.

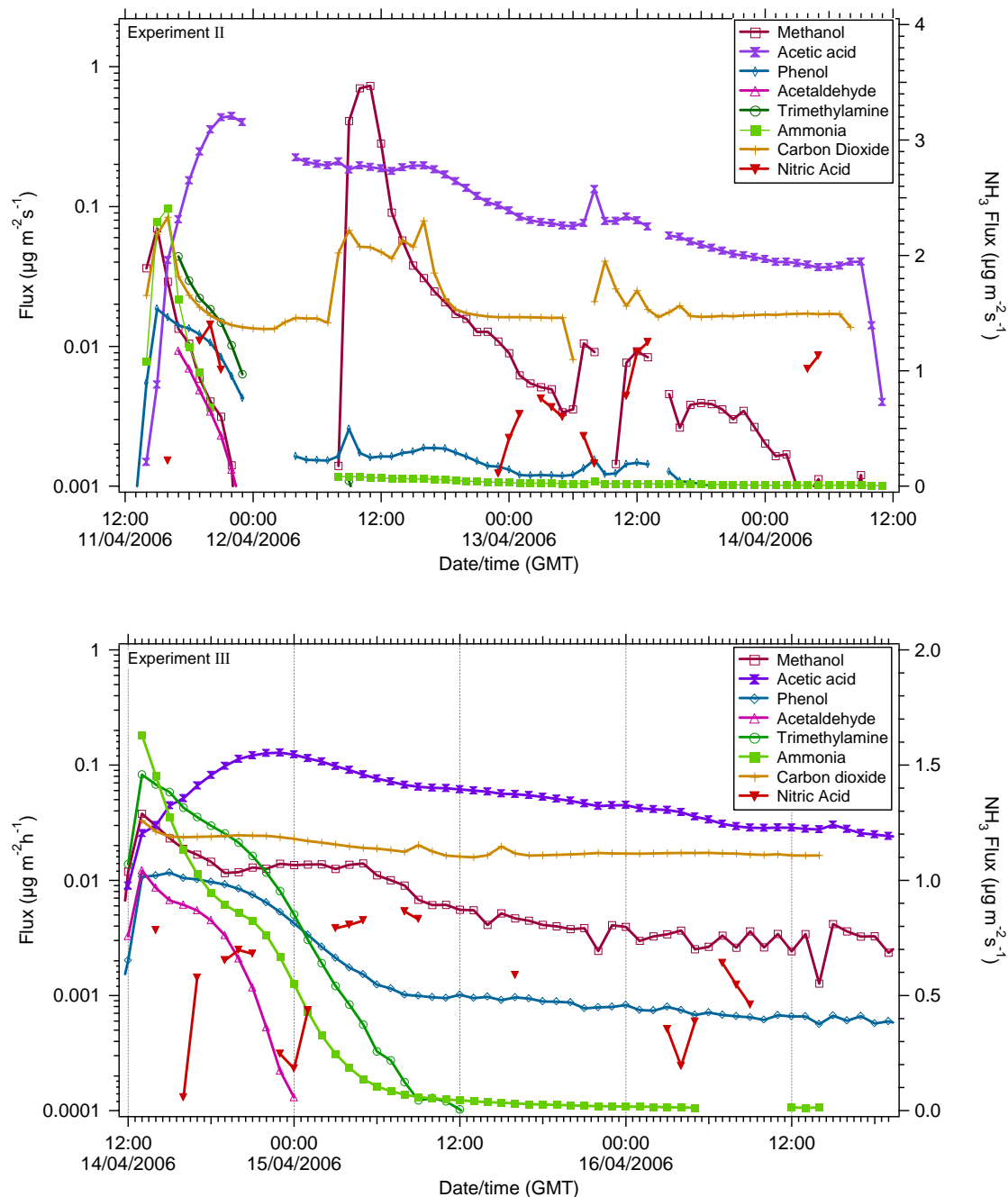


Figure 1.58. Graphs illustrating the sequence of emission fluxes during Experiments II and III.

FIELD EXPERIMENT OF SLURRY APPLICATION

Sizeable field experiments were conducted in the autumn 2004 and spring 2005, in order to quantify the emission of HNO_3 from slurry applied to grassland and to investigate the potential for associated aerosol formation. Measurements include:

- fast concentration of NH_3 and HNO_3 by TDL-AS (see above);
- concentration gradients of gaseous HNO_3 , HCl , HONO and SO_2 as well as aerosol NO_3^- , Cl^- and SO_4^{2-} using a combination of wet rotating denuder and steam jet aerosol collector (GRAEGOR);
- concentration and flux measurements of volatile organic compounds by proton transfer reaction mass spectrometry;

- concentrations, size-distributions and fluxes of aerosol NO_3^- using an aerosol mass spectrometer (AMS);
- particle number fluxes by condensation particle counter (CPC).

The NH_3 concentrations and fluxes measured during these campaigns were presented above (e.g. Tables 1.1 to 1.4). The concentrations and fluxes of HNO_3 , NO_3^- aerosol and SO_4^{2-} aerosol are shown in Fig. 1.59 for the 2005 campaign for the days following slurry application.

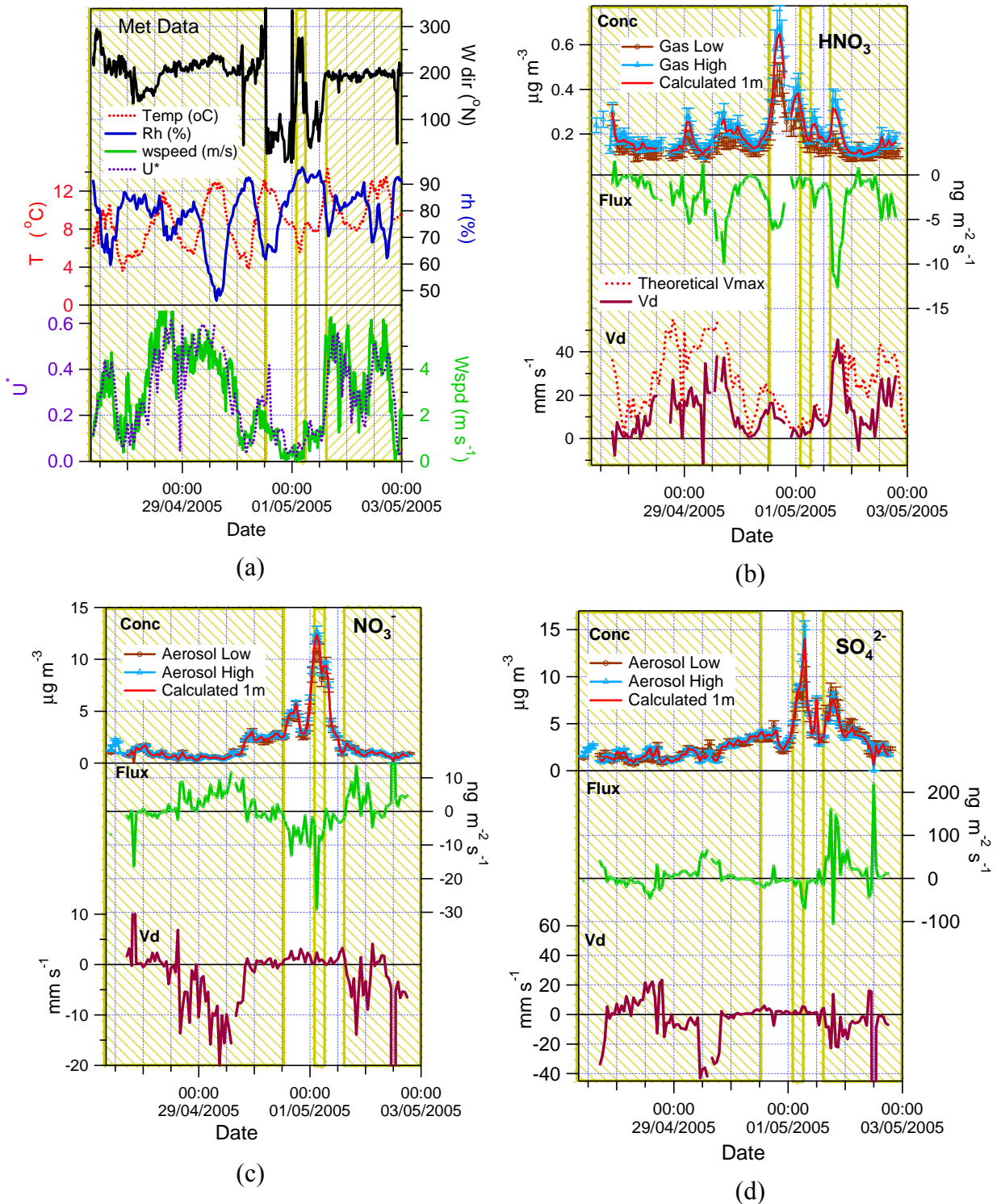


Figure 1.59. Concentrations, fluxes and deposition velocities of selected compounds during the 2005 slurry experiment. Hatched areas indicate periods were the wind was coming from the fertilised South field.

The measurements were made on the boundary of two fields and only one field (the S field) was fertilised. Wind direction from this fertilised field is indicated by hatched background. The measurements show that, during northerly winds, HNO_3 was deposited at a rate close to its theoretical maximum, while the aerosols were deposited with a V_d in the range of 1 to 3 mm s^{-1} . By contrast, during southerly winds, HNO_3 shows a deposition slower than theoretically predicted, while NO_3^- is emitted during these periods. Quantitatively, the NO_3^- emission flux approximately balances the HNO_3 deposition, leading to a flux of total nitrate ($\text{TN} = \text{NO}_3^- + \text{HNO}_3$) that is close to zero. No significant HNO_3 emission was observed during the campaigns.

By contrast, unexpectedly, HONO emission was observed during the first four days following slurry application (Fig. 1.60). A similar observation has since been reported by Stemmler *et al.* (2006), who observed HONO emission from NO_x reaction with humic acid.

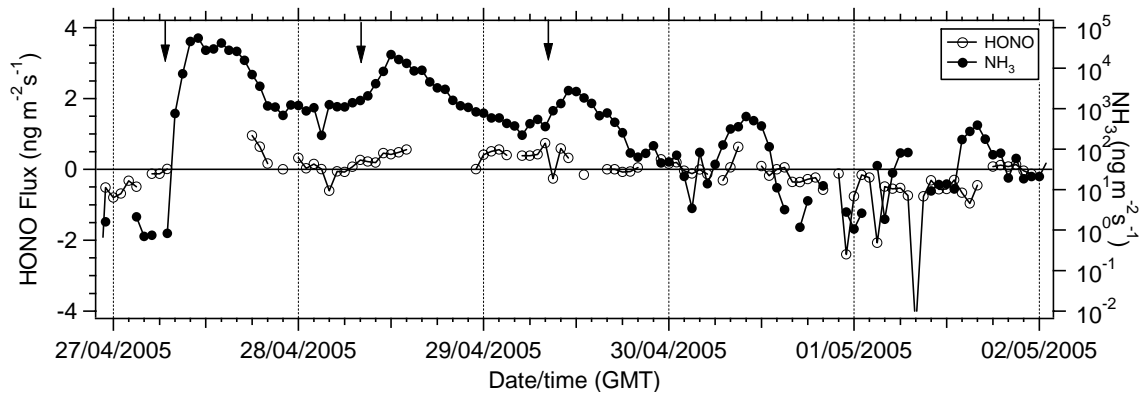


Figure 1.60. Graph demonstrating the relationship between NH_3 and HONO fluxes in relation to emissions from slurry.

The ptrms measurements in the field are consistent with the cuvette measurements and indicate, inter alia, that acetic acid is emitted from the slurry (Fig. 1.61). Note that Fig. 1.61 shows air concentrations rather than fluxes, which for compounds with a low ambient background is directly related to the emission flux, while for other compounds is also affected by background concentrations. In particular, the elevated concentrations in HNO_3 and HONO during 30-Apr and 2-May are due to polluted air masses arriving at the site (as also reflected in high aerosol concentrations, Fig. 1.59) rather than emission from the field.

SCALING-UP OF THE EFFECTS OF AGRICULTURAL HNO₃ EMISSIONS ON UK BUDGETS

An initial investigation was undertaken into the effect of including agricultural primary HNO₃ emissions on the agreement between the FRAME model predictions and the measurements, assuming that primary HNO₃ emission from livestock wastes amounts to 4% of the NH₃ emissions. In the light of the new investigations presented here, this is likely to be an overestimate.

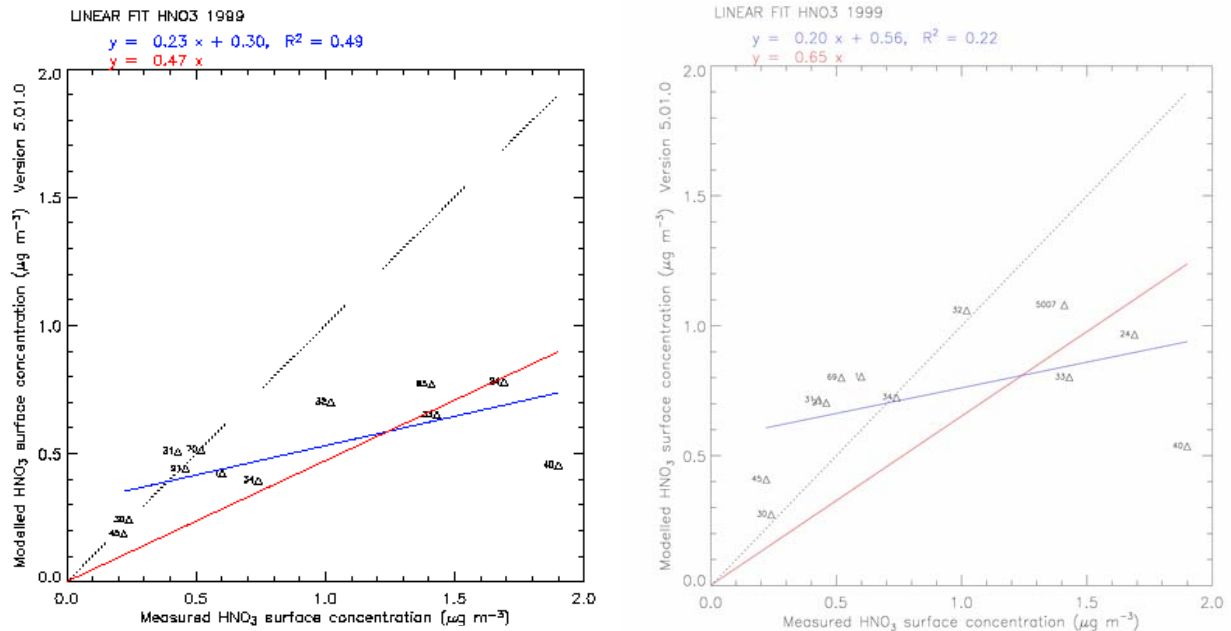


Figure 1.62. Comparison of annual HNO₃ concentration predicted by FRAME with data from the UK Nitric Acid Network (a) before and (b) after inclusion of primary HNO₃ emission.

SUMMARY OF THE CURRENT UNDERSTANDING OF HNO₃ EMISSION FROM LIVESTOCK WASTES

From the old investigations, based on measurements with batch wet denuders and analysis by ion chromatography, it had been hypothesised that HNO₃ emission is emitted from livestock wastes (in particular cattle), amounting to approximately 5 % of the NH₃ emission. It was thought that the time lag between NH₃ and HNO₃ emissions in the earlier measurements could be due to the fact that the surface pH decreases as NH₃ is lost from the slurry, eventually enabling HNO₃ to come off as well. One conundrum of this interpretation was that, at high concentrations, NH₃ would normally react with HNO₃ to form NH₄NO₃ aerosol.

Based on the new observations the following picture starts to emerge:

1. The measurements here confirm large NH₃ emissions from slurry application (in cuvette and field).
2. Significant HNO₃ emission (at the level of a few % of the NH₃ emission) was not confirmed during the measurements analysed so far (neither at farms, during cuvette or during the field experiments). It is possible that such emission may occur in special situations such as slurry application to soils already high in NO₃⁻ or with very low pH, but they are certainly not widespread.
3. Slurry spreading appears to lead to NH₄NO₃ aerosol formation. As a consequence, the HNO₃ from the atmosphere does not reach the ground but is incorporated into aerosol by reaction with the emitted NH₃. This reduces the N deposition during these periods (NO₃⁻ aerosol deposits more slowly than the HNO₃ would have done), but the relative contribution to the overall N budget is small as NH₃ dominates the exchange.

4. Although HNO₃ emission was not detected, emission of an organic acid (acetic acid) was observed. This indeed lagged behind the emission of NH₃, supporting the hypothesis that changes in pH and solubility with time govern the sequence of the emissions.
5. HONO emission was detected following slurry spreading, consistent with recently published work (Stemmler *et al.*, 2006), which shows HONO production from humic acid. During the Easter Bush experiment this emission did not amount to 5%, but the importance may vary with slurry type as well as meteorological and soil conditions.
6. It is possible that the HNO₃ emission detected in the earlier studies, in reality, represented HONO emissions. Capture of HONO would result in NO₂⁻ in solution, which, during storage, may have been further oxidised to NO₃⁻ and thus been interpreted as HNO₃.
7. Emissions of HONO and amines appear to be a larger additional N source from livestock wastes than HNO₃ which deserve better quantification.

References

- Famulari, D.; Fowler, D.; Hargreaves, K.; Milford, C.; Nemitz, E. and Weston, K. (2004). Measuring eddy-covariance fluxes of ammonia using tunable diode laser absorption spectroscopy. GaNE special issue of *Water, Air and Soil Pollution – Focus* 4(6), 151-158.
- Fowler, D., Mueller, J., Smith, R.I. and Cape, J.N., 2005. Non-linearities in source receptor relationships for sulfur and nitrogen compounds. *Ambio*, 34: 41-46.
- Nemitz, E., Gallagher, M.W., Duyzer, J.H. and Fowler, D., 2002. Micrometeorological measurements of particle deposition velocities to moorland vegetation. *Quarterly Journal of the Royal Meteorological Society*, 128: 2281-2300.
- Nemitz, E. and Sutton, M.A., 2004. Gas-particle interactions above a Dutch heathland: III. Modelling the influence of the NH₃-HNO₃-NH₄NO₃ equilibrium on size-segregated particle fluxes. *Atmospheric Chemistry and Physics*, 4: 1025-1045.
- Stemmler, K., Ammann, M., Donders, C., Kleffmann, J., and George, C. 2006. Photosensitized reduction of nitrogen dioxide on humic acid as a source of nitrous oxide. *Nature* 440:195-198.
- Twigg, M. (1996) Application of tunable diode laser absorption spectroscopy for the investigation of surface-atmosphere exchange of ammonia. PhD Thesis. 218 pp. University of Ulster.
- Thomas, R., Trebs, I., Otjes, R., Jongejan, P.A.C., ten Brink, H., Phillips, G., Meixner, F.X., Nemitz, E. (2007) A continuous analyser to measure surface / atmosphere exchange fluxes of water soluble inorganic aerosols and reactive trace gases. In preparation for *Environmental Science and Technology*
- Whitehead, J.D. 2006. Atmospheric ammonia measurements using a quantum cascade tunable diode laser absorption spectrometer. PhD Thesis. 189 pp. Manchester University.

2.10. Bias from dry deposition – Dry deposition on bulk rain collectors

USE OF ‘FLUSHING’ RAIN GAUGES TO ESTIMATE THE CONTRIBUTION OF DRY DEPOSITION TO BULK RAIN COLLECTORS.

J Neil Cape

Background

As reported at the meeting with Defra at CEH Edinburgh in February 2006, the initial operation of the set of 3 ‘flushing’ gauges in parallel with 3 standard bulk collectors was described, and a significant discrepancy in volume of precipitation collected was noted. Since then, new software has been installed and the funnel/bottle connectors have been redesigned to avoid that problem.

Methods

Between March and June 2006 the 3 ‘flushing’ gauges were operated in parallel with 3 standard bulk gauges (Figure 1.63), but with the flushing mechanism turned off – i.e. this was a direct comparison of the two types of gauge, the only difference being that in the standard gauge, the sampling funnel is connected directly into the sample bottle, whereas for the ‘flushing’ gauge, the rain passes from the funnel through a short length of silicone tubing to the valve that separates the washings from the rain sample, and then down ca. 1.5 m silicone tubing to the sample bottle which is kept in the dark at ground level.

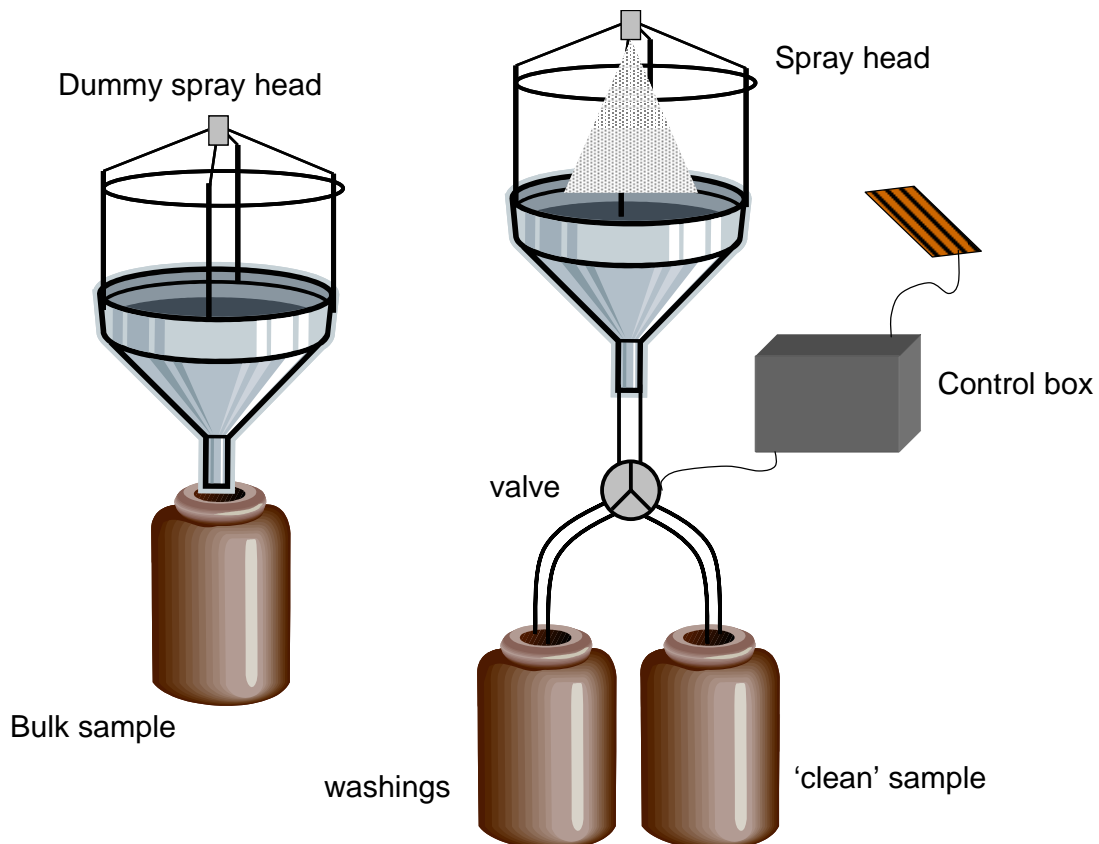


Figure 1.63. Diagram of standard bulk collector (left) fitted with dummy spray head for direct comparison with the flushing gauge (right). When rain is detected, the funnel surface is flushed with a 10% methanol solution for 10 seconds, the washings being collected in one bottle. The valve then switches so that the rain collected by the cleaned funnel is diverted to the ‘clean’ sample bottle.

Between June and September, the flushing gauges were operated as designed, with a 20 second rinsing of the funnel surface using 10% methanol solution, when rain is detected, collected separately from the main sample. In principle, the amount of dissolved material collected in the washings and the sample should equate to that collected by the bulk collector.

In the following data analysis, the dataset has been restricted to those weeks for which there was a valid sample from all 6 collectors – a sample might be lost through wind displacing a funnel (a recurrent problem which has been fixed), or through contamination by birds (detected in terms of high ammonium and potassium concentrations).

Results

March-June

The total amount of material deposited to the 3 flushing gauges is expressed as a % of the total deposited to the 3 standard bulk collectors in Figure 1.64. The error bars refer to the combined uncertainties of 3 replicate collectors of each type, and the asterisk denotes a statistically significant difference (two-sided t-test) between the gauge types.

The amount of water collected in the flushing gauge was only slightly (but consistently and significantly) less than in the bulk collectors (95%). The geometry of the two types of funnel is identical, suggesting that there may have been a small amount of evaporation from water retained in the silicone tubing between the funnel of the flushing gauge and the valve, which caused a restriction to the flow. There was no obvious leakage of water from the valve or tubing connectors. As the 6 gauges are all deployed within an area 5 m x 5 m it is unlikely that there was a real difference in the amount of precipitation between the two sets of gauges. More puzzling is the consistent difference in amounts of deposited solutes in the two types of gauge, with the flushing gauge having only 70-80% of the solutes deposited in the bulk collector. This difference cannot be explained by the slightly smaller volume of rain collected in the flushing gauges. The measured ion concentrations in the flushing gauges were consistently less than for the standard bulk collector. There are three possible explanations: (1) that there were losses of all ions (cations and anions) in the sample tubing between the funnel and the sample bottle, or from the sample bottle itself during sampling; (2) that there was additional (dry) deposition of material to the bulk collector, because of the proximity of the sample to the open air, immediately below the funnel; or (3) that prior use of the flushing gauges with the methanol solution had altered the properties of the funnel surfaces, leading to less dry deposition. The first explanation seems unlikely, that all types of ion could be consistently retained within the sampler over a period of 3 months. However, the second also seems unlikely, that particles (Na and Cl) should give the same level of additional dry deposition, by diffusion through the funnel into the sampling bottle, as water soluble gases (NH₃ and SO₂). If the third explanation were to be true, it would imply that a subtle difference in funnel surface altered dry deposition by up to 30% of the total deposition, and would be of concern for all studies using bulk collectors.

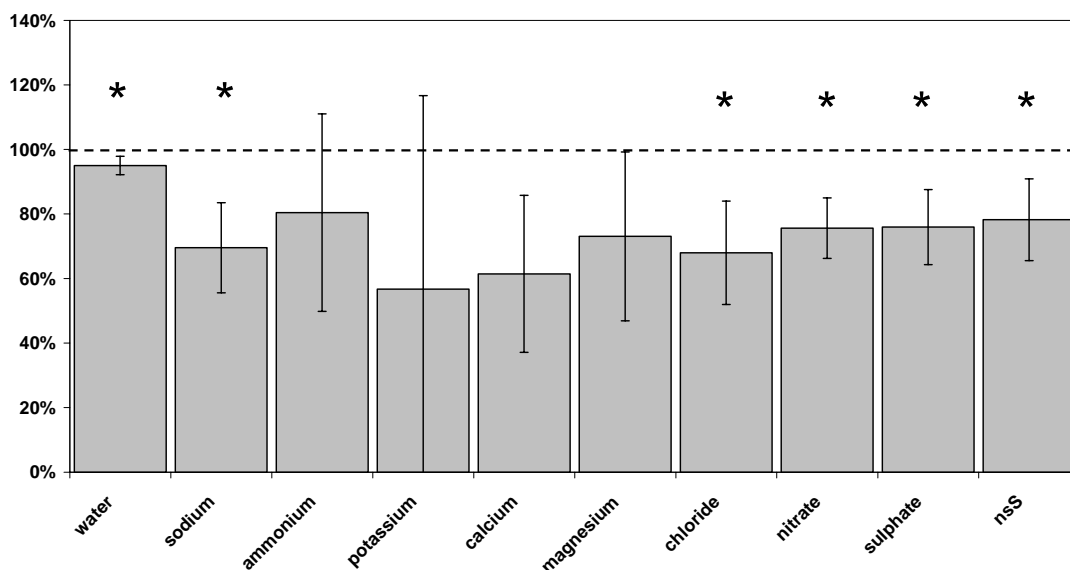


Figure 1.64. Comparison of deposition to permanently open flushing gauges and to standard bulk collectors – ratio of deposit in flushing gauges to standard collectors as %

June-September

There were 6 weeks with valid samples from all 6 gauges during the period. The flushing gauges operated as designed during the period, and showed a similar pattern of water capture as in the previous period, with 96% of rainfall amount collected in the flushing gauge as rain sample (Figure 1.65). Total deposition of ions, in the funnel washings and in the rain sample, were more variable than in the previous experiment, with ‘losses’ relative to the bulk collector of ammonium, nitrate and sulphate, and ‘gains’ of calcium, magnesium and chloride. Separation of the total into the ‘clean’ sample and the funnel washings is shown in Figure 1.66. The behaviour of the solutes reflects different sources; deposition of particulate material (calcium, magnesium, sodium, chloride), likely to be in the form of ‘large’ particles (diameter > 1 micron), was enhanced, and much of the enhancement was in the funnel washings (i.e. dry deposition to the funnel). There may also be a contribution from trace amounts of calcium and magnesium in the washing solution, because overall concentrations of Ca and Mg were small. Concentrations of 1-4 μM of Ca and Mg were measured in samples of the wash solution, with no measurable contribution from other ions. Sodium and chloride deposition were similar in both types of gauge, but variable across gauges, reflecting the random sampling of large sea-salt particles, which contribute to solution composition differences across gauges, regardless of type. For the other ions, the total amount deposited to the flushing gauges was, as before, 60-80% of that deposited to the standard bulk collector.

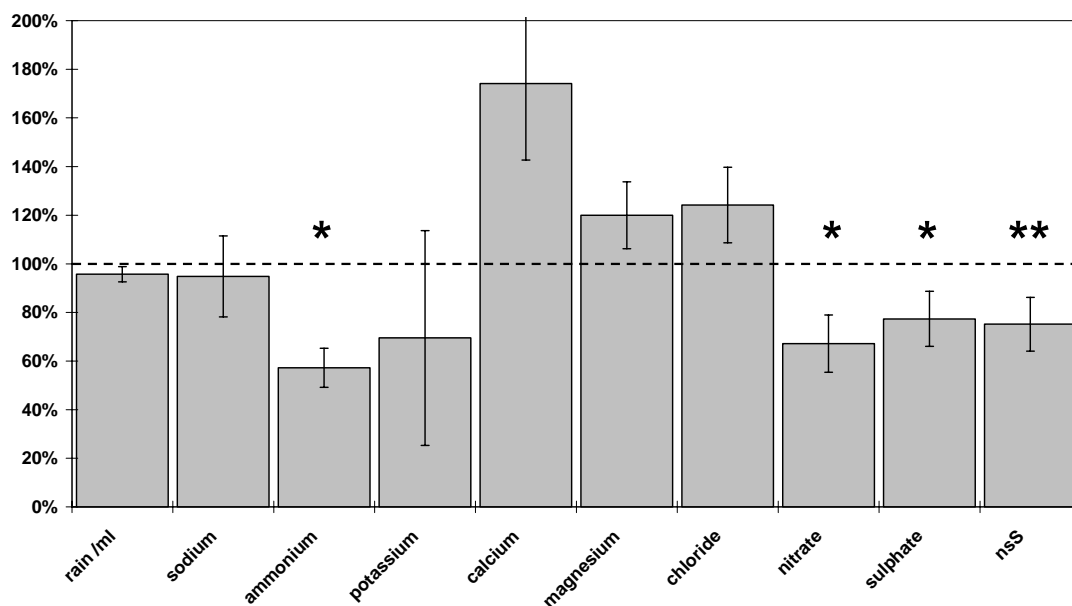


Figure 1.65. Total amount (washings + 'clean' sample) deposited in flushing gauge as ratio to amount deposited in standard bulk collector (%)

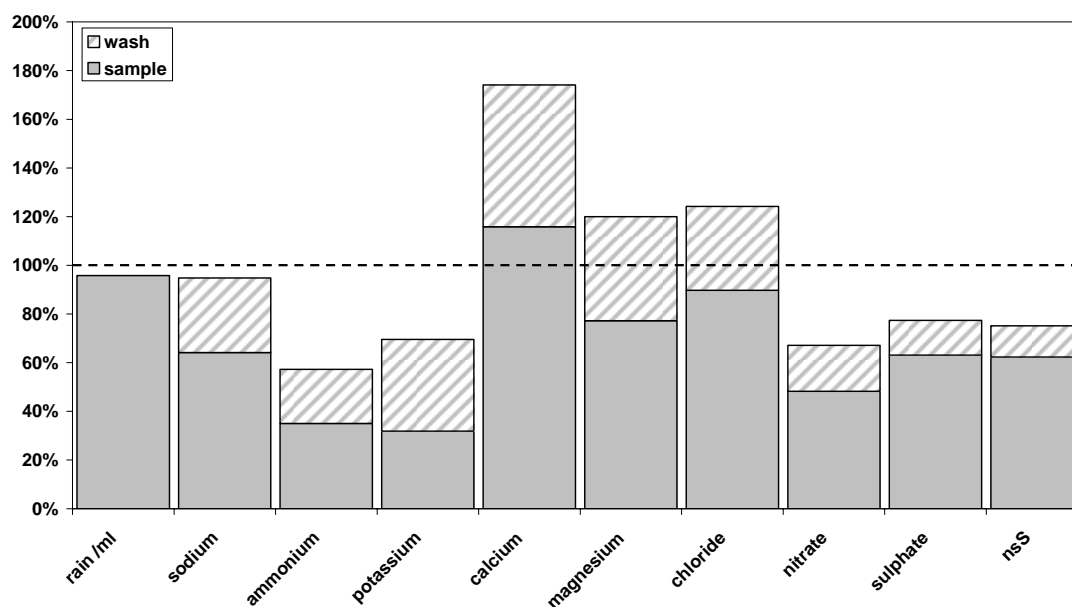


Figure 1.66. As Figure 1.65, but showing separately the amount deposited in the washings and in the 'clean' sample.

The data in Figure 1.66 suggest that the contribution of dry deposition (measured as the funnel washings) to the total collected in the flushing gauges was: ammonium $39 \pm 21\%$, nitrate $28 \pm 15\%$ and non-sea sulphate $17 \pm 6\%$. If the explanation for the consistently lower deposition to the flushing gauges than to the standard bulk collectors, seen in both sets of data, is related to additional dry deposition to the bulk collector, then the overall contribution of dry deposition would be even greater.

Absolute deposition (micromoles/sampler) is shown for each of the ions in Figure 1.67. This figure also shows the maximum contribution from dry deposition (assuming this to be the main source of difference) by direct comparison of the amounts deposited in the standard bulk collector (hatched) and in the sample bottle from the flushing gauge (grey).

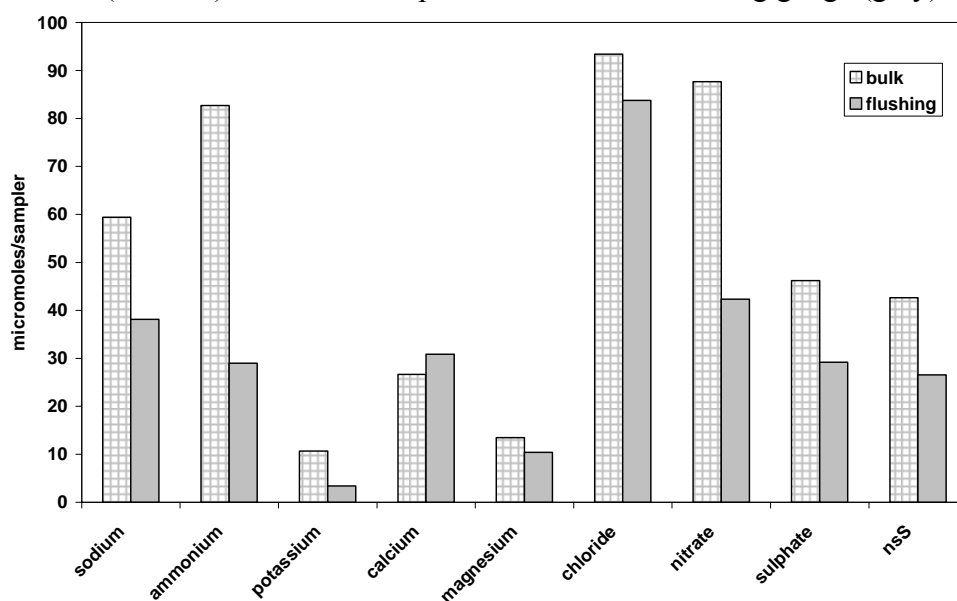


Figure 1.67. Deposition of ions to standard bulk collectors (hatched) and in ‘clean’ samples from the flushing rain gauges.

Conclusions

These results imply a significant contribution from dry deposition for some ions at this site. The measurements are continuing into 2007, operated by a PhD student as part of his research into organic N in rain. The samplers will be deployed to 3 separate sites, as originally planned, during spring 2007. Future results will be reported to Defra.

3. MAPPING DEPOSITION

3.1 UK 5km wet deposition maps

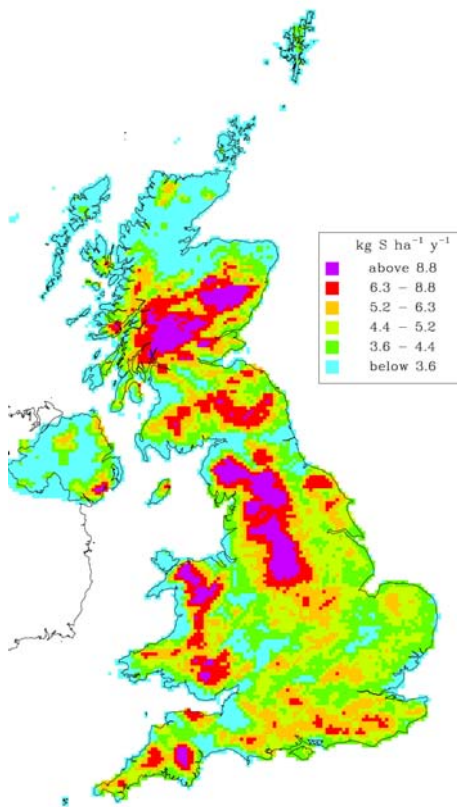
Rognvald Smith

MODELLING WET DEPOSITION ACROSS THE UK

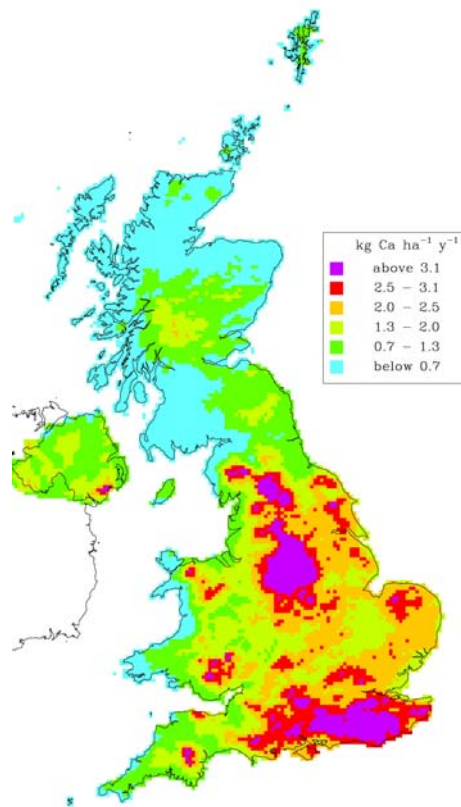
Maps of rainfall concentration are derived using kriging interpolation from the measurements at between 30 and 40 sites within the Acid Deposition Monitoring Network. The rainfall amounts are taken from annual maps at the 5km scale supplied by the Meteorological Office.

Over hill terrain, both rainfall amount and rain concentration are increased by the presence of orographic cloud (see section 1.6 above). The seeder-feeder enhanced wet deposition is calculated by partitioning the rainfall amount into its two components and by assuming that concentration of the feeder component, formed from the orographic cloud, is a factor of 2 greater than the concentration in the seeder component.

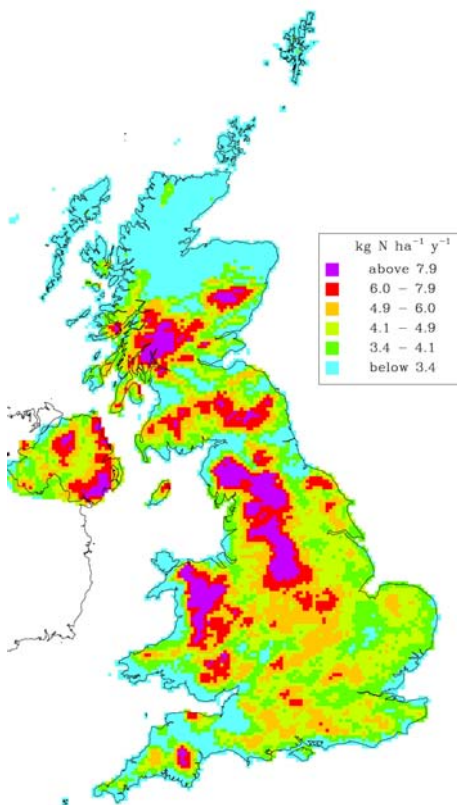
Annual maps of seeder-feeder enhanced wet deposition for non-seasalt sulphate, non-seasalt calcium, ammonium and nitrate are shown in Figure 2.1 (a-c).



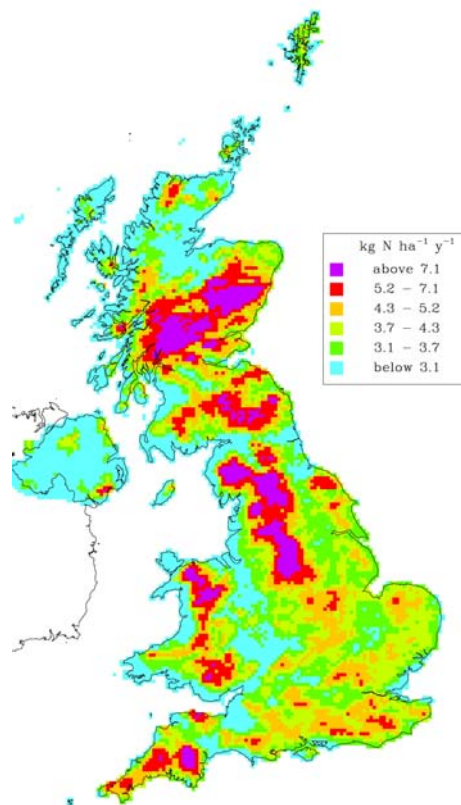
Wet deposition, non-seasalt Sulphur, 2002



Wet deposition, non-seasalt Calcium, 2002

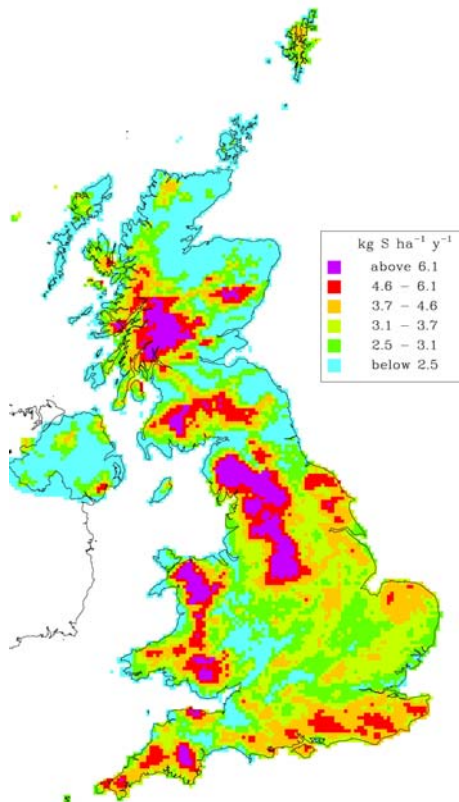


Wet deposition, Ammonium, 2002

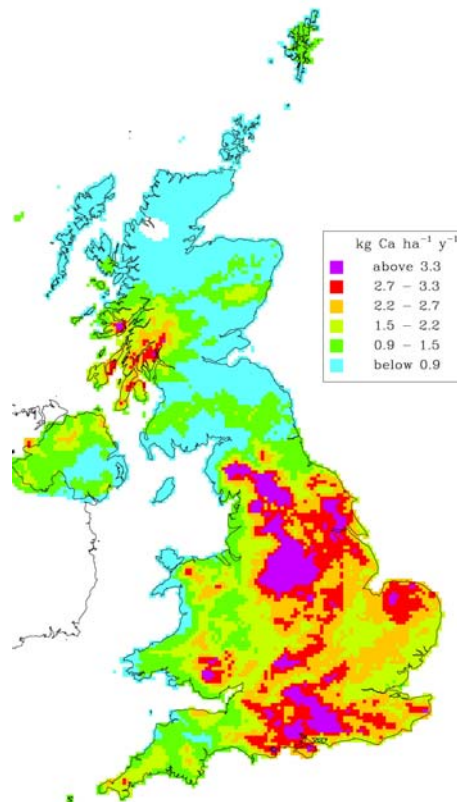


Wet deposition, Nitrate, 2002

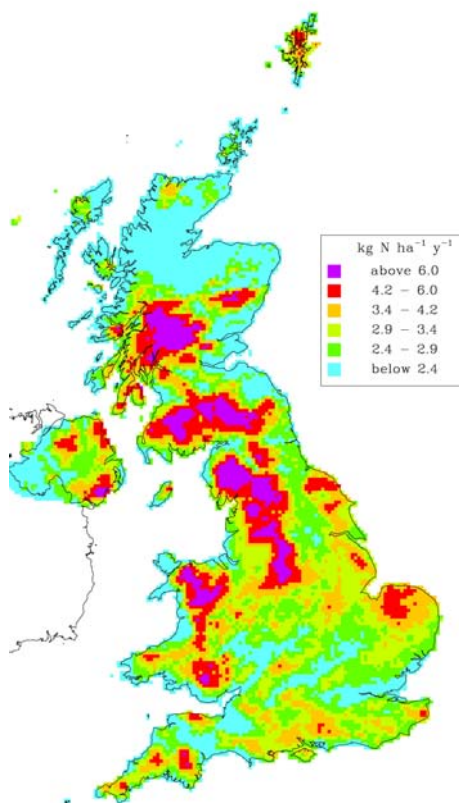
Fig 2.1(a) Maps of wet deposition of non-seasalt sulphur, nitrogen and non-seasalt calcium for 2002.



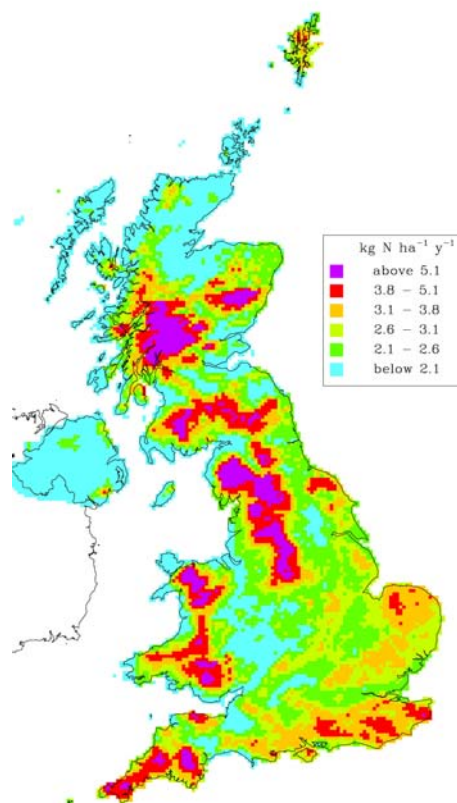
Wet deposition, non-seasalt Sulphur, 2003



Wet deposition, non-seasalt Calcium, 2003

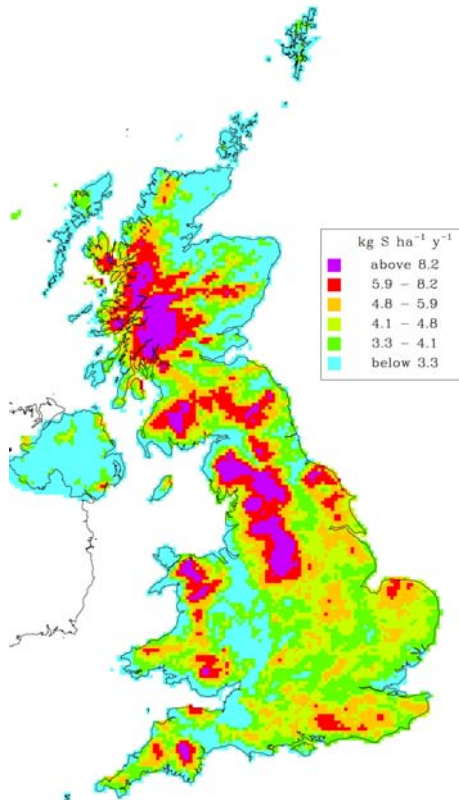


Wet deposition, Ammonium, 2003

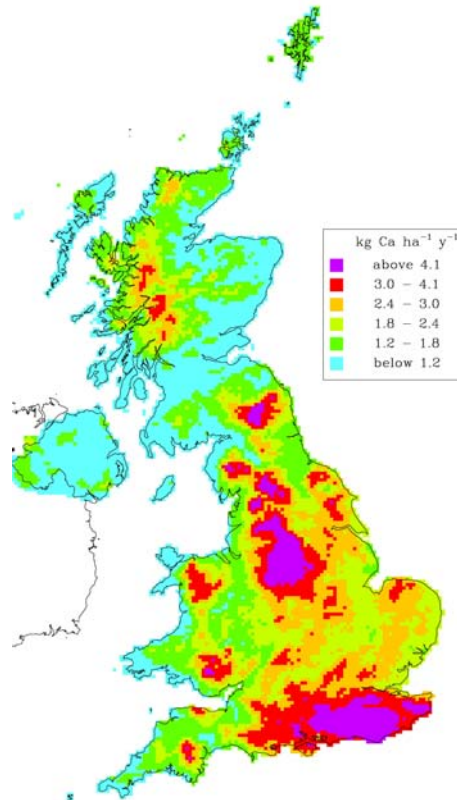


Wet deposition, Nitrate, 2003

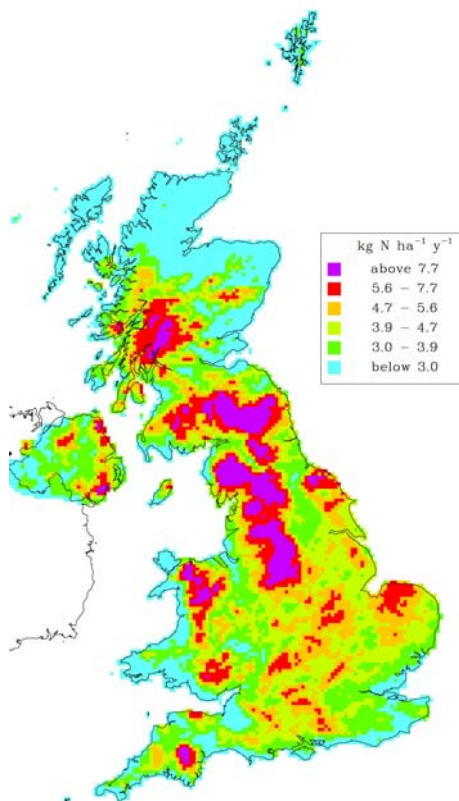
Fig 2.1(b) Maps of wet deposition of non-seasalt sulphur, nitrogen and non-seasalt calcium for 2003.



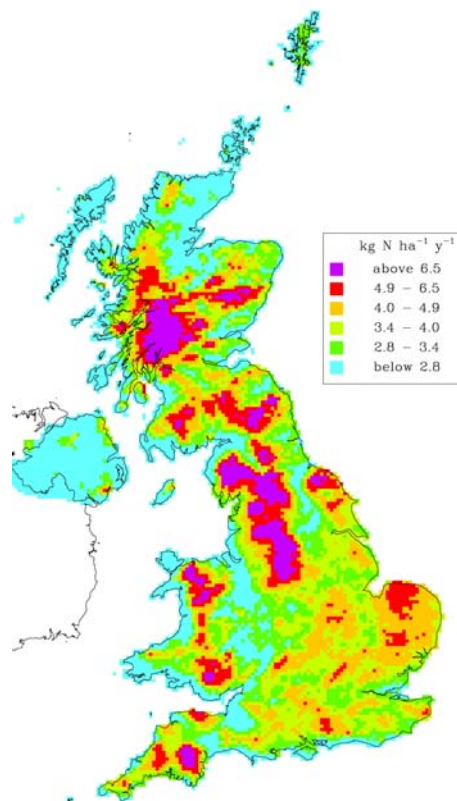
Wet deposition, non-seasalt Sulphur, 2004



Wet deposition, non-seasalt Calcium, 2004



Wet deposition, Ammonium, 2004



Wet deposition, Nitrate, 2004

Fig 2.1(c) Maps of wet deposition of non-seasalt sulphur, nitrogen and non-seasalt calcium for 2004.

3.2 Total deposition to the UK

Rognvald Smith

UK BUDGETS

The budget deposition values for the UK are calculated as the area-weighted sum of deposition to the 5 landuses in the models, namely arable, forest, grassland, moorland and urban. Table 2.1 shows the budget values for all modelled pollutants.

Table 2.1 Budget deposition to UK (gG y⁻¹) for 2002-2004

	Ion	2002	2003	2004
wet	nss SO ₄	124	87	114
	NO ₃	102	72	94
	NH ₄	113	81	107
	nss Ca	39	43	52
	nss Mg	1	0	1
	nss Cl	5	2	2
	Cl	1933	1292	1618
	Na	1102	773	946
	H	8	5	4
	Ca	81	73	88
	Mg	127	86	106
	SO ₄	214	147	184
	cloud	nss SO ₄	6	6
NO ₃		5	5	5
NH ₄		5	6	5
nss Ca		2	3	2
nss Mg		0	0	0
nss Cl		0	0	0
Cl		89	86	76
Na		50	50	44
H		0	0	0
Ca		3	5	4
Mg		6	6	5
SO ₄		10	10	9
dry	SO ₂	53	64	47
	NO ₂	22	25	17
	HNO ₃	62	87	57
	NH ₃	51	58	48
	nss Ca	6	11	9
	nss Mg	0	0	0
	Ca	10	14	12
	Mg	11	11	10
aerosol	SO ₄	11	15	10
	NO ₃	9	13	9
	NH ₄	7	9	7

The inter-annual variability is quite pronounced with some pollutants, with the dry summer in 2003 leading to, for example, higher dry deposition of SO₂, HNO₃, and NH₃ and lower wet deposition of non-seasalt SO₄²⁻, NO₃⁻ and NH₄⁺. Non-seasalt Cl⁻ and Mg²⁺ are now small components of the deposition budget at the UK scale. The modelled dry deposition of aerosols at the UK scale is about 50% greater than cloud droplet deposition for NH₄⁺ and about 100% greater for SO₄²⁻ and NO₃⁻.

Table 2.2 Trends in UK budget deposition for major ions (gG y⁻¹), 1995-2004

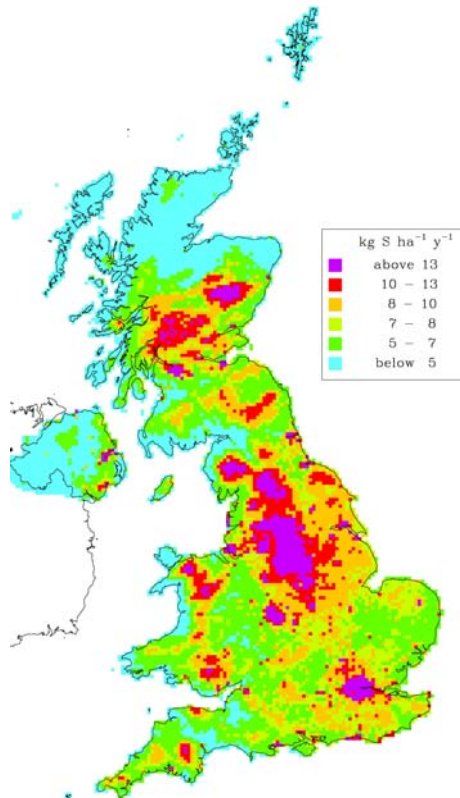
		1995	1996	1997	1998	1999	2000	2001	2002	2003	2004
nss SO _x	wet+cloud	164	183	148	162	149	138	133	129	93	120
	Dry	146	145	111	94	82	73	76	53	64	47
	Aerosol						9	12	11	15	10
	Total						221	221	194	172	176
NO _y	wet+cloud	101	104	102	98	103	98	105	107	77	99
	dry (NO ₂)		27	37	33	31	32	28	22	25	17
	dry (HNO ₃)						57	73	62	87	57
	Aerosol						7	9	9	13	9
	Total						163	186	178	176	164
NH _x	wet+cloud	120	135	116	121	121	104	120	118	87	112
	Dry			62	53	50	43	52	51	58	48
	Aerosol						6	7	7	9	7
	Total						154	180	176	154	166
nss Ca	wet+cloud						53	47	40	46	55
	Dry						7	8	6	11	9
	Total						60	55	47	57	64
nss Cl	Total	24	14	8	11	3	11	6	7	1	1

Total inputs, including seasalt contribution:

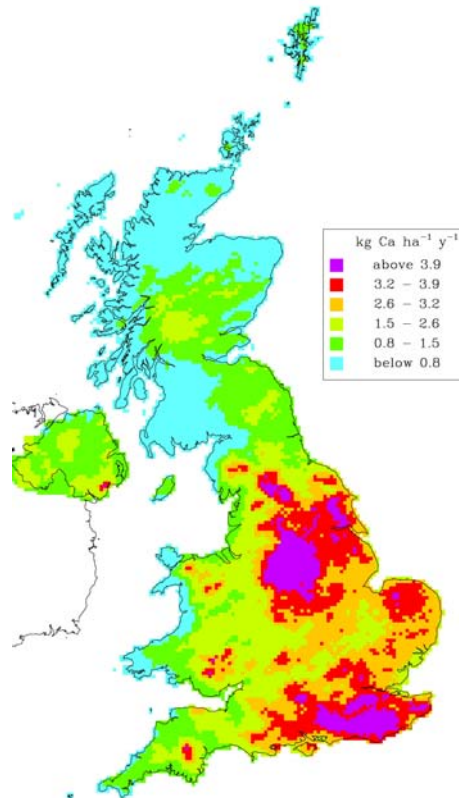
SO _x	Total	384	395	332	345	326	298	265	277	221	240
Ca+Mg	Total						245	170	239	194	225
Na	Total	842	755	845	1002	1156	1008	641	1102	773	946
Cl	Total	1498	1356	1470	1749	1979	1847	1119	1933	1292	1618

The trends from 1995 to 2004 in the main components of the UK budget (Table 2.2) confirm the substantial drop in deposition of non-seasalt sulphur and non-seasalt chloride. For nitrogen, the only statistically significant linear trends are the decrease in NO₂ dry deposition and NH₄ wet deposition, and there is little evidence of trend in the other components.

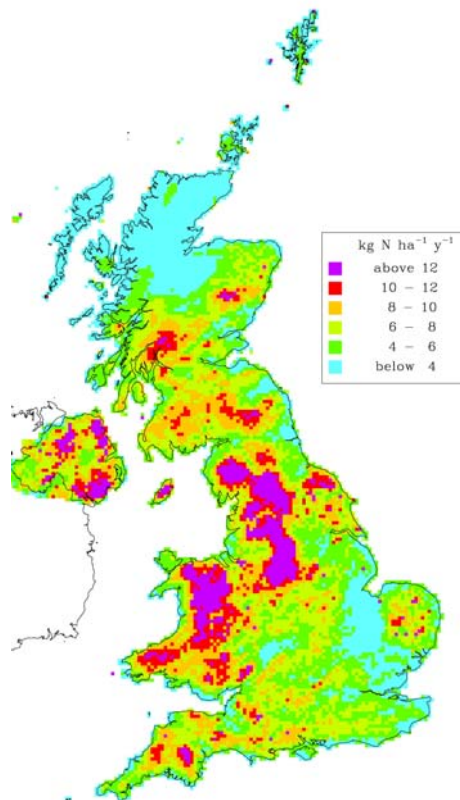
MAPS OF TOTAL DEPOSITION



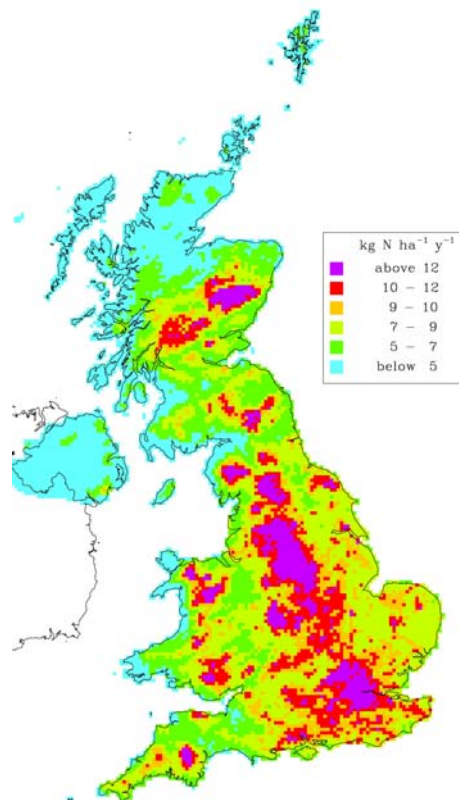
Total deposition, non-seasalt Sulphur, 2002



Total deposition, non-seasalt Base Cations, 2002

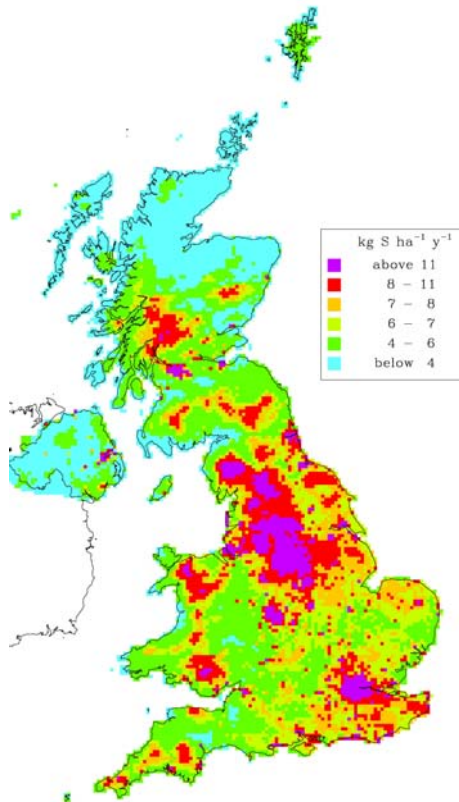


Total deposition, Reduced Nitrogen, 2002

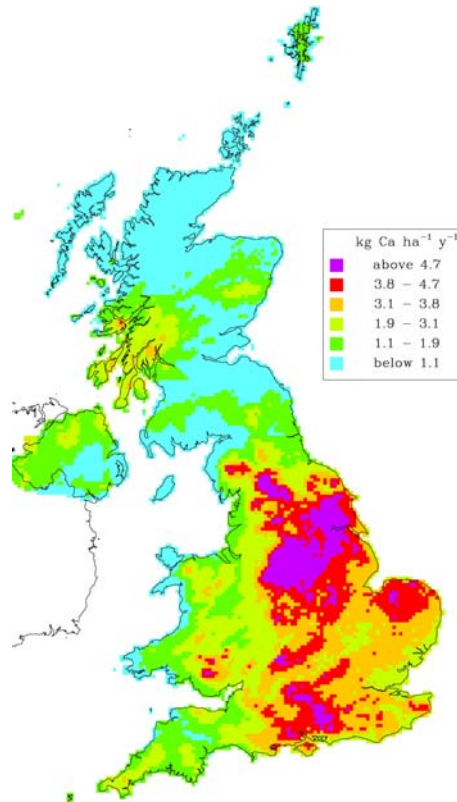


Total deposition, Oxidised Nitrogen, 2002

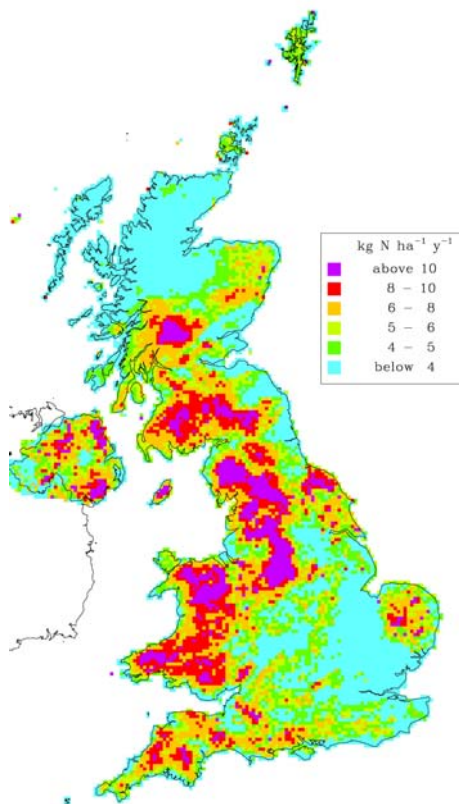
Fig 2.2(a) Maps of total deposition of non-seasalt sulphur, nitrogen and non-seasalt base cations for 2002



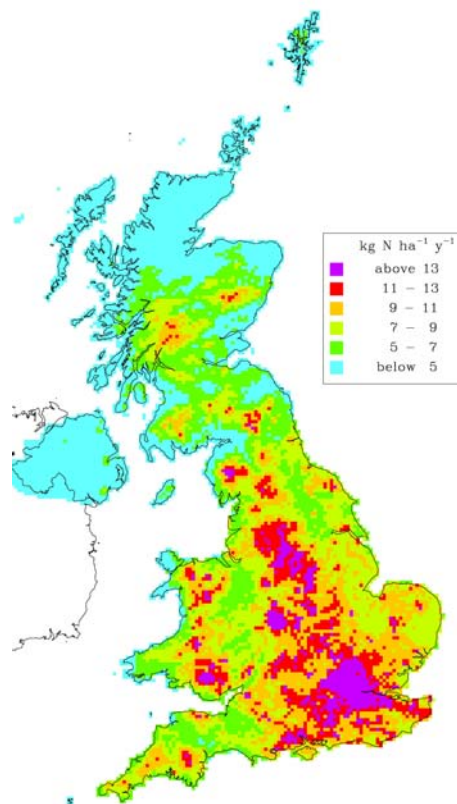
Total deposition, non-seasalt Sulphur, 2003



Total deposition, non-seasalt Base Cations, 2003

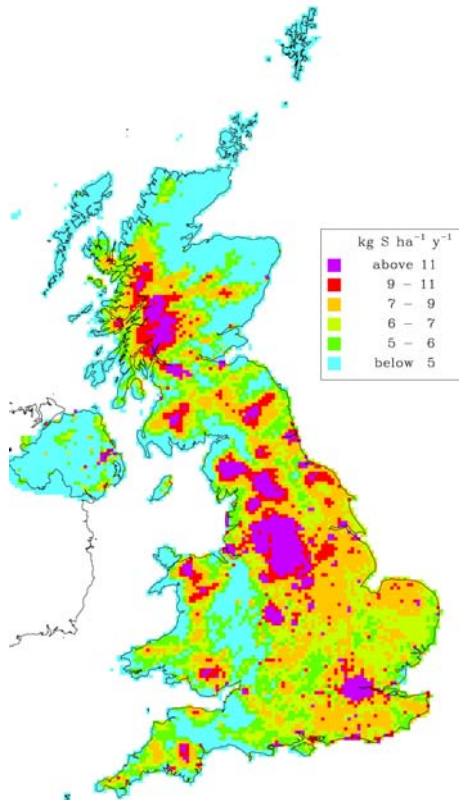


Total deposition, Reduced Nitrogen, 2003

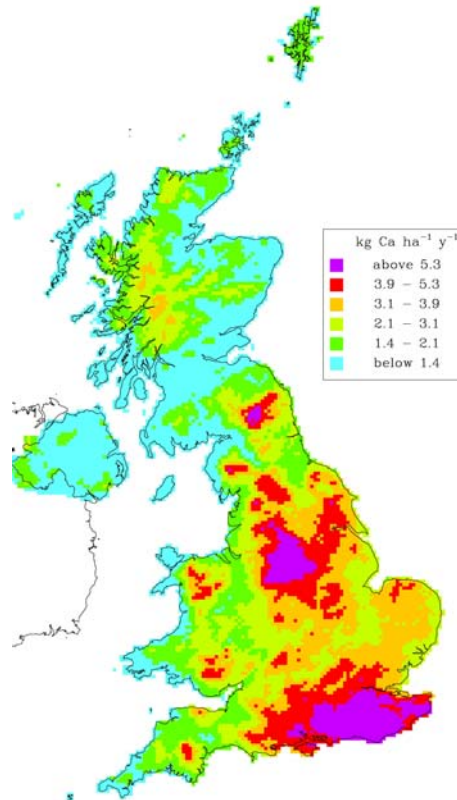


Total deposition, Oxidised Nitrogen, 2003

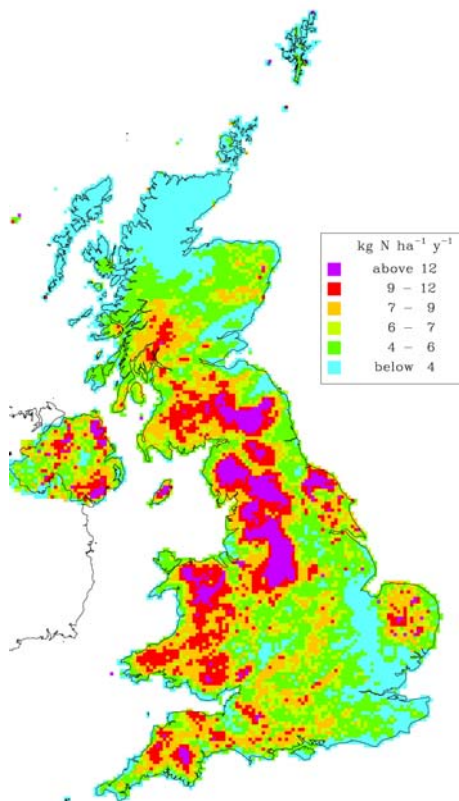
Fig 2.2(b) Maps of total deposition of non-seasalt sulphur, nitrogen and non-seasalt base cations for 2003



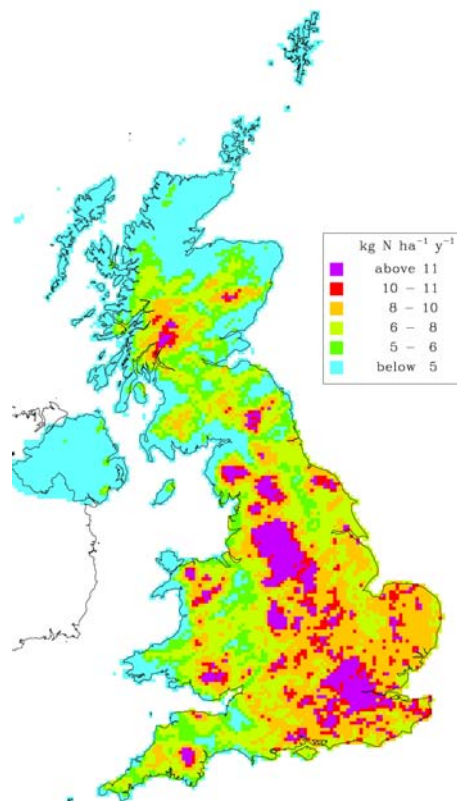
Total deposition, non-seasalt Sulphur, 2004



Total deposition, non-seasalt Base Cations, 2004



Total deposition, Reduced Nitrogen, 2004



Total deposition, Oxidised Nitrogen, 2004

Fig 2.2(c) Maps of total deposition of non-seasalt sulphur, nitrogen and non-seasalt base cations for 2004

Figures 2.2(a-c) give the annual maps of total deposition of non-seasalt sulphate, non-seasalt base cations, reduced and oxidised nitrogen for 2002-2004. The base cation maps are for the sum of Ca^{2+} and Mg^{2+} expressed as if it were all Ca^{2+} . Total deposition is the sum of deposition by all modelled pathways, in this case dry, wet, cloud droplet, and aerosol.

Over the three years, there is little difference in pattern of total sulphur deposition except over Scotland, where there is a shift in area of highest total deposition from the Cairngorms (in the north-east) to the southern Highlands between 2002 and 2004. For base cation deposition, which increases from 2002 to 2004, the pattern of deposition in the dry year of 2003 is different to the other two years with a noticeably smaller area of high deposition along the south coast. The maps of total deposition of reduced nitrogen show no substantial changes in pattern over the three years, although there appears to be the development of an area of higher deposition in the eastern areas of the Scottish-English border. For oxidised nitrogen deposition, the maps show similar patterns over the three years, but for the loss of deposition over the Cairngorms as occurred for sulphur deposition.

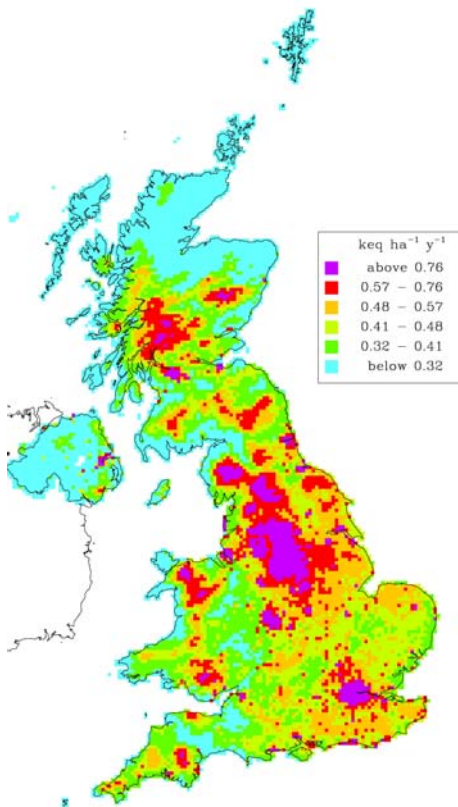
DEPOSITION FOR CRITICAL LOAD EXCEEDANCES

The calculation of critical load exceedances uses three-year average deposition data to smooth out some of the between-year variability. The current version of this data set is for the period 2002-2004.

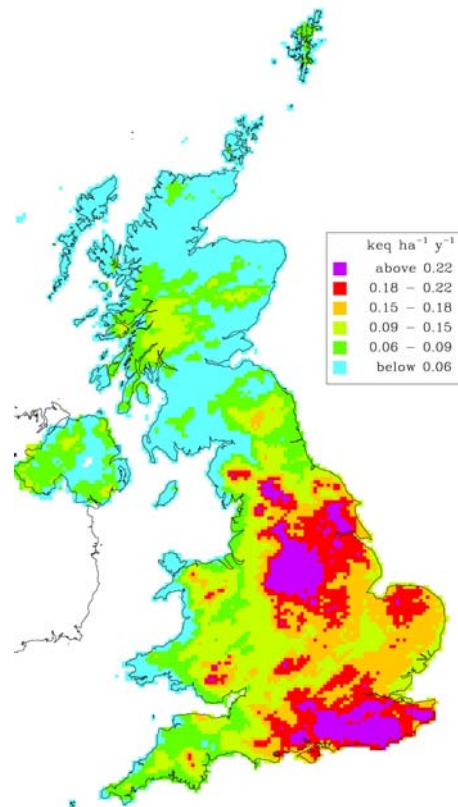
Figure 2.3 shows the maps of the main components in calculating deposition for critical loads (non-seasalt sulphate, oxidised nitrogen, reduced nitrogen and non-seasalt base cations) as averaged for the three-year period 2002-2004. There are no major changes to note between this data set and the previous 3-year average data for 1999-2001.

Deposition to specific land use categories varies from the above deposition to the average land use for each 5km x 5km square. This is illustrated with the deposition of reduced nitrogen to Norway Spruce forest (ns) and to acid grassland (ag) in Figure 2.4. In both cases NH_3 is deposited more rapidly to these landuses than to the other rural land use categories (arable or grassland), so the landuse specific deposition is generally greater than the average deposition in the area. However these maps do not take into account the presence of the specific landuse on the ground, and so are useful only for ecosystem studies and are not indicators of deposition in a particular area.

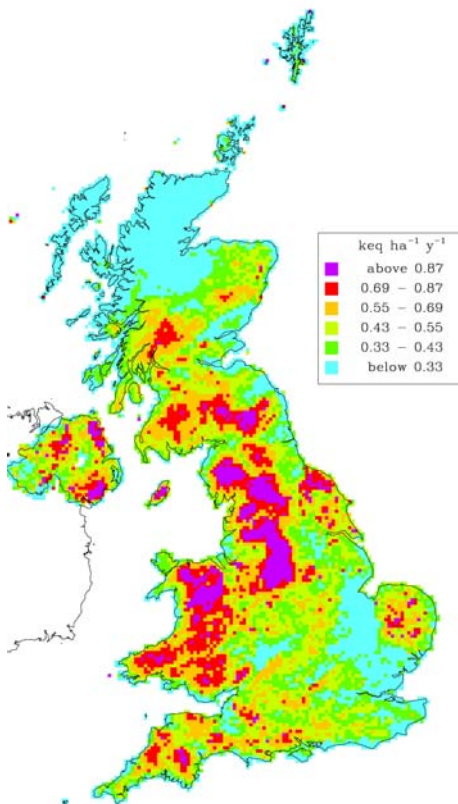
The use of seasalt base cation deposition along with the weathering rate as input to the calculation of a mass balance critical load has raised the issue of the appropriate averaging period. As can be seen in the above UK budget for deposition of sodium, the range of annual total deposition was 667 to 1207 Gg y^{-1} for the ten years indicates a year-to-year variability of the order of a factor of 2 attributable solely to changes in rainfall amount. This can be confirmed by reference to data at individual sites, particularly those in the remoter regions of the UK. Therefore, a ten-year average seasalt Ca^{2+} deposition is calculated from the ten-year average Na^+ (1995-2004), using a standard ratio of Ca^{2+} to Na^+ in sea water. This map is given in Figure 2.5.



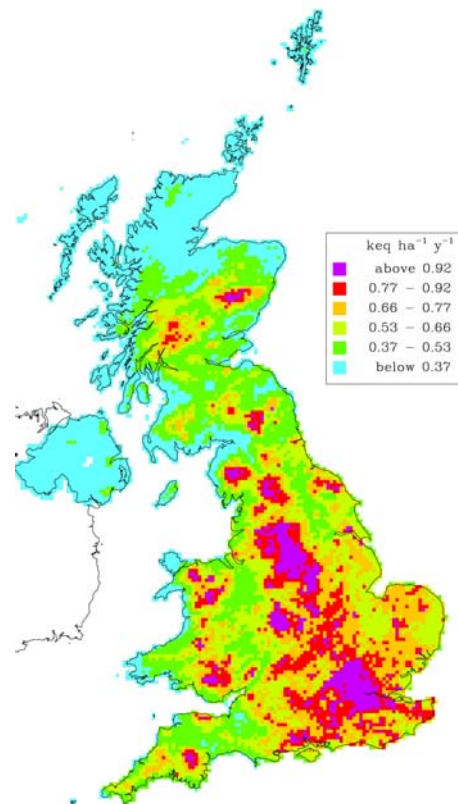
Deposition, non-seasalt Sulphur, 2002-2004



Deposition, non-seasalt Base Cations, 2002-2004

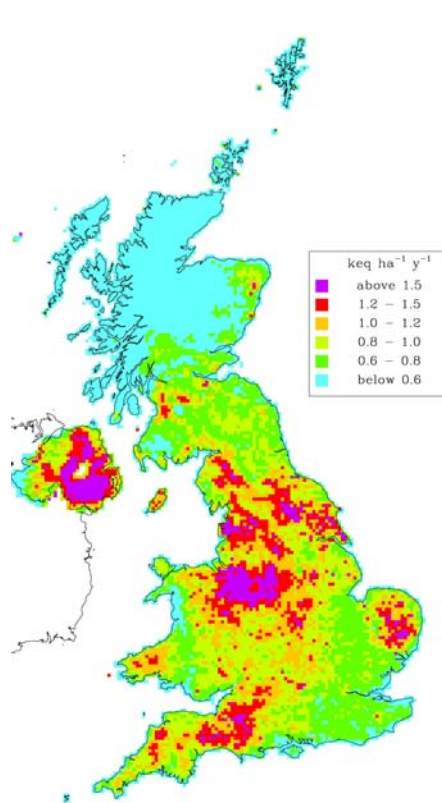


Deposition, Reduced Nitrogen, 2002-2004

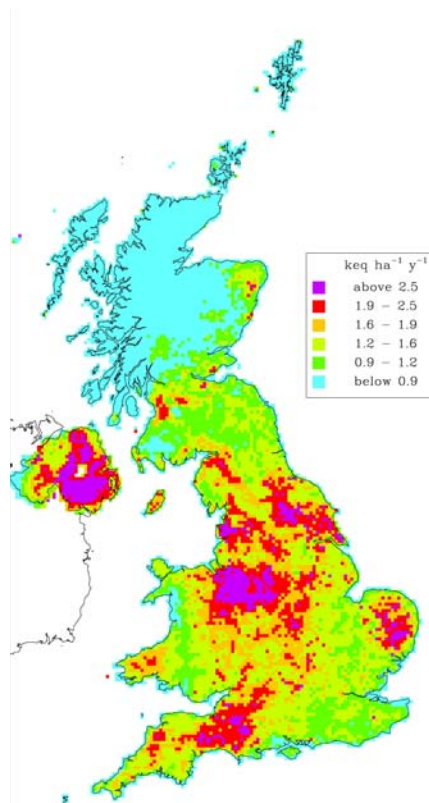


Deposition, Oxidised Nitrogen, 2002-2004

Fig 2.3 Maps of total deposition of non-seasalt sulphur, nitrogen and non-seasalt base cations for the average of the three-year period 2002-2004, as used for critical load exceedance calculations

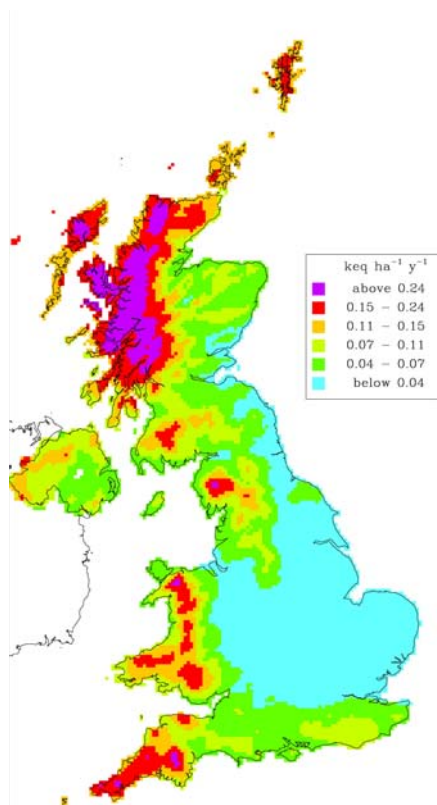


NH_x deposition to acid grassland

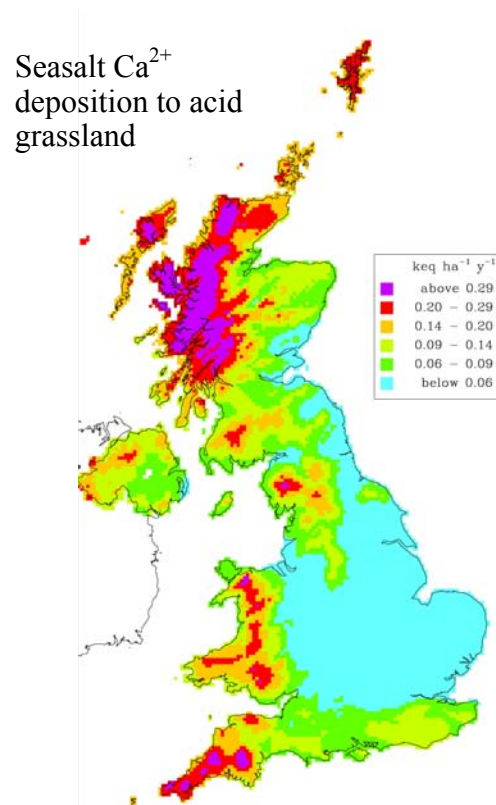


NH_x deposition to Norway spruce

Fig 2.4 Maps of ecosystem-specific total deposition of reduced nitrogen to acid grassland and to Norway spruce for the average of the three-year period 2002-2004, as used for critical load exceedance calculations



Seasalt Ca²⁺ deposition to acid grassland



Seasalt Ca²⁺ deposition to Norway spruce

Fig 2.5 Maps of the 10-year average total deposition of seasalt Calcium (1995-2004) to acid grassland and to Norway spruce, as used for the mass balance critical load.

4. AOT 40

4.1. Mapping annual AOT40

Ron Smith and Mhairi Coyle

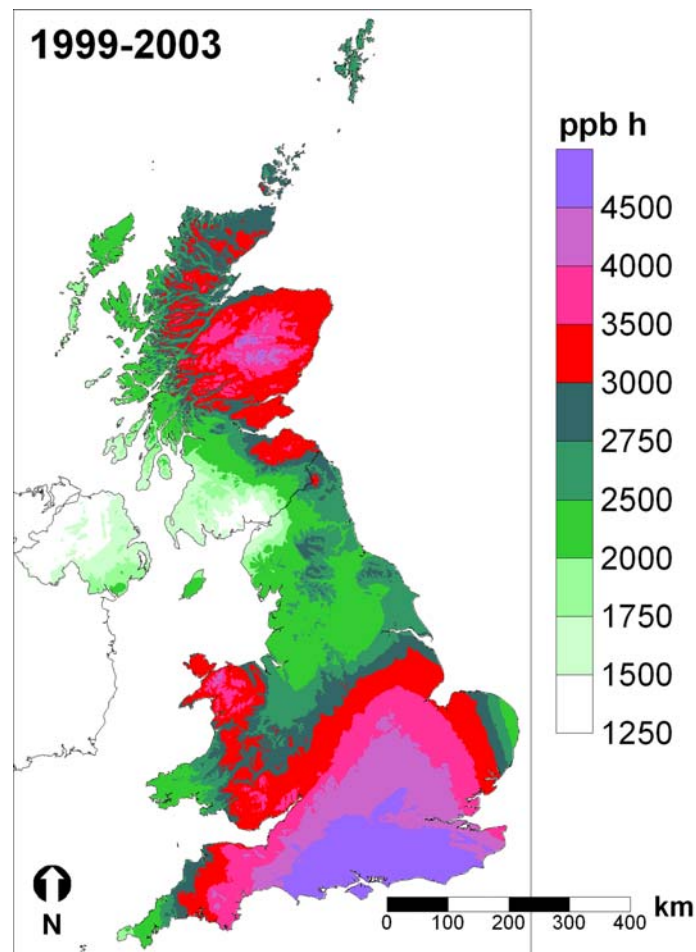


Figure 3.1. Five year mean (1999-2003) of AOT 40 (ppb) for crops and semi-natural vegetation.

The current target value and long-term objective for the protection vegetation is defined under the 3rd Daughter Directive are AOT40s of $18000 \mu\text{g.m}^{-3}.\text{h}$ (~ 9000 ppb h) as a 5 year mean from May to July (0800 to 2000 CET) and $6000 \mu\text{g.m}^{-3}.\text{h}$ (~ 3000 ppb h) from May to July (0800 to 2000 CET) respectively. The UNECE-ICP vegetation has also defined similar values for critical levels of 3000 ppb.h ($6000 \mu\text{g.m}^{-3}.\text{h}$) during May to July daylight hours for crops and semi-natural vegetation and 10000 ppb.h ($20000 \mu\text{g.m}^{-3}.\text{h}$) during April to September daylight hours for forests, both of which are assessed on a 5-year mean.

The AOT40 for crops/semi-natural vegetation and forests as defined by the ICP-Vegetation have currently been calculated for 1999-2003 and mapped across the UK at a 1 km a 1km scale using the methodology described in Coyle et al. 2002. Maps of the number of days the eight-hour running mean exceeds 50 ppb, the summer (April to September) mean and annual mean for 2003 are also available.

Reference:

Coyle, M., R. I. Smith, et al. (2002). "Quantifying the spatial distribution of surface ozone concentration in the UK." *Atmospheric Environment* **36**(6): 1013-1024.

5. SYNTHESIS

5.1. *Synthesis of UK trends to support policy negotiations*

In addition to the introductory discussion to this report which provides the historical perspective, the following papers provide a synthesis on trends and non-linearities, supported by the Acid Deposition Processes contract.

- Fowler, D., Muller, J., Smith, R.I., Cape, J.N., Erisman, J.W. 2005. Nonlinearities in source receptor relationships for sulphur and nitrogen compounds. *Ambio*, 34, 41-46.
- Fowler, D., Smith, R.I., Muller, J.B.A., Hayman, G., Vincent, K.J. 2005. Changes in the atmospheric deposition of acidifying compounds in the UK between 1986 and 2001. *Environmental Pollution*, 137, 15-25.
- Fowler, D., Smith, R.I., Muller, J., Cape, J.N., Sutton, M.A., Erisman, J.W., Fagerli, H. Long term trends in sulphur and nitrogen deposition in Europe and the cause of non-linearities. (Presented at Acid Rain Conference 2005 in Prague) *Water, Air, Soil Pollution Focus* (online first doi:10.1007/s11267-006-9102-x)

5.2 *Communication, Reporting and Development of internet site*

A website - <http://www.uk-pollutantdeposition.ceh.ac.uk> - has been set up and it has been conceived that not only data and information from “Acid Deposition Processes” will be published, but also complemented by additional material and datasets e.g. heavy metal deposition, wet and dry deposition datasets etc. A password restricted access area was created for downloading of data files and beta versions of datasets. The site is currently being developed and links to the site will be provided via the new CEH website, other Defra Project websites hosted by CEH, e.g. CARA, and other relevant sites such APIS.